University of Zurich[UZH]

Effect of climate change on human health: Case studies from Switzerland

GEO 511 Master's Thesis

Author
Fabian Weibel
16-701-278

Supervised by
Dr. Veruska Muccione
Dr. Seyed Saeid Ashraf Vaghefi

Faculty representative
Prof. Dr. Christian Huggel

29.09.2022
Department of Geography, University of Zurich

Abstract

An increasing number of severe and long-lasting heat waves all over the world during the last decades clearly points out that climate change is real. Global warming is especially pronounced in urban areas due to a phenomenon called the Urban Heat Island effect (UHI effect). A lack of vegetation, dense house constructions, missing water bodies, sealed surfaces, and an increased production of anthropogenic heat lead to significantly increased temperatures in cities. This poses a real threat to human health, whereby elderly people, people with chronic diseases, and small children are the most affected.

The aim of this master's thesis is to investigate the current and future thermal situation in Basel and Zurich and based on the findings, to discuss appropriate adaptation actions to reduce heat stress in the cities. In a first step, the UHI effect in Basel was explored to get an overview of hot and cool spots in the city. In a second step, the wet-bulb globe temperature (WBGT) was calculated for both a historic time period (1981-2020) and future simulations (1981-2099) using empirically derived mathematical equations and basic climate variables as input. The data for the future simulations are based on the three RCP scenarios (Representative Concentration Pathway) initially developed for the IPCC Climate Change Report 2014 (IPCC 2014). To handle the complexity of the climate system and the associated uncertainties, approaches of Decision Making under Deep Uncertainties (DMDU) were used (Exploratory Modeling (EM), Dynamic Adaptive Policy Pathways (DAPP)).

The gained results show that thermal stress will increase in the upcoming years, both in Basel and Zurich. However, the differences among the three RCPs are quite substantial. Where under RCP2.6, a stabilization in the next few years can be determined, one has to expect a gradually increasing number of extreme days and events per year until the end of this century under RCP8.5. The kind of necessary adaptation measures and where to implement them in a city are therefore really dependent on the chosen climate scenario.

A literature review as well as the results of a sensitivity analysis revealed that an optimized urban geometry and an increased amount of green spaces (e.g. trees, urban parks, rooftop gardens) in combination with open water surfaces (e.g. fountains, rivers, lakes) are the most efficient measures. Increasing the surface albedo on the other hand, even though comparatively easy and low in costs to implement, probably leads to rather small changes in the thermal situation.

In the end, it all comes down to how decision-makers work together and how they incorporate all occupants, the politicians, and the private sector in their work. What can be said for sure is that thermal stress will increase in the future and adaptation measures of any kind are urgently needed to protect the population in a sustainable way.

Zusammenfassung

Eine Zunahme von akuten und langanhaltenden Hitzeperioden auf der ganzen Erde während der letzten Dekaden deutet klar darauf hin, dass der Klimawandel Realität geworden ist. Die globale Erderwärmung ist besonders spürbar in urbanen Gebieten aufgrund eines Phänomens namens Hitzeinseleffekt. Eine niedrige Vegetationsdichte, dicht gedrängte Gebäude, fehlende Wasserflächen, versiegelte Oberflächen und eine erhöhte Produktion anthropogener Wärme führen dazu, dass Temperaturen in Städten signifikant erhöht sind. Das stellt eine reale Gefahr für die Gesundheit dar, wobei ältere Personen, Personen mit chronischen Krankheiten und Kleinkinder besonders darunter leiden.

Das Ziel dieser Masterarbeit ist es, die gegenwärtige sowie zukünftige Hitzesituation in Basel und Zürich zu untersuchen and basierend auf den erworbenen Erkenntnissen geeignete Anpassungsmassnahmen, um den Hitzestress zu minimieren, zu diskutieren. Als erstes wurde der Hitzeinseleffekt in Basel untersucht, um einen groben Überblick über lokale Hot und Cool Spots zu erlangen. In einem zweiten Schritt wurden mit Hilfe empirischer Formeln und simplen Klimavariablen für eine historische Zeitperiode (1981-2020) und Zukunftssimulationen (1981-2099) tägliche wet-bulb globe Temperaturen (WBGT) berechnet. Die Daten für die Zukunftssimulationen basieren auf den drei RCP Szenarien (Repräsentativer Konzentrationspfad), welche im Rahmen des IPCC Climate Change Reports 2014 berechnet wurden (IPCC 2014). Um die Komplexität des Klimasystems und die damit verbundenen Unsicherheiten berücksichtigen zu können, wurden verschiedene Konzepte von Decision Making under Deep Uncertainties angewendet (Exploratory Modeling (EM), Dynamic Adaptive Policy Pathways (DAPP)).

Die Resultate haben ergeben, dass sowohl in Basel als auch in Zürich die Hitzebelastung in den nächsten Jahren zunehmen wird. Die Stärke der Zunahme ist allerdings stark vom gewählten RCP Szenario abhängig. Während unter RCP2.6 eine Stabilisierung erwartet wird, muss unter RCP8.5 von einer beschleunigenden Zunahme von Hitzetagen und -events bis zum Ende des Jahrhunderts ausgegangen werden. Die Art und Weise wie Anpassungsmassnahmen umgesetzt werden sollten, ist also stark vom eintretenden RCP Szenario abhängig.

Eine Literaturrecherche sowie eine Sensitivitätsanalyse haben ergeben, dass eine Optimierung der Stadtgeometrie und eine Erhöhung der Vegetationsdichte in Kombination mit offenen Wasserflächen die effizientesten Massnahmen sind. Eine Erhöhung der Albedo von Oberflächen, trotz des vergleichsweise geringen Aufwands, erzeugt hingegen nur einen minimal kühlenden Effekt.

Letztendlich hängt alles davon ab, wie Entscheidungsträger zusammenarbeiten und inwiefern sie die beteiligte Bevölkerung, die Politik und den Privatsektor in den Erarbeitungsprozess miteinbeziehen. Klar ist aber, dass die Hitzebelastung wohl trotz dieser Massnahmen in Zukunft weiter zunehmen wird und deshalb dringend effiziente Lösungen, um die Bevölkerung davor zu schützen, nötig sind.

Table of Contents

Figures

Appendix:

Tables

Appendix:

Abbreviations

Meteorological parameters:

e	Vapor pressure (hPa, kPa)
PET	Physiological equivalent temperature (°C)
Q	Radiation (w/m^2)
rh	Relative humidity (%)
Ta	Air temperature / Dry bulb temperature (°C)
Tg	Globe temperature (°C)
Tnwb	Natural wet-bulb temperature (°C)
Tpwb	Psychrometric wet-bulb temperature (°C)
WBGT	Wet-bulb globe temperature (°C)
ws	Wind speed (m/s)

Greenhouse gases:

CH_4	Methane
CO_2	Carbon dioxide
N_2O	Nitrous oxide

Others:

CH2018	Swiss Climate Scenarios 2018
DAPP	Dynamic Adaptive Policy Pathways
DMDU	Decision Making under Deep Uncertainties
EM	Exploratory Modeling
EMA Workbench	Exploratory Modeling and Analysis Workbench
GCM	Global/General Climate Model
GDP	Gross Domestic Product
HHWS	Heat-Health Warning System
IPCC	The Intergovernmental Panel on Climate Change
LEE	Average length of extreme events
NED	Number of extreme days
NEE	Number of extreme events
NCCS	Nation Centre for Climate Services
RCM	Regional Climate Model
RCP	Representative Concentration Pathway
RDM	Robust Decision Making
SD	Scenario Discovery
SSP	Shared Socio-economic Pathway
SUHI	Surface Urban Heat Island
UHI	Urban Heat Island

1 Introduction

1.1 Relevance

Climate change poses one of the most substantial threats for humanity in the past and upcoming decades. Global surface temperatures are increasing with an extraordinary rate which has never been seen in Earth's history before. Future projections even predict an acceleration of global warming during the next decades (IPCC 2021a). As experienced in the summers of 2003, 2015, 2018, and 2022 in Europe, increasing temperatures directly lead to an intensification of extreme events such as heat waves and droughts. They become more severe, long-lasting, and more frequent. The chance of combined events increases as well, leading to unpredictable impacts on the environment and many parts of our society (Niggli et al. 2022).

Shrinking glaciers, missing precipitation, and a strong evapotranspiration directly affect the water cycle and finally lead to extensive water shortages. This causes troubles in many sectors, such as the agricultural sector, the energy sector, or the drinking water supply.

High temperatures could also cause direct impacts on human health, especially in regions with a high degree of urbanization. Due to an accelerating population growth in cities and consequently a densification and expansion of urban places, more and more people are becoming exposed to extremely high temperatures. Overheating, circulatory problems, or a loss of labor productivity are just a few of many possible threats of heat waves for human beings. The consequences of hot temperatures can be quite dramatic which is why it is important to gain a profound knowledge of how thermal conditions are developing in the future and what possibilities exist or should be developed to mitigate the impacts on human health. Suitable adaptation measures are therefore in high demand in order cool down hot spots in cities as efficient and economically as well as ecologically friendly as possible.

1.2 Research questions

The overall goal of this master's thesis is to understand **how climate change, in particular how increasing temperatures and intensifying heat waves, affect human health** through an analysis of the Urban Heat Island effect (UHI effect) and wet-bulb globe temperatures (WBGT). On the basis of the results, suitable adaptation measures will be assessed in order to mitigate the impacts of heat waves in urban areas. The analysis of the UHI effect and WBGT will primarily be applied for Basel. Additionally, Zurich will be investigated for future WBGT in order to gain a broader picture of possible impacts of climate change in two big Swiss cities.

The following three research questions should help to reach the overarching goal:

1. What is the **UHI effect** in **Basel**? Where are current and future hot spot areas?
2. How does future climate change affect **WBGT** in Basel? How does it compare to Zurich?
3. What **adaptation measures** are the most suitable to reduce hot spots in Basel?

To answer the first research question, a deep analysis of the UHI effect in Basel will be made. The goal is to locate current hot and cool spots and to analyze the characteristic land use classes, the topography, and building constructions at these places. Important to consider for this part of the study are the locations of vulnerable facilities, like for example nursing homes, hospitals, kindergarten, and schools.

The second and third research questions will be tackled by applying an approach of Decision Making under Deep Uncertainties (DMDU). The Exploratory Modeling and Analysis Workbench (EMA Workbench) developed by Kwakkel (2017) will be used to simulate future WBGT for three different climate projections (RCP2.6, RCP4.5, RCP8.5). Based on the outcomes, suitable adaptation measures to reduce heat stress in the city will be discussed.

1.3 Structure

After a brief introduction of the main goals and the research questions of this master's thesis, chapter 2 introduces important scientific and theoretical background knowledge in order to emphasize the relevance of this work and to explain some basic concepts. The focus of chapter 3 lies on presenting the study areas which are Basel and Zurich. Chapter 4 explains the main methods applied in this study. After introducing the used measuring stations and the data in chapter 5, chapters 6 and 7 summarize and discuss the most important findings. According to the outcomes, suitable adaptation measures and their efficiencies to handle a potentially increasing heat stress are covered. After a short conclusion of the most important findings in chapter 8, the final two chapters present the used literature as well as an appendix of additional figures and tables which were not showed in chapter 6.

2 Scientific and theoretical background

2.1 Climate change and global warming

Climate change is more than ever highly discussed in the society and thus a controversial topic in politics. During the last several years, governments as well as large parts of the population in many countries argued for fighting against climate change and stood up for drastic changes in politics and the society. The latest IPCC report from 2021/22 once again bore out that the atmosphere, ocean, and land surfaces are warming unusually fast compared to historic temperature fluctuations and that this warming unequivocally can be attributed to human induced changes in the climate system. The projected goal of the Paris Agreement of a limited warming of 1.5° C will be exceeded unless the current burning rate of fossil fuels will not be reduced as soon and as rigorously as possible. Otherwise, the frequency and amount of weather and climate extremes will increase in every region on Earth (IPCC 2021b). According to the report, scientists expect that poor people in developing countries are going to be disproportionately affected. They oftentimes live in regions where climate change has very strong impacts on the environment. Furthermore, developing countries have much less financial possibilities and infrastructural facilities to fight against climate catastrophes and extreme events. Therefore, the scientists stated that beside of the projected impacts of climate change, socio-economic developments should be considered as well (IPCC 2022, IPCC 2014).

Climate change has many different impacts on both humans as well as the environment. Different regions in the world face different challenges. These are mainly dependent on the prevalent climate conditions and the characteristics of the environmental system. Indeed, the residents and the local infrastructure have an important influence as well. Usually, the food production and agricultural sectors, the people's livelihoods, and human health are the most vulnerable to any kind of climate change. Whether it concerns heavy rainfall events, extensive droughts, severe heat waves, or globally rising sea levels. In the end, it all leads to economical, ecological, social, and health issues.

A global phenomenon which can be observed almost everywhere on Earth are rising air and water temperatures, mainly due to extensive emissions of anthropogenic greenhouse gases (CO_2, CH_4, N_2O) (IPCC 2014, CH2018 2018, Hansen et al. 2006). Detailed observations of surface air temperatures are available for the period between 1850 to present. During the 19th century, climatologists began to systematically install and maintain surface temperature sensors in order to gain a better understanding of the climate system and its impacts on the environment. Whereas for information about the temperature fluctuations before 1850, one has to consult indirect techniques like analyzing tree rings, corals, sediments, or ice boreholes. Using all these sources of information about the past climate, researchers could reconstruct a relatively stable temperature between 1000 and 1850. Since 1900, they observed an abrupt warming trend (Chapman & Davis 2010). This represented major changes for

life on Earth. Higher temperatures do not only lead to shrinking glaciers and ice shields and consequently to globally rising sea levels. Higher temperatures do also influence the occurrence and intensity of heat waves and droughts. Indeed, the probability and severity of extreme heat events are expected to increase much faster compared to global changes of mean surface temperatures (Vautard et al. 2014, IPCC 2018).

There are spatial differences in the magnitude and speed of the climate change among different regions on Earth. Vautard *et al.* (2014) found that some parts in Europe experienced a stronger warming than the global average, whereas other places on Earth even cooled down slightly. The spatial and seasonal pattern of warming and cooling in Europe is not evenly distributed either. A stronger warming is expected in Northern and Eastern Europe during the winters, whereas in Southern Europe, the summers will probably get hotter (Vautard et al. 2014). Climatologists agree that the strongest changes will experience high latitudinal regions. They already measured a stronger increase in mean annual temperatures at the poles compared to the global average and they expect it to become even more pronounced in the upcoming years (Hansen et al. 2006, IPCC 2014). This phenomenon of an increased warming at high latitudes is described as the arctic amplification (Previdi, Smith & Polvani 2021).

An investigation of climate change on a smaller and more local scale points out that highly urbanized areas do suffer disproportionately under very strong increased temperatures. One reason for this phenomenon can be attributed to the so-called Urban Heat Island effect. More information about this phenomenon can be found in chapters 2.4 and 6.1. However, the vulnerability and exposure of urban areas to increasing temperatures do not only rapidly increase due to the global warming. Rapid expansions of cities and fast growing urban populations are additional reasons for an increased proneness to climate extremes, independent of the global climate change (Dodman et al. 2022).

Therefore, it is no surprise that the Intergovernmental Panel on Climate Change (IPCC) ranks increasing temperatures and associated heat waves as one of the most severe risks related to climate change (Burgstall et al. 2019). Beside of financial burdens, societies and environments will have to change in the future in order to adapt to the upcoming climatic conditions.

2.2 Heat waves and human health

Heat waves all over the world lead to a massive increase of thermal stress both for plants, animals, or humans. Scientists observed an increase of dangerous heat exposure in cities during the period from 1980 to 2017 of about 500%. As a result, over 1 billion people every year experienced very hot conditions leading to significant death tolls and hospitalization rates (Cissé et al. 2022, Li, Stringer & Dallimer 2021, Li, Ferreira & Smith 2020). The next sections briefly outline some key issues and the most substantial impacts of recent heat wave events in Australia, South Asia, and Europe.

Heat wave in eastern Australia (2019/20):

A very strong heat event occurred in the eastern part of Australia in 2019/20. The event led to massive damages in ecosystems through extensive forest fires and droughts (Bowman et al. 2021, Abram et al. 2021). It is expected that over 20% of Australia's temperate broadleaf and mixed forests were burned during the 2019/20 summer season (Boer, de Dios & Bradstock 2020). Additionally, it is assumed that over one billion animals were killed in the forest fires (Filkov et al. 2020). Beside of huge environmental and agricultural impacts, the heat wave also heavily affected human health.

Heat wave in India and Pakistan (2022):

The latest series of heat waves in Asia was experienced by the population in India and Pakistan in 2022. They suffered under extremely hot temperatures leading to widespread crop failures, drinking water shortages, and power failures. Simultaneously, extensive floods due to an increased glacial melting in the Himalayas damaged important parts of infrastructural facilities and agricultural fields (Fountain 2022).

Heat waves in Central Europe (2003, 2015):

During the summers of 2003 and 2015, the population in Central Europe was exposed to unnatural high air temperatures. As the heat wave in eastern Australia (2019/20), these two events led to extensive droughts and widespread forest fires. In fact, the summers of 2003 and 2015 were two of the hottest and driest summers in Central Europe ever registered. The temperatures were 20-30% higher compared to normal summers in the past decades. The agricultural productivity suffered under extensive crop failures. Alpine glaciers lost up to 10% of their mass. Additionally, the heat waves caused problems in the energy sector like for example issues in the cooling process of power plants. Combined with an increased need of energy for air conditioners, this led to widespread energy shortages, especially in countries where most of the energy was generated by nuclear power plants (e.g. France) (De Bono et al. 2003, Dong et al. 2016, Kovats & Hajat 2008).

The events in Central Europe unambiguously bore out that heat waves strongly influence affected people's everyday life. Beside the aforementioned impacts on the environment, heat waves do also negatively influence the health of the human body. Hot temperatures during the day and a missing cooling during the night can represent a threat, especially for vulnerable people like elderly people, people with chronic diseases, and small children. In addition to extremely high temperatures, heat waves are oftentimes coupled with severe air pollution in urban areas (Kovats & Hajat 2008). Especially ozone and particulate matter are significantly increased during heat waves. Ozone is readily formed under hot and sunny weather conditions (Fischer, Brunekreef & Lebret 2004). Fischer, Brunekreef and Lebret (2004) investigated the excess deaths due to the summer heat wave 2003 in the Netherlands. They found that a large part of the excess deaths initially attributed to high temperatures were actually

caused by increased ozone and particulate matter concentrations. This finding demonstrates that indirect effects of heat waves on human health can be as impactful or even worse than direct effects. There are many other studies which observed an excess death in Central Europe during the heat waves of 2003 and 2015. De Bono *et al.* (2004) even described the extreme event in 2003 as one of the deadliest natural disasters in Europe of the last 100 years. They estimated an excess of about 30'000 deaths during the summer season. Ragettli *et al.* (2019) did a similar study about the impacts of the 2003 and 2015 heat waves on mortality and morbidity rates in Switzerland. Although they estimated an increased mortality rate during both heat waves, Ragettli *et al.* (2019) observed a smaller excess during 2015 compared to 2003. They stated an improved public awareness of heat threats as well as implemented mitigation measures after the 2003 event as two possible explanations for the reduced excess death rate.

Table 1 summarizes increased mortality rates attributed to the 2003 heat wave in Switzerland, France, and the Netherlands.

Table 1: *Increased mortality due to the 2003 summer heat wave in Switzerland, France, and the Netherlands* (Kovats & Hajat 2008).

Country	Excess death (increase in %)
Switzerland	975 (6.9%)
France	14'802 (60%)
Netherlands	1400

Human health:

Multi-country studies about health impacts related to climate change are rare. An example of such a study was conducted by Vicedo-Cabrera et al. (2021). They investigated heat-related health impacts in 43 countries. The scientists analyzed heat-related deaths between 1991 and 2018 and found that on average, 37% of these deaths could be attributed to anthropogenic climate change (Cissé et al. 2022, Vicedo-Cabrera et al. 2021).

Elderly people, people with chronic diseases, and small children are the groups which are the most vulnerable to very hot thermal conditions. Some studies also name females as slightly more endangered than males (Ragettli et al. 2017). Hot temperatures during the day and a missing cooling during the night in combination with a strong exposition to solar radiation and a high relative air humidity are the major causes for dehydration and hyperthermia. People with already weak capacities of internal thermoregulatory mechanisms and a debilitated circulatory system cannot balance the excessive heat anymore (Ragettli et al. 2019, Matzarakis & Amelung 2008). In cases when the air temperature is higher than the skin temperature, the body tries to cool down via direct heat exchange

and sweat evaporation. However, if the humidity gradient between the body and the surrounding air is very low, this cooling mechanism is disturbed. Heat strokes, heat exhaustions, heat syncopes, heat cramps, and even dysfunctions of multiple organs are possible health consequences (Burgstall et al. 2019). Combined with a reduced physical activity due to hot weather, the risk of cardiovascular diseases becomes an additional threat for vulnerable people. Cardiovascular diseases could for example be a coronary heart disease or a peripheral arterial disease (Cissé et al. 2022, Obradovich & Fowler 2017). Besides circulatory problems, some affected people could also suffer from endocrine or mental disorders, or other psychological disturbances (Kovats & Hajat 2008, Bi et al. 2011).

If an already harmful heat stress during the day gets prolonged by considerably high minimum temperatures during the night, heat waves are even worse for human health. Nocturnal rest and sleep are very important for our body, especially during periods of extensive thermal exposure during the day. Royé *et al.* (2021) found a clear relationship between the duration and excess of hot nights and sleep disturbances. Beside light and noise, they determined the thermal environment as the most important parameter that influences our sleep quality (Royé et al. 2021).

In addition to health problems for vulnerable people, heat waves can also lead to a reduction in labor productivity and thus in extreme cases to a decreased economic output (Tuholske et al. 2021, Dodman et al. 2022). Too high or too low thermal conditions can cause a strongly declined productivity in physically demanding activities (Burke, Hsiang & Miguel 2015). A loss of concentration, a reduced brain function, fatigue, or dehydration are, amongst others, some possible impacts which outdoor workers could suffer under uncomfortable climatic conditions (Cissé et al. 2022). Kjellstrom (2016) investigated current and future impacts on the work capacity in the agricultural and industrial sector in South and South-East Asia. His analyses highlighted that extreme hot days currently cause a loss of 15-20% of annual work hours. He even calculated a doubling by 2050 if global climate change will develop as expected. In terms of economic output, this results in additional costs of up to several percentages of GDP in some countries. Another study estimated the amount of lost work hours due to heat for the time period between 2000 and 2018 on a global scale. The scientists concluded that there was an increase of about 45 billion lost work hours in 2018 compared to 2000 (Cissé et al. 2022, Watts et al. 2019).

These observations indicate that climate change, and especially globally increasing temperatures and heat extremes, may amplify the economic inequalities between developing and developed countries. Social conflicts and disrupted trades are preprogrammed challenges (Burke, Hsiang & Miguel 2015).

2.3 Climate scenarios

It is tremendously difficult to get a thorough understanding of the entire climate system. Even after many years of intense scientific work, research, data collection, and data analysis, there are still a lot

of unknown processes and unexplored feedback mechanisms. Making accurate predictions about the future state of the climate system is not easy and always related to various kinds of uncertainties. Moreover, the influence of randomness and nonlinearity must not be disregarded since many processes in the chaotic behavior of the climate system do actually happen by pure coincidence (Thompson & Sieber 2012). Consequently, it is impossible to estimate one single future scenario which holds true for the entire Earth. It is much more common to make region specific predictions and split the future time into three to four distinct time periods. Furthermore, every determined future scenario only holds for a certain time since a constantly improved understanding of all processes, newly developed models, and additional data allow to refine every existing scenario.

Most climate scenarios nowadays are based on global/general as well as regional climate models (GCM, RGM). It depends on the size and the complexity of the topography of the region of interest as well as on the scope of application whether spatially high-resolved regional models are required, or if global models already deliver adequate results (CH2018 2018).

For this master's thesis, the Swiss Climate Scenarios 2018 (CH2018) were used to calculate future WBGT values. They are based on an ensemble of RCMs (combination of several RCMs with different initial conditions). Three different scenarios for Switzerland were generated according to the three Representative Concentration Pathways (RCP2.6, RCP4.5, RCP8.5) developed for the IPCC Climate Change Report 2014 (IPCC 2014, CH2018 2018). As input for each simulation, anthropogenic forcing scenarios, like the emission of greenhouse gases and aerosols and changes in land use classes, were included. RCP2.6 is a very optimistic scenario whereas RCP8.5 represents a future without any climate protection measures. RCP4.5 stands in between RCP2.6 and RCP8.5. It includes some mitigation measures which however are less strict and short-term compared to those of RCP2.6. Regarding the current developments and policies set by most nations, RCP4.5 is probably the most realistic scenario. In the specific case of air temperatures, the scenarios translate into an increase of 0.3° C to 1.7° C or 2.6° C to 4.8° C by the end of the 21st century relative to the reference period between 1986 and 2005 under RCP2.6 and RCP8.5 respectively (table 2) (IPCC 2014).

Table 2: *Representative Concentration Pathways (RCP) used in the IPCC Climate Change Report* (Burmeister, Büter & Trute 2019, IPCC 2014).

Scenario	Change of anthropogenic forcings	Change of global mean surface temperatures
RCP2.6	Strong reduction of greenhouse gas emissions	0.3 – 1.7° C
RCP4.5	Emissions decline after 2050	1.1 – 2.6° C
RCP8.5	Continuously increasing emissions until the end of this century	2.6 – 4.8° C

In addition to different anthropogenic forcing scenarios, the National Centre for Climate Services (NCCS) developed states for three different future time periods (2035, 2060, 2085) and five model regions (eastern and western region for north of the Alps, Alpine area and a region for south of the Alps) (CH2018 2018).

Figures 1 and 2 exhibit a closer look at Switzerland. The projected temperature changes for the scenarios RCP2.6 and RCP8.5 were applied to calculate how the number of tropical nights ($T_{min} \geq 20°$ C) and hot days ($T_{max} \geq 30°$ C) could change in the future. As expected, the Swiss Plateau and the valleys in Ticino are going to experience the biggest changes (CH2018 2018).

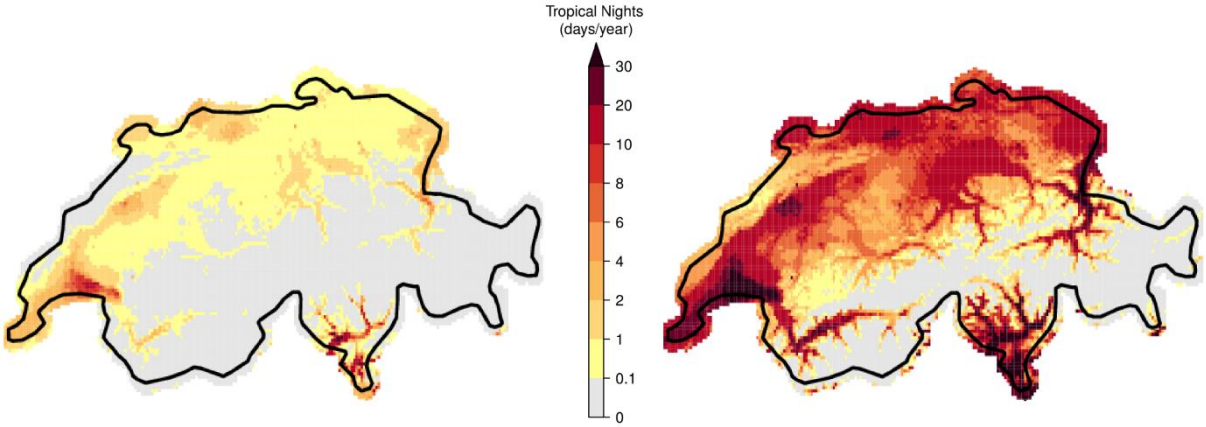

Figure 1: *Expected number of tropical nights ($T_{min} \geq 20°$ C) per year for the future scenarios RCP2.6 (left) and RCP8.5 (right) in the year 2085 (CH2018 2018).*

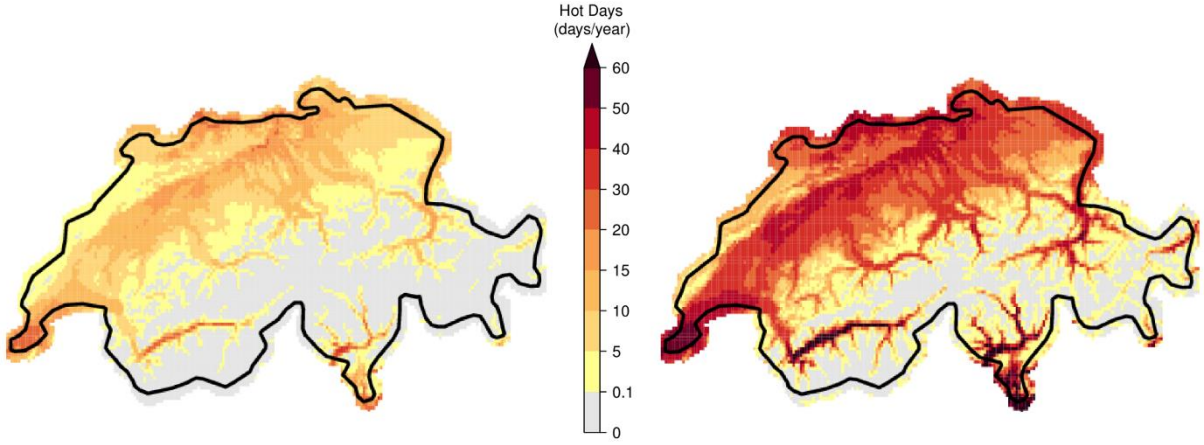

Figure 2: *Expected number of hot days ($T_{max} \geq 30°$ C) per year for the future scenarios RCP2.6 (left) and RCP8.5 (right) in the year 2085 (CH2018 2018).*

In the latest IPCC Report (AR6), the climatologists refined their future scenarios from the IPCC Report 2014 (AR5). The new projections not only differentiate between climate radiative forcings, but also consider socio-economic estimations (Shared Socio-economic Pathway (SSP) (IPCC 2021a)). However, the data for Switzerland which has to be calculated specifically is not available yet. Which is why the future scenarios in this paper still relay on the RCPs introduced in the IPCC Report 2014.

Figure 3 shows the spatial distribution of globally increasing temperatures estimated for the scenarios SSP1-2.6 (comparable with RCP2.6) and SSP3-7.0 (between RCP4.5 and RCP8.5) (O'Neill et al. 2016, Lee et al. 2021). It clearly shows that the temperature increase is stronger over the continents than over the oceans. Furthermore, higher temperature changes are expected on the Northern compared to the Southern Hemisphere. There are four main reasons leading to this pattern: First, water has a higher heat capacity than continental surfaces and thus warms up less quickly. Second, a major part of anthropogenic greenhouse gases originates from the higher populated Northern Hemisphere and thus heats up the atmosphere and surface faster. Third, a strong positive feedback mechanism is observed in high latitudinal regions. A warmer climate leads to less extensive and short-lasting snow and sea ice covers. This results in an increased warming due to a lowered albedo and therefore to a stronger absorption of shortwave radiation by the Earth's surface and ocean (Previdi, Smith & Polvani 2021). Finally, the moisture content on land is limited compared to oceans. Once all water is evaporated (water limitation), the heat cannot anymore be buffered by the latent heat flux which in the end leads to a strong sensible heat flux and increased temperatures over land (Byrne 2020, Fendt & Schlosser 2021, Sutton, Dong & Gregory 2007).

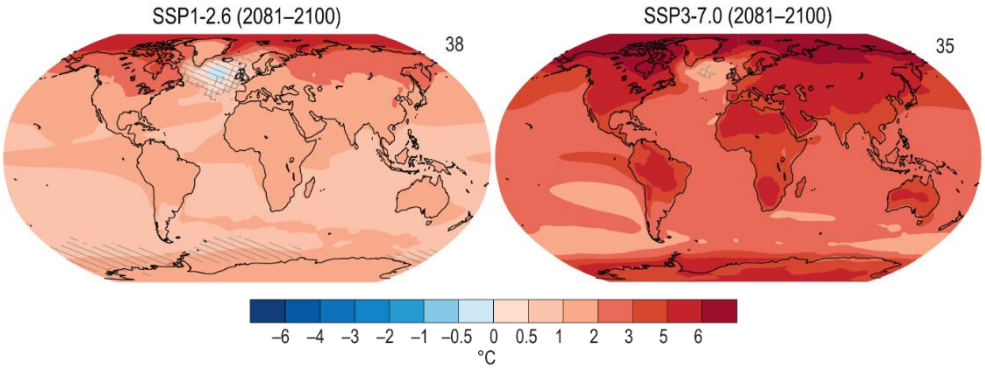

Figure 3: *Spatial distribution of the global annual mean temperature change relative to the period between 1995 and 2014 for the scenarios SSP1-2.6 and SSP3-7.0 (Lee et al. 2021).*

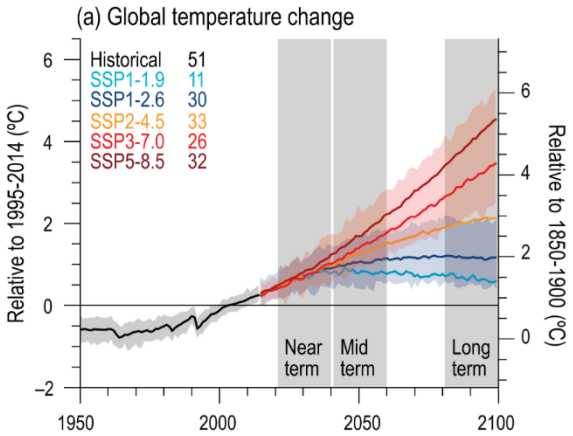

Figure 4: *Global average surface temperature change relative to the period between 1995 and 2014 (left axis) and the period between 1850 and 1900 (right axis) for different SSP scenarios (Lee et al. 2021).*

2.4 The Urban Heat Island effect

Cities almost all over the world experience significantly higher thermal conditions compared to their rural vicinities. This effect of locally increased temperatures in urbanized regions is called the Urban Heat Island effect (UHI effect). By definition, the UHI effect is the temperature difference between urban and rural landscapes in comparable macro-climatic conditions. In general, the phenomenon is stronger the larger and more compact a city is and gets increased with larger population sizes (Parlow, Vogt & Feigenwinter 2014, Burgstall 2019).

In the literature, one distinguishes between surface and atmospheric UHI effects (SUHI and UHI). Whereas the SUHI is generally determined with remote sensing techniques (e.g. satellites, airplanes, drones), the atmospheric UHI must be observed directly with in-situ measurements (e.g. simple thermometers) (Voogt & Oke 2003, Burgstall 2019, Parlow, Vogt & Feigenwinter 2014). Furthermore, some scientists introduced a third category, namely subsurface heat islands. Although this effect is much less discussed in the literature, it can induce important micro-climatic impacts. Especially in regions with widespread and deep permafrost layers or cities with shallow aquifers in their underground (Yow 2007). Even though the SUHI and UHI influence each other, for this master's thesis, the atmospheric UHI effect was considered since air temperatures are much more important than surface temperatures when investigating the impacts of climate change on human health. Moreover, this study is based on data of measuring stations in Basel and Zurich which permanently collect meteorological variables on-site like the air temperature, air humidity, wind speed, and global radiation. It is beneficial to have all meteorological data from the same location to get rid of potential data inaccuracies due to different measuring conditions at various places.

There are many reasons leading to the UHI effect. Specific characteristics of cities lead to altered thermal, aerodynamic, radiative, and moisture properties (Burgstall 2019). Highly urbanized areas have a high aerodynamic surface roughness. The regional wind field as well as local vertical and horizontal turbulences are altered. Additionally, the heat budget is completely different in urban compared to rural areas. The used construction materials in cities have specific physical and thermal properties which decisively change the radiation balance (Parlow, Vogt & Feigenwinter 2014). In the next sections, the most relevant causes of the UHI effect are shortly summarized.

One of the most important causes of the UHI effect is the high degree of sealing in combination with a lack of vegetation. Plants feature two beneficial properties to regulate and cool down local air temperatures. On the one hand, they provide extended shadow areas and thus reduce the incoming shortwave radiation. There is less energy reaching the ground which results in decreased air temperatures. On the other hand, they are able to reduce the air temperature through evapotranspiration. During the process of photosynthesis, water vapor transpires through the stomata. This chemical reaction needs energy which is being taken from the surrounding air. As a

result, vegetation is able to locally decrease the air temperature by both minimizing the sensible heat (blocking of shortwave radiation) as well as the latent heat flux (evapotranspiration of water) (Burgstall 2019, Burmeister, Büter & Trute 2019, Parlow, Vogt & Feigenwinter 2014). However, one has also to keep in mind that the process of water transpiration slightly increases the air humidity. This could potentially lead to a negative thermal comfort. Nevertheless, the cooling by far outweighs potential warming effects (Kühnle 2021).

Beside of sealed places and the lack of vegetation, buildings and other infrastructural facilities heavily affect the intensity of the UHI effect. The height, geometry, and density of house constructions could lead to altered air flows and extenuated wind systems. The surface roughness is different in cities compared to places dominated by vegetation. Furthermore, high buildings can block natural wind systems which leads to an increased accumulation of hot air in the inner districts of a city. The orientation of buildings and street canyons is an important factor hereby. Continuous rows of houses have different effects on altering air currents than perimeter block developments (Weber et al. 2018, Burgstall 2019, Parlow, Vogt & Feigenwinter 2014, Burmeister, Büter & Trute 2019). Almost as important as the orientation and geometry of buildings is the energy efficiency of their walls and roofs. Buildings with high insulation values and airtightness can effectively help to protect inhabitants from overheating. Cool indoor places are especially important for facilities with vulnerable people like for example hospitals or nursing homes. An additional positive effect of properly insulated buildings is that less energy is needed for heating or cooling. This has a direct effect on the produced anthropogenic heat and thus on the UHI effect. Furthermore, a decreased energy consumption is beneficial to mitigate the long term climate change (Dodman et al. 2022).

Unlike high and dense house constructions, water bodies often have beneficial impacts on local air flow patterns in urban places. Thanks to specific properties of water (high heat capacity, evaporation), rivers or lakes can lead to a natural ventilation effect. Refreshing air from the surrounding is pulled into the center of the city. Hot and polluted air cannot accumulate as easily as without the ventilation effect (Chen et al. 2014, Burmeister, Büter & Trute 2019). If larger water bodies are missing in a city or if the induced wind field is blocked by buildings, the UHI effect gets amplified.

Finally, the residents of cities produce heat themselves and thus further enhance the UHI effect. This so-called anthropogenic heat originates mainly from extensive traffic loads and industrial heat waste (Weber et al. 2018, Burgstall 2019, Burmeister, Büter & Trute 2019). Another important source of anthropogenic heat stems from air conditioners and heating installations. This results in a positive feedback effect. The hotter it gets in cities during the summer season, the more air conditioners are used. Consequently, the energy consumption increases which accelerates the global climate change. A negative feedback can be attributed to the winter or cities in high latitudes. A warmer climate results

in a reduced need of heating installations and this in turn is beneficial to reduce global warming (Lokoshchenko 2014).

In order to improve the understanding of the UHI effect in cities, the causes can be grouped into external and internal drivers. External drivers are for example the topography (e.g surrounding hills or depressions), altitude, geographic location of the city (latitude and longitude), or the distance to big open water bodies (e.g. lake, river, sea). Internal drivers are for example the anthropogenic heat production, geometry and orientation of buildings and street canyons, reflectance and thermal properties of surfaces, or vegetation density (Parlow, Vogt & Feigenwinter 2014).

The UHI effect is a very complex phenomenon. Not all of the above-mentioned causes are important for every urban place. Therefore, it is crucial to investigate the UHI effect for each city separately in order to get real information about the local thermal conditions. Manoli *et al.* (2019) for example could observe big differences in the intensity of the UHI effect between cities in humid and cities in arid regions. They observed a nonlinear increase in the urban-rural temperature difference with precipitation. There is a linear relationship for climate regimes where precipitation rates are lower than 1500 mm/year. Above this threshold, UHI are not in a linear relation with precipitation anymore. Manoli *et al.* (2019) stated the energy limitation in humid cities as the major reason for this nonlinearity. One result of this finding is that green spaces in tropical urban environments are not as effective to cool down cities as they are in arid regions. While the energy availability is the main limitation for evaporative cooling in humid cities, water scarcity mainly dampens evapotranspiration and thus latent heat flux in arid regions (Manoli et al. 2019).

The findings of Manoli *et al. (*2019) show that in order to gain a thorough understanding of specific UHI effects, one should not only consider the air temperature, but the entire energy balance and climate regime as well. This includes the net radiation (shortwave and longwave), the latent and sensible heat flux, the ground storage, the anthropogenic heat flux, and the precipitation rates. Nonetheless, air temperatures are a very good proxy and therefore oftentimes used as suitable simplification (Parlow, Vogt & Feigenwinter 2014).

Long-term observations of the UHI effect show clear diurnal cycles. Parlow, Vogt and Feigenwinter (2014) and Burgstall (2019) identified a peak temperature difference during the first half of the night, especially directly after sunset. A similar result was observed by Lokoshchenko (2014). He measured a maximal UHI effect in Moscow during late evening and early morning. Consequently, he observed a minimum during the day. Under specific circumstances, even a weak cooling effect in the middle of the day could be detected (daytime urban cool island effect) (Burgstall 2019, Lokoshchenko 2014, Theeuwes et al. 2015).

As mentioned in the previous sections, the UHI effect is a very local phenomenon. It is crucial to entirely understand the nature of the UHI effect in a city in order to devise suitable adaptation measures. They

should always be applied to local conditions to achieve an optimized cooling effect. Efficient adaptation measures will become crucial in the near future since climate change and global warming will be amplified in cities due to the effects of urban heat islands. Furthermore, heat stress becomes even more impactful in settlements due to the fact that many vulnerable people live in a considerably small area (heat exposure). Depending on the future emission pathway, researchers expect that 50% (RCP2.6) to 75% (RCP8.5) of the global human population could suffer under strong heat stress by the end of this century (Dodman et al. 2022).

2.5 Quantifying heat stress

The air temperature is a meteorological variable which can be measured very easily without the need of any complicated measuring stations nor the knowledge of complex analysis techniques. Using the air temperature as a proxy to estimate the impacts of heat waves on human health is therefore a common method used by various scientists (Morabito et al. 2012, Kovats & Hajat 2008). A simple linear regression between the air temperature and mortality rates for example delivers a first overview of the current state of relationship between these two variables. Changes of possible future mortality rates due to increased air temperatures can quickly be derived. Potential global warming can be transferred to mortality rates by using the previously generated correlation model.

However, to thoroughly understand the health impacts of climate change, in particular of an increased UHI effect, a much more extended analysis must be undertaken. Beside of the air temperature, supplementary meteorological variables such as the air humidity, wind speed, or radiation must be considered. There exist different approaches which make use of this additional information. Some heat stress indices are based on objective and subjective strains (empirical thermal indices). Others include physiological parameters like for example metabolic activities or clothing (Burgstall et al. 2019).

An example for an empirical thermal index is the physiological equivalent temperature (PET). This measure incorporates several different meteorological parameters (air temperature, air humidity, solar radiation, wind speed), but also includes thermo-physiological variables (e.g. clothing and physical activity) (Matzarakis & Amelung 2008). In fact, the coverage and thickness of clothing play a considerable role in the relationship between meteorological conditions and human health (Steadman 1994). Calculating PET can be very complicated since processes like the constriction or dilatation of peripheral blood vessels or the physiological sweat rate are needed and thus must be measured or estimated separately. This process is difficult and laborious. The skin temperature or skin wetness are good indicators to use, however, they are strong simplifications of the heat balance within a body and thus a major source of uncertainties (Matzarakis & Amelung 2008).

Instead of PET, the wet-bulb globe temperature is used in this master's thesis. WBGT is a heat index which takes the air temperature, air humidity, wind speed, and global radiation (incoming shortwave

radiation) into account. WBGT is a measure to estimate risks related to heat stress. Initially, this heat exposure index was developed during the 1950s by US military ergonomists to control heat risks for their soldiers during training camps (Budd 2008, Lemke & Kjellstrom 2012). Nowadays, it is commonly used in diverse civil applications to study the effect of increasing environmental heat exposure due to climate change on workers with physically demanding jobs, elderly people, or people with chronic diseases.

Clark (2018) published a study where he investigated the relationship between WBGT and the risk of cardiovascular-related deaths. He compared the results to air temperatures. The scientist found that WBGT clearly outperformed the air temperature in estimating the mortality rate. He got a similar result for estimating the risk of renal diseases. The measured relationship between the maximal WBGT and the relative risk of cardiovascular causes of death is pictured in figure 5.

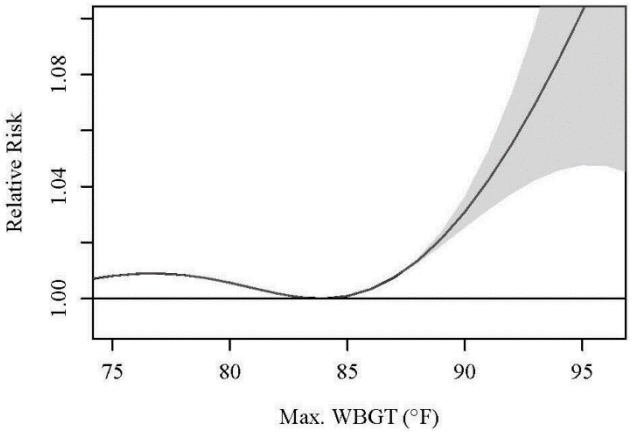

***Figure 5**: Relative risk of cardiovascular causes of death (y-axis) based on maximal WBGT (x-axis). Urban Piedmont, North Carolina (Clark 2018).*

WBGT is a meteorological parameter which, in contrast to PET, does not directly consider people's activity, internal thermoregulatory mechanisms, or clothing. Instead, the latter must be incorporated when defining individual-related threshold values for certain heat indicators (see chapter 4.3).

WBGT is a weighted temperature measure composing of three inputs (equation 1): The natural wet-bulb temperature (Tnwb, °C, measured with a thermometer wrapped in a wet wick), the black globe temperature (Tg, °C, measured with a thermometer inside a black globe), and the air temperature (Ta, °C) (Lemke & Kjellstrom 2012, Patel, Mullen & Santee 2013, Liljegren et al. 2008). The black globe temperature incorporates radiant heat, air temperature, and wind, whereas the natural wet-bulb temperature shows the amount of cooling by humidified air and wind (Heo, Bell & Lee 2019).

$$WBGT = 0.7 * Tnwb + 0.2 * Tg + 0.1 * Ta \quad (1)$$

To directly measure WBGT in the field, costly and maintenance-heavy sensors must be installed. Three different instruments are necessary: A natural wet-bulb thermometer to measure Tnwb, a globe thermometer for Tg, and a dry-bulb (air) thermometer for Ta (Bernard 1999). A regular recalibration of electronic monitors as well as replenishing of the wet-bulb thermometer's water reservoir need expertise and takes a lot of time (Patel, Mullen & Santee 2013). Therefore, various scientists developed

mathematical models in order to calculate WBGT using a few meteorological variables as input. Most of them are based on empirically derived formulas, developed by using regression models (Lemke & Kjellstrom 2012, Steadman 1994, Carter et al. 2020, Heo, Bell & Lee 2019, Ono & Tonouchi 2014, Bernard 1999). The theoretical background is the same for all approaches, however, the calculation steps as well as the incorporated weather data can differ, depending on how the physical models were deduced. For this master's thesis, three different approaches were evaluated. All of them need measurements of the air temperature, relative air humidity, wind speed, and global radiation as input variables. By assessing different approaches of various scientists, more robust heat indices can be calculated. Further information about the three approaches and their exact equations can be found in chapter 4.2 (Steadman 1994, Bernard 1999, Ono & Tonouchi 2014).

2.6 Decision Making under Deep Uncertainties

Deep uncertainty:

The climate on Earth is a highly complex system. There are many processes and phenomena which are not fully understood or even discovered yet. In 2002, United States Secretary of Defense Donald Rumsfeld once stated during a press conference:

> '…there are known knowns; …there are known unknowns; … But there are also unknown unknowns …'.

This statement can easily be applied to the climate system as there exist many processes which are still unknown and thus have to be discovered first (Rumsfeld 2021, Marchau et al. 2019a, p. 6). A lot of external factors, including positive and negative feedback loops, make the understanding of the climate and weather phenomena even more complicated. Finding the causes and their corresponding effects are heavily impeded in a very dynamic system (Stanton & Roelich 2021, Marchau et al. 2019a). In fact, the highest uncertainties in climate models can be attributed to internal climate variabilities and randomness, sometimes called 'climate noise' (Deser et al. 2012).

Predicting future states of the climate and estimating potential impacts on human health is an additional challenge. Not only the magnitude and speed of climate change are hard to predict, but also the order of social and health consequences. Decision-makers are faced with deep uncertainties and forced to find strategies to handle those reasonably and as broad-based as possible. Not exactly knowing the external context of the system, its boundaries, and the specific initial conditions are three major problems decision-makers must cope with (Marchau et al. 2019a).

Oftentimes, there are many stakeholders involved with different needs, interests, motivations, societal backgrounds, and financial resources. Decision-makers with various scientific backgrounds must work

together to find solutions that are suitable for as many occupants as possible (Stanton & Roelich 2021, Marchau et al. 2019a, Kwakkel & Haasnoot 2019). This becomes even more important for human-natural systems, like the relationship between climate change and human health. Schneider, Turner & Garriga (1998, p. 170) put it in an understandable and cogent nutshell:

> '… uncertainty is not purely of a technical or physical or biological character,
> but also social, cultural, and institutional in nature.'

To handle all uncertainties and unpredictable developments, the use of approaches for Decision Making under Deep Uncertainties are needed. In the following sections, some common practices to handle deep uncertainties are presented.

Exploratory Modeling and Dynamic Adaptive Policy Pathways:

Scientists of different fields developed specific practices to handle deep uncertainties to improve the forecasting of non-linear systems and accordingly to support the process of decision making. In order to be prepared as good as possible for uncertain events and corresponding impacts, the paradigms of 'prepare and adapt' and 'monitor and adapt' are followed. The monitoring part is important to always have an up-to-date state of the climate system and the connection to human health. The adaption part allows decision-makers to constantly adjust their strategies according to newly gained findings and unexpected changes in the system (Marchau et al. 2019a).

An important part of many DMDU approaches is a tool called Exploratory Modeling (EM). EM is a practice where a wide range of possible future states of the system under investigation are produced. Each model run is the result of a randomly chosen combination of external factors and policies. This technique of handling deep uncertainties allows decision-makers to gain insight into the behavior of a complex system under a bunch of different influencing factors (Ashraf Vaghefi et al. 2021, Kwakkel 2017, Moallemi et al. 2020, Marchau et al. 2019b, Marchau et al. 2019a).

Strongly connected to EM is Scenario Discovery (SD). In Scenario Discovery, an ensemble of model runs generated with an EM experiment is systematically analyzed in order to identify certain combinations of external factors and policies which are most responsible for a specific outcome (Kwakkel, Auping & Pruyt 2013, Ashraf Vaghefi et al. 2021). In the case of the climate system, this could be specific weather conditions leading to extreme events like for example heat waves, droughts, or heavy rainfall events.

The results of EM and SD can further be used as starting point for adaptive decision-making approaches like Dynamic Adaptive Policy Pathways (DAPP) or Robust Decision Making (RDM).

DAPP approaches are characterized by developing a series of actions over time, called pathways, and constantly adapting these pathways to the current state of knowledge. In order to achieve this, the ensemble of future scenarios generated during EM must be considered and accordingly, various

strategies to react to the vast number of outcomes have to be developed. The models and data which are used for DAPP are therefore used in an exploratory rather than a projective way. The basic idea behind this procedure is strongly aligned to the proverb 'All roads lead to Rome' (Haasnoot, Warren & Kwakkel 2019, p. 71, Haasnoot, van 't Klooster & van Alphen 2018, p. 274). There exist different procedures or routes which can achieve the intended goals. To develop an adaptive plan, short-term actions and long-term options are essential. All long-term options must be kept open as long as possible. New actions are activated only if remaining on the current path is no longer sufficient to reach the initial goal. Finding the right points in time for path changes is not straight forward. Oftentimes, a so-called metro map or decision tree is used to visualize the different pathways. Tipping points are pictured with nodes and denote the points in time when new decisions should be taken (Haasnoot, Warren & Kwakkel 2019, Haasnoot, van 't Klooster & van Alphen 2018, Ashraf Vaghefi et al. 2021, Lempert 2019, Lawrence & Haasnoot 2017). Usually, tipping points are defined based on specific thresholds a decision-maker sets in advance. In the case of UHI and human health, this could be a temperature or WBGT value, above which vulnerable people suffer under overheating or dehydration. Or it could be a certain number of extreme days or events per year. The goal of any decision-maker is to avoid reaching a tipping point because once a tipping point is reached, it is hard or even impossible to go back to a former state. The system could become unstable and thus difficult to predict the direction of prospective developments (Ashraf Vaghefi et al. 2021).

RDM is strongly linked to DAPP and therefore in many cases applied complementary. Based on the multiple future scenarios calculated with EM, the goal of RDM is to develop various strategies to deal with the most unfavorable scenarios. To achieve this, SD comes into play again. Decision-makers evaluate in an iterative process various alternative strategies and try to identify the most robust ones based on predefined robustness criteria. Robust strategies are mainly characterized by a high level of performance over and adaptability to a wide range of unexpected changes in the future. Since this always comes with trade-offs, finding the most appropriate strategies is not easy and therefore requires multiple iterations in the decision process. At the start, a bunch of different strategies is considered as appropriate. This initial selection is then constantly refined until the most robust strategies remain (Hall et al. 2012, Lempert 2019).

All of these theories and tools (EM, SD, DAPP, RDM) are not very useful if they are applied independently. In order to manage DMDU extensively, it always requires a combination of all.

3 Study areas

The main focus of this master's thesis lies on investigating the impacts of heat waves on human health in the city of Basel. The UHI effect as well as historic and future WBGT are deeply analyzed. To be able to compare the results from Basel to a second urban place and to gain a broader knowledge, future WBGT are also calculated for Zurich. Figure 6 shows an overview of the Alpine range including the locations of the two study sites. The climate in both cities is heavily affected by the surrounding topography (Vosges, Black Forest, Jura Mountains, Alps) as well as nearby water bodies (Rhine, Limmat, Sihl, Lake Zurich).

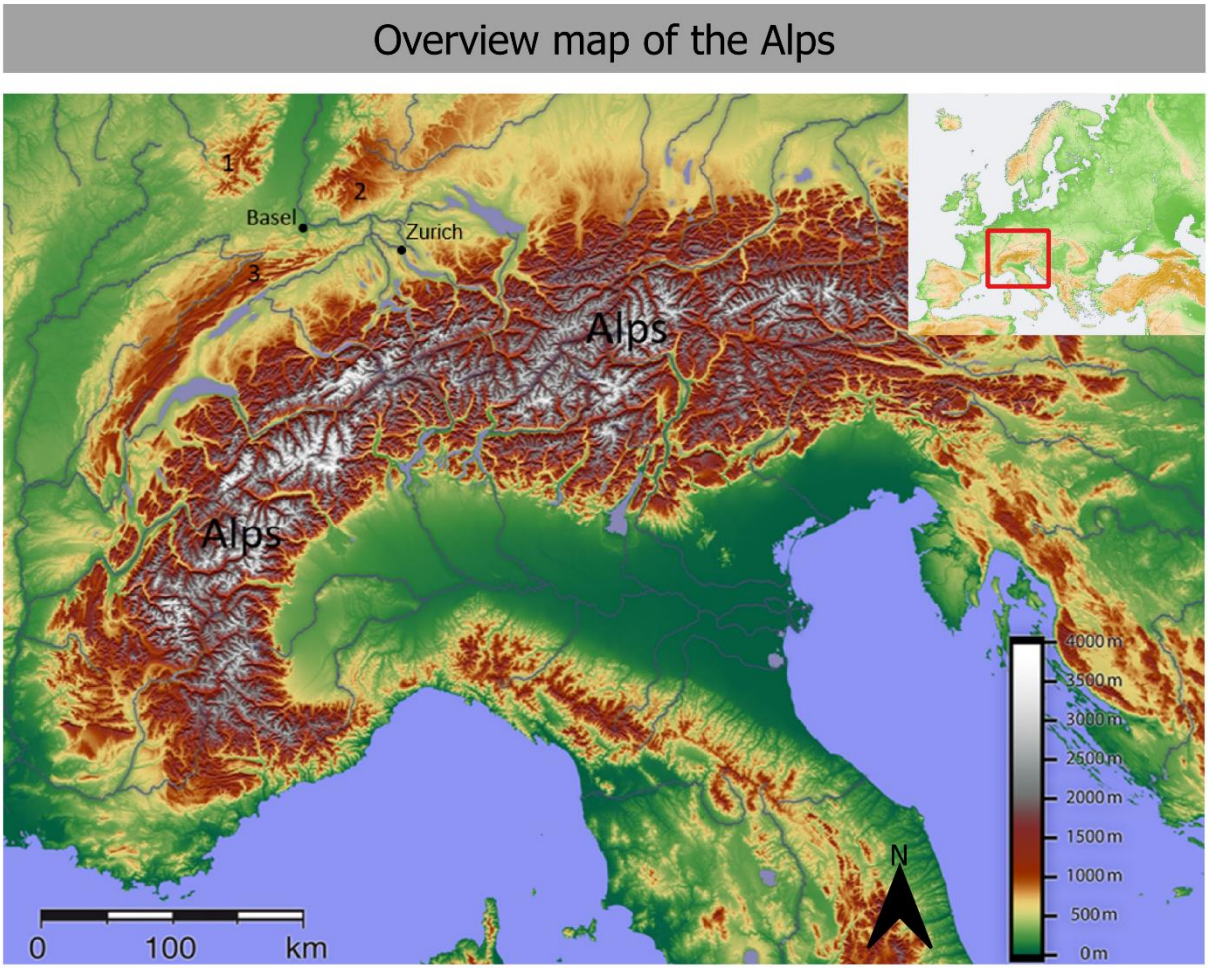

Figure 6: *Overview map of the Alpine range and Switzerland, showing Basel, Zurich, the Vosges (1), the Black Forest (2), the Jura Mountains (3), and the Alps (own figure, according to Wikipedia (2006)).*

Basel:

Basel is a half canton in Switzerland located in the northwestern part of the country. It acts as border region to the neighboring countries France and Germany. With a total area of about 37 km^2 and a population of slightly over 190'000, it is a rather densely populated region. Considering the whole metropolitan area which also includes other cities in Germany, France, and Switzerland, the

approximate total population is much higher. The city has an altitude range between 244 and 522 m a.s.l. However, the major part and the city center are below 300 m a.s.l. Basel is surrounded by small mountain ranges, namely the Vosges to the northwest in France (1), the Black Forest to the northeast in Germany (2), and the Jura Mountains to the southwest in Switzerland (3). The city is located in the southern part of the Rhine rift (figure 6) (Burmeister, Büter & Trute 2019, Wikipedia 2006, Wicki, Parlow & Feigenwinter 2018).

Basel is reckoned as one of the most dynamically active economic regions in Switzerland. During the last several years, a strong economic growth was measured. Over 190'000 employees (Swiss and abroad) are currently working in the city, many of them in the pharmaceutical industry. A second big economic sector is the cargo shipping industry. Basel is located at the Rhine knee and thus a very important place for cargo traffic and maritime trade (Kanton Basel-Stadt 2021a, Wikipedia 2021). Beside the importance of Basel as business and industrial location, tourism is a major sector as well. Many tourists visit Basel every year. Two of the most important events are the Art Basel and the Shrove Tuesday (Kanton Basel-Stadt 2021b).

Climate change could have a huge impact on the productivity of the city. Especially, increased temperatures could lead to a reduced labor productivity and thus to a lower economic output (Tuholske et al. 2021). Furthermore, heat waves in combination with droughts could pose a problem for the shipping industry (Basel-Stadt 2021a, Basel-Stadt 2011). Therefore, it is important to investigate future climate conditions in the city and to evaluate the impacts which rising temperatures could have on the local population and the economic sector.

Zurich:

With a population of over 400'000 inhabitants and an urbanized area of about 90 km^2, Zurich is the biggest city in Switzerland. Zurich is located at the northern end of Lake Zurich where the main outflow of the lake, the Limmat, converges with the Sihl. These three water bodies play an important role for the microclimate in the city. To the southwest of Zurich, a small hill range (Üetliberg) separates the urban areas from less populated regions. As the aforementioned water bodies, the hill range is evident for the microclimate as well, since they all generate a ventilation effect and thus vertically transport hot or cool air masses through the streets. Zurich has an altitude of about 400 m a.s.l., however, there is a big altitude range between different districts of the city. Combined with the temperature contrast between districts located on a north- and on a south-facing slope, considerably high thermal differences can be found.

As Basel, Zurich is an important business hub and tourist region of Switzerland. Over 450'000 employees are currently working in the city, whereby the banking industry is one of the most important sectors (Stadt-Zürich 2022).

3.1 Climate

The predominant climate in Basel and Zurich is a mixture between maritime and continental (Wikipedia 2022a). The mean air temperature in Basel is about 11.5° C, whereas in Zurich it is slightly lower with 9.6° C. During the winter seasons, mean air temperatures are about 2° C in Basel and 1.3° C in Zurich. During the summers, they are about 18° C in both cities. On average, one measures 52 summer days per year in Basel and 42 days in Zurich (T_{max} > 25° C). Hot days (T_{max} > 30° C) and tropical nights (T_{min} > 20° C) are possible, but they appear irregularly.

Precipitation occurs throughout the whole year with a maximum in late spring to early summer and a minimum in winter.

The relative air humidity is higher during the winter season than it is during summer. This annual pattern is due to the fact that cold air can hold less moisture. Consequently, the air is saturated much faster although the absolute water content is considerably lower in winter than in summer.

A closer look at the global radiation at the Earth surface reveals a maximum in summer and a minimum in winter. The reason is mainly due to an extensive and longer-lasting cloud coverage during the winter above the city which blocks shortwave radiation from hitting the ground.

Figures 7 and 8 below (Basel) and figures 51 and 52 in the appendix (Zurich) show a graphical overview of some important climatic variables for Basel and Zurich. The observations stem from weather stations of MeteoSwiss situated in Basel-Binningen (MeteoSwiss 2021, more information about the measuring station can be found in chapter 5) and Zurich-Fluntern (MeteoSwiss 2022). The figures show the annual course of the temperature (daily mean, daily max, and daily min), the relative air humidity (figure 7 and figure 51), the global radiation, and the wind speed (figure 8 and figure 52).

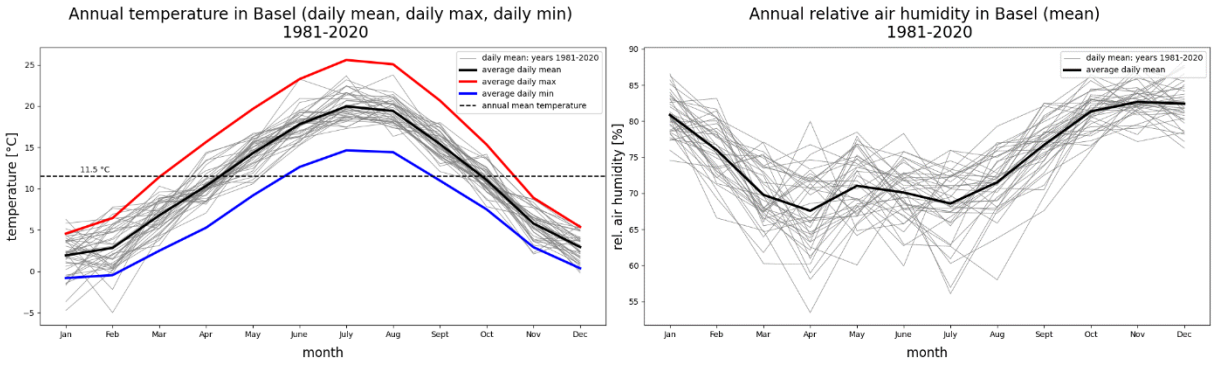

Figure 7: *Left: Annual temperature in Basel-Binningen. Daily means of each year (grey), averaged daily mean (black), averaged daily max (red), and averaged daily min (blue). Annual mean temperature (dashed line). Right: Annual relative air humidity in Basel-Binningen. Daily means of each year (grey) and averaged daily mean (black) (own figure, based on data from MeteoSwiss (2018) and (2020)).*

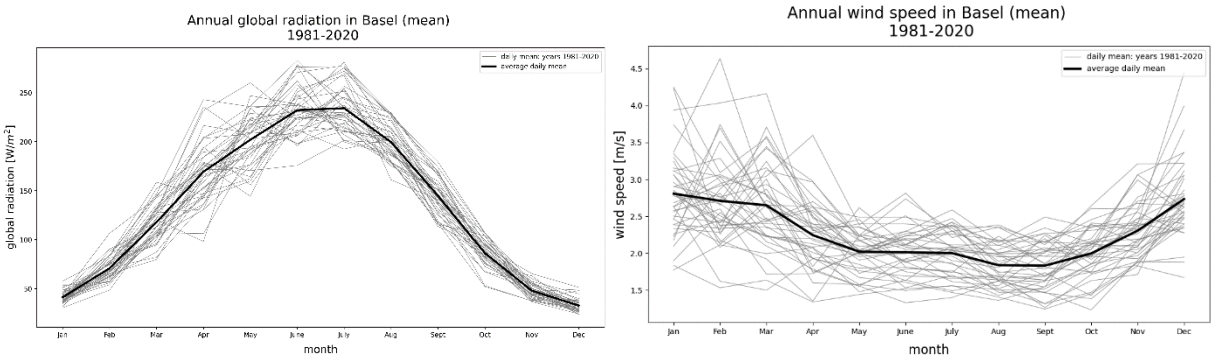

Figure 8: *Left: Annual global radiation in Basel-Binningen. Daily means of each year (grey) and averaged daily mean (black). Right: Annual wind speed in Basel-Binningen. Daily means of each year (grey) and averaged daily mean (black) (own figure, based on data from MeteoSwiss (2018) and (2020)).*

4 Methods

4.1 The Exploratory Modeling and Analysis Workbench

DMDU is an essential theory of this study. Exploratory Modeling (EM) is a common technique to deal with uncertainties within a human-natural system. The results of EM are the basis for many adaptive and robust decision-making procedures. With the help of EM, the future climate can be explored in a what-if approach. Conditions under which WBGT or other heat indicators are below/above a certain threshold in the future can be identified (Kwakkel & Haasnoot 2019, Ashraf Vaghefi et al. 2021).

For this study, the Exploratory Modeling and Analysis Workbench (EMA Workbench) was applied. This EM tool was developed by Kwakkel (2018). The script and all its dependencies are open-source and can be downloaded from GitHub (https://github.com/quaquel/EMAworkbench). The programming language of the program is Python. The code framework which makes use of the EMA Workbench and includes the climate model, the data preprocessing, and the visualizations was initially written by Dr. Seyed Saeid Ashraf Vaghefi for another climate study. For the case of this master's thesis, necessary customizations and additions were realized (e.g. implementing the WBGT equations, setting the thresholds for extreme days, creating appropriate visualizations).

The EMA Workbench makes use of the so-called XLRM framework. This framework treats the climate system as if it was a simple mathematical function. As input, it takes external factors (X, e.g. RCPs, climate models) and policy leavers (L, e.g. thresholds and adaptation measures). The performance metrics (M) are the model outputs (Kwakkel 2017, Ashraf Vaghefi et al. 2021). A schematic overview of the XLRM framework is illustrated in figure 9.

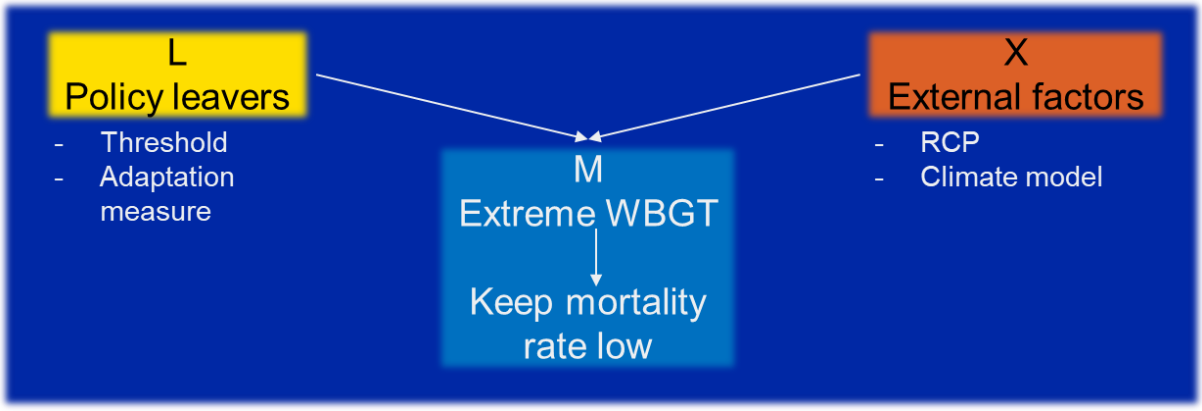

Figure 9: *Schematic of the XLRM framework of the EMA workbench (own figure, according to Kwakkel (2017)).*

In order to get as robust outcomes as possible, 4080 future projections (scenarios) were executed for each individual experiment (136 different climate realizations * 30 different policy leavers). During each experiment, one RCP scenario (either RCP2.6, RCP4.5, or RCP8.5 and slightly different realizations thereof (climate models)) and one WBGT threshold (out of a predefined threshold range, see chapter

4.3) were randomly chosen to generate one single future projection. All 4080 scenarios together delivered a robust picture of possible future states of the climate in Basel (or Zurich). Both, the raw WBGT values and different heat indicators (extreme day, extreme event, length of extreme event) were analyzed afterwards. Various visualizations and statistical evaluations were used to compare the different future projections and to develop appropriate adaptation strategies.

4.2 Calculating wet-bulb globe temperatures

This chapter gives an understanding of three different ways to calculate WBGT. All three approaches are based on the four basic meteorological variables air temperature, relative air humidity, wind speed, and extra radiation. The benefit of investigating multiple approaches is to gain a broader and more robust picture of potential WBGT at a specific location. Depending on the calculated values, the most appropriate approach for Basel and Zurich was chosen to perform the EMA Workbench.
In the following sections, the equations of the three investigated approaches are presented in order to give some background information about the empirical derivation and to be able to reproduce the presented results.

(1) WBGT by Steadman (1994):

The first approach was developed by Steadman (1994) and incorporates the air temperature, vapor pressure, wind speed, and radiation:

$$WBGT = Ta + 0.348 * e - 0.7 * ws + 0.7 * \frac{Q}{ws + 10} - 4.25 \quad (2)$$

where e is the vapor pressure (hPa), ws is the wind speed (m/s), and Q is the net radiation (w/m^2).
The vapor pressure can be calculated with the following equation:

$$e = \frac{rh}{100} * 6.105 * e^{17.27 * \frac{Ta}{237.7 + Ta}} \quad (3)$$

where rh is the relative humidity (%).

(2) WBGT by Bernard (1999):

This approach was initially developed by Bernard (1999) to predict workplace WBGT in an aluminum smelter by an empirical model which only needs ambient conditions of outside the faculty (Bernard 1999). For further information about another application of Bernard's model, the paper of Carter *et al.* (2020) provides an illustrative example. They applied the model to estimate WBGT for a heat stress study in Central Alabama. Their goal was to find out, how good the model of Bernard (1999) performs against direct measurements of Tg and Tnwb by using a specific heat stress tracker.

Bernard's equations are as follows:

If Tg – Ta < 4:

$$Tnwb = Ta - C1(Ta - Tpwb) \quad (4)$$

where C1 is

$$C1 = 0.85\ for\ ws < 0.03\ \left(\frac{m}{s}\right)$$
$$C1 = 1.0\ for\ ws > 0.3\ \left(\frac{m}{s}\right)$$
$$C1 = 0.96 + 0.069 * log10(ws)\ for\ 0.03\ \leq ws \leq 3.0\ \left(\frac{m}{s}\right)$$

If Tg – Ta ≥ 4:

$$Tnwb = Tpwb + 0.25 * (Tg - Ta) + C2 \quad (5)$$

where C2 is

$$C2 = 1.1\ for\ ws < 0.1\ \left(\frac{m}{s}\right)$$
$$C2 = -0.1\ for\ ws > 1.0\ \left(\frac{m}{s}\right)$$
$$C2 = \frac{0.1}{ws^{1.1}} - 0.2\ for\ 0.1\ \leq ws \leq 1.0\ \left(\frac{m}{s}\right)$$

The psychrometric wet-bulb temperature (Tpwb, °C) is estimated with the following equations:

$$Tpwb = 0.376 + 5.79 * e + (0.388 - 0.0465 * e) * Ta \quad (6)$$

and

$$e = \frac{rh}{100} * 0.6107 * e^{\frac{17.27 * Ta}{Ta + 237.3}} \quad (7)$$

where e is the vapor pressure (kPa).

Tg is estimated with the following equation:

$$Tg = 0.009624 * Q + 1.102 * Ta - 0.00404 * rh - 2.2776 \quad (8)$$

The approach of Bernard (1999) suggests two different equations to calculate Tnwb, depending on the magnitude of the difference between Tg and Ta. The scientist recommends to consider the effect of radiant heat (Tg) only if the difference between Tg and Ta is at least 4° C. Otherwise, Tg can be neglected to calculate Tnwb.

(3) WBGT by Ono and Tonouchi (2014):

Ono and Tonouchi's model was applied by Heo, Bell and Lee (2019) to estimate WBGT for a heat stress study in South Korea. They compared different thermal comfort indices (air temperature, heat index (HI), and WBGT) and examined which of those is the best one to study the impact of heat waves on human health.

Ono and Tonouchi's equation is as follows:

$$WBGT = 0.734 * Ta + 0.0374 * rh + 0.00292 * Ta * rh + 7.619 * Q - 4.557 * Q^2 - 0.0572 * ws - 4.064 \quad (9)$$

The presented approaches of Steadman (1994), Bernard (1999), and Ono and Tonouchi (2014) are three amongst many others. Some of them are more straight forward to implement, whereas others are fairly complicated and rely on expert knowledge. There are also minor differences between the required input variables. A detailed collection of various WBGT approaches is collated in the paper Lemke and Kjellstrom (2012).

After bringing together all the needed formulas and required data, the equations of the three chosen approaches were implemented in the climate model section of the EMA Workbench. The program reads in the input data and calculates various time series of WBGT for either the observed or the simulated period.

4.3 Defining thresholds for extreme days/events

Defining a threshold for extreme events is not straight forward. Various aspects must be considered. There is not one single threshold which holds for every human or every application. Thresholds always depend on specific circumstances and therefore have to be adapted correspondingly.

Critical values of WBGT can be defined for different age groups, classes of people (e.g. elderly people, small children, workers, sportspersons), and for different classes of metabolic rates (e.g. resting, low, moderate, heavy, very heavy workloads). Or they can be fixed for distinct time periods during which

persons are exposed to heat stress. The grade of acclimatization and the individual clothing are important as well (Casanueva et al. 2020, Jacklitsch et al. 2016). The grade of acclimatization and thus the subjective vulnerability to heat is different for people living in high latitudinal regions compared to people living in the tropics or subtropics. Furthermore, it can fluctuate over the course of one year meaning that after a cold winter, humans are oftentimes more sensitive to high temperatures compared to the time in late summer and autumn (McGregor et al. 2015, Tuholske et al. 2021, Ragettli et al. 2017, Ragettli et al. 2019, Kovats & Hajat 2008).

Normally, the thresholds are determined by looking at mortality data. These data are collected regularly and standardized and thus comparatively easily accessible. For more in-depth studies, heat-budget models are considered instead to estimate the thermal stress of a body (McGregor et al. 2015). Various scientists generated threshold tables in order to quantitatively assess the impacts of heat on human health. These tables were used as basis to develop Heat-Health Warning Systems (HHWS). Table 3 shows an example of possible threshold values for heat exposures of outdoor workers recommended by the World Meteorological Organization (WMO) and the World Health Organization (WHO) (McGregor et al. 2015).

***Table 3**: Threshold values for extreme events recommended by* McGregor *et al.* (2015*). WBGT values in ° C indicate thresholds for outdoor workers above which heat stress could lead to a reduction in labor productivity or to health problems. The table is split into four different work/rest regimes (rows) and three different workloads (columns)* (adapted from OSHA (2017)).

Work/rest regime	Light	Moderate	Heavy
100% work, 0% rest, each hour	30.0° C	26.7° C	25° C
75% work, 25% rest, each hour	30.6° C	28.0° C	25.9° C
50% work, 50% rest, each hour	31.4° C	29.4° C	27.9° C
25% work, 75% rest, each hour	32.2° C	31.1° C	30.0° C

For the case study of this master's thesis, three distinct threshold ranges were chosen. A lower one (26° C to 30° C) which represents the case of heavy outdoor workers (100% physical work) and very vulnerable people. An intermediate one (28° C to 32° C) which represents the case of moderate outdoor workers (25-50% physical work) and younger people or humans which are better acclimatized to heat. And an extreme one (32° C to 35° C) which is meant for people coming from very hot climatic regions and healthy young people.

These ranges were chosen in a way that they roughly cover the classification shown in table 3. The chosen threshold ranges were implemented in the EMA Workbench as a policy leaver.

The EMA workbench randomly selected one threshold within the defined range during every model run. As a result, various different thresholds were defined (but always out of the set range). This

procedure makes the model outcomes more robust and minimizes the uncertainties compared to an approach which only considers one single threshold for all model runs.
A second advantage of this approach is that it is possible to estimate the relative importance of the chosen WBGT threshold on the outcomes by conducting a sensitivity analysis (feature scoring).

4.4 Sensitivity analysis of threshold range and external factors (feature scoring)

A sensitivity analysis was executed in order to evaluate the importance of certain factors on the heat indicators. The goal was to figure out the effect of the choice of a WBGT threshold on the projected number of extreme days or a specific climate scenario on the outcome of the future simulations. The results of a feature scoring delivered an understanding of the relevance of policy leavers (threshold range) and future scenarios (RCP, climate model).

4.5 Effects of adaptation measures on heat indicators

The intention of this part of the study is to investigate the sensitivity of WBGT and consequently of heat indicators to changes in the air temperature, air humidity, global radiation, or wind speed. Based on information from the literature, the input data sets were changed accordingly in order to mimic potential climatic effects of certain adaptation measures. For example, a reduction of global radiation can simulate the effect of planting trees or installing other sun shields (shadowing effect). Decreased air temperatures by a certain amount can imitate the effect of evaporative cooling of vegetation or water bodies. Altered wind speed data can deliver information about the ventilation effect in the city (urban geometry, water bodies).
Five different scenarios were executed (reduced global radiation, three scenarios of decreased air temperatures, increased wind speed). The results were compared to normal conditions (data without simulated adaptation effects). This evaluation delivered a rough estimation of the effectiveness of certain adaption measures.
Special attention in the sensitivity analysis was put on the effect of wind and urban ventilation. In a separate simulation, the modelled wind speeds were reduced by 3 m/s if the value is greater than 3 m/s or set to 0 m/s if the values are smaller or equal than 3 m/s. The goal was to investigate the thermal effects in the city in the case when no explicit measures are being taken to enhance the aerodynamic situation (e.g. air flow barriers, no open water bodies, no vegetation, wrong orientation of street canyons). The outcome of this scenario was then compared to normal conditions and conditions with a slightly enhanced ventilation effect.

4.6 Difference from the measuring station to the hottest places in the city

Due to the elevated locations and environmental vicinity of the measuring stations, it is possible that the measured and simulated data do not perfectly reflect the real thermal conditions of the sites in the city centers (see chapter 5). To handle this issue, an additional EMA Workbench run was conducted for Basel and Zurich where the calculated WBGT values were manually adjusted to potential urban heat conditions. Daily WBGT were not modified, if the value was below 20° C. Values between 20° C and 25° C were increased by 1° C, values between 25° C and 30° C by 3° C, and values higher than 30° C by 5° C. This approach imitates potentially increased urban heat conditions which cannot be measured with the used measuring stations.

4.7 Metro map and feasibility-effectiveness diagram

The intention of this part of the study was to generate three simple DAPP plans (RCP2.6, RCP4.5, RCP8.5) for the time until 2100. As starting point for each map, four main adaptation options were considered, namely generating green spaces (e.g. trees, green roofs/facades), realizing blue spaces (e.g. water bodies, porous surfaces, fountains), adapting the urban geometry (e.g. shape of buildings or orientation of buildings and street canyons), and increasing the surface albedo (bright surfaces/facades). Using the outcomes of the EMA Workbench, the results of the sensitivity analysis as well as information from other studies, different pathways were developed. The timing of adaptation tipping points is mainly based on qualitative estimations under consideration of the three different future scenarios RCP2.6, RCP4.5, and RCP8.5.

The metro maps were generated using a specific software. The 'Pathways Generator' application is available from https://publicwiki.deltares.nl/display/AP/Pathways+Generator (25.08.2022) and can be used free of charge on any Windows computer. No additional soft- or hardware was required.

In a second step, a feasibility-effectiveness diagram of the discussed adaptation measures was generated. This illustration gives a schematic overview of the effectiveness of each measure in terms of reducing heat stress and the expected costs in terms of money, time, and feasibility. The effectiveness of each adaptation measure is based on the outcomes of the sensitivity analysis as well as on results from other studies. Based on the classification of the adaptation measures in the feasibility-effectiveness diagram, the most optimal paths of the metro map could be determined.

5 Data

5.1 Observations (1981-2020)

The input data used for this master's thesis stem from meteorological measuring stations maintained by the Federal Office of Meteorology and Climatology (MeteoSwiss). The station for the study in Basel is located in Basel-Binningen (figure 10). Its altitude is 316 m a.s.l. and thus a few meters higher than the center of the city (about 252 m a.s.l. (map.geo.admin.ch)) and the Rhine (about 245 m a.s.l. (map.geo.admin.ch)). The station is situated between a small grove to the north and some agricultural fields to the south. The measuring devices are on a small meadow between the observatory Basel and some garden plots. See figure 11 for an overview of the measuring site.

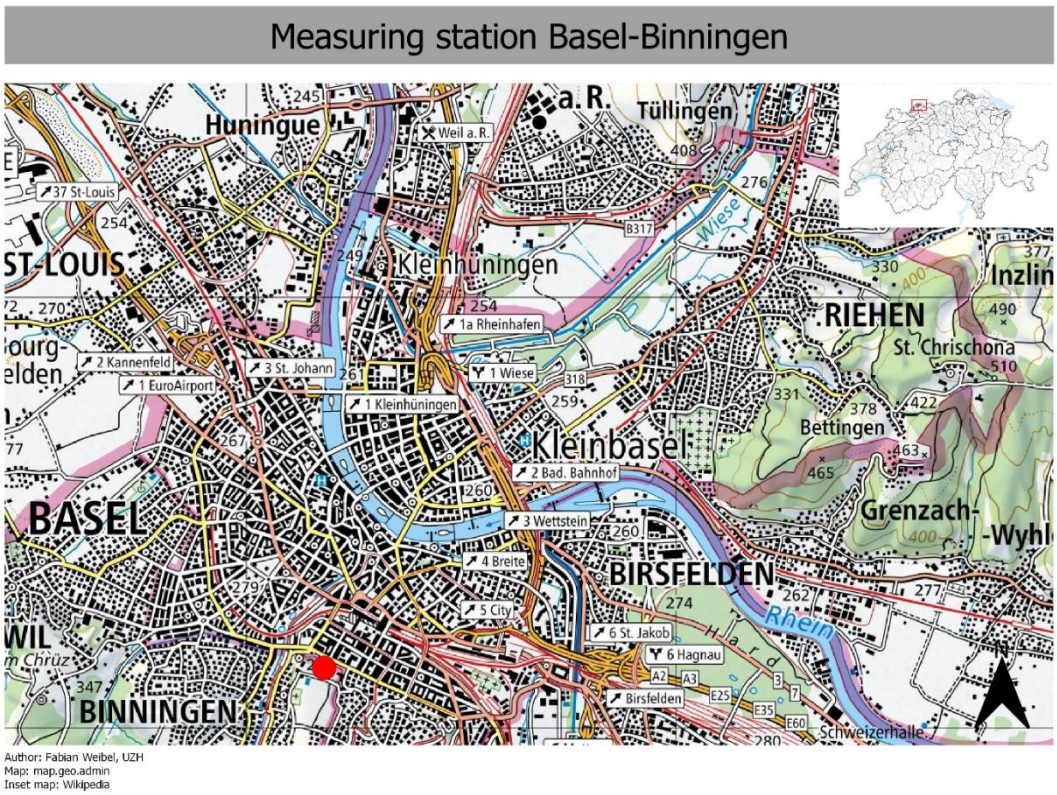

Figure 10: *Location of the MeteoSwiss measuring station in Basel-Binningen (red dot), 316 m a.s.l., 47.541142/7.583525 (map.geo.admin.ch, created with QGIS Desktop).*

Figure 11: *Station photo of the MeteoSwiss station in Basel-Binningen (own image).*

The measuring station for the study in Zurich is located in Zurich-Fluntern in the eastern part of the city (figure 12). It is slightly elevated to the main city and lies on a southwest facing slope at an altitude of 556 m a.s.l.

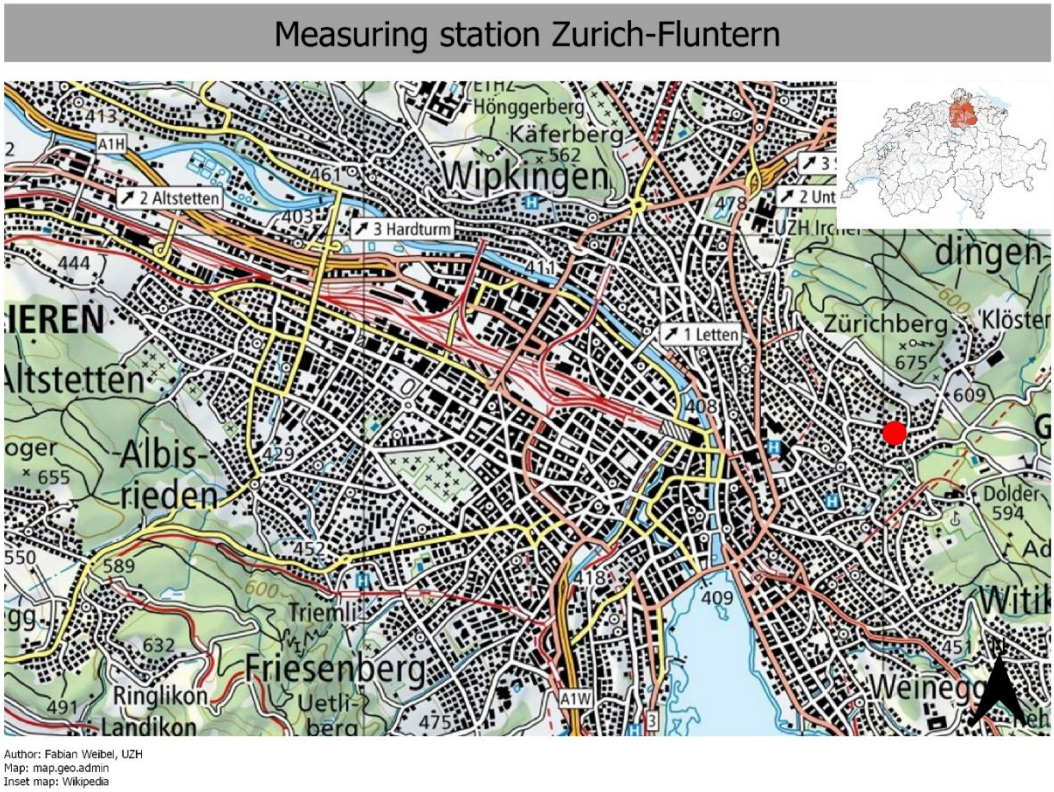

Figure 12: *Location of the MeteoSwiss measuring station in Zurich-Fluntern (red dot), 556 m a.s.l., 47.377925/8.565742 (map.geo.admin.ch, created with QGIS Desktop).*

The elevated locations and environmental vicinity of both stations could lead to improved thermal conditions compared to some spots in the city centers. This certainly has to be considered when analyzing the results later on.

Both measuring stations are part of a countrywide network of evenly distributed weather stations, developed and maintained by MeteoSwiss. The so-called SwissMetNet was initialized in 2003 in Aigle and since then constantly developed and expanded. It now consists of about 160 stations. The network distribution follows the complex topography of Switzerland to optimally represent the different regional climates of the country. The overall goal of SwissMetNet is to improve the meteorological forecasting and climate observation of the Alpine region in general and of Switzerland in particular.

Each station of this network contains state-of-the-art measuring technologies. The measurement equipment and data processing are standardized across all stations which also includes several quality checks. This simplifies the comparison of the data and makes the analysis more robust against inconsistencies.

The measuring stations in Basel-Binningen and Zurich-Fluntern compose several different sensors. They contain a wind mast (10 m above the ground), a monitoring bridge (2 m above the ground), a

precipitation gauge, and a radioactivity sensor. Attached to the monitoring bridge are air temperature, air humidity, and radiation sensors. Each sensor automatically measures every ten minutes its respective meteorological variable and immediately transmits it to a MeteoSwiss database (MeteoSwiss 2020, MeteoSwiss 2018).

The important meteorological variables for this study are the daily air temperature (mean, maximum, minimum), the daily mean relative air humidity, the daily mean global radiation, and the daily mean wind speed. The air temperature, the relative air humidity, and the global radiation are constantly measured 2 m above the ground, the wind speed although is measured 12 m above the ground (MeteoSwiss 2020, MeteoSwiss 2018). The global radiation is the combination of the direct solar radiation, the reflected radiation at the surface, and the diffuse radiation which was scattered in the atmosphere by atoms, molecules, water droplets, and other larger particles floating in the air (Gebhardt et al. 2016).

The time frame for the historic period of this study is 30 years and covers the years 1981 to 2020.

A graphical summary of the input data for Basel can be found in chapter 3.1. Similar graphics for Zurich are in the appendix.

5.2 Simulations (1981-2099)

As for the historic data, the simulated datasets for the future predictions also include the four meteorological variables air temperature (daily mean, maximum, minimum), relative air humidity (daily mean), global radiation (daily mean), and wind speed (daily mean). However, the values are not real observations, but projections based on the Climate Scenarios for Switzerland 2018 (CH2018). MeteoSwiss provides simulations for several SwissMetNet stations for the time period between 1981 and 2099. An ensemble of GCM and RCM was used by MeteoSwiss to capture as many uncertainties due to complex physical processes within the climate system as possible. To get localized projections for specific stations in Switzerland, they used an ensemble of RCM and statistical downscaling techniques (quantile mapping → matching the distribution of observed and simulated climate variables). All simulations were projected for three different emission scenarios (RCP2.6, RCP4.5, RCP8.5) For each of these three emission scenarios, multiple variations of data sets (8 variations/climate models for RCP2.6, 17 for RCP4.5, 22 for RCP8.5) with slightly changed values were generated. This variety of future data sets is necessary to capture uncertainties of socio-economic dynamics and arising from difficulties in estimating the impacts of climate change mitigation measures (CH2018 2018, Kotlarski & Rajczak 2018). Further information about RCPs and emission scenarios are summarized in chapter 2.3.

The investigated time period in this study for the simulations ranges from 1981 to 2099.

6 Results

6.1 The urban heat island effect in Basel

The first part of the results section presents the UHI effect in Basel. After a short description of the temporal variations, emphasis is put on the spatial variabilities. The goal is to show how hot and cool districts are distributed in the city and what their building characteristics and vegetation covers are. After looking on the current thermal situation in the city, a comparison to a projected future state is presented (2030).

In summary, it can be stated that both large spatial differences within the urban area and an inhomogeneous temporal course, throughout the year as well as a single day, could be observed. This made analyzing the UHI effect and finding suitable adaptation measures more complex and sophisticated.

6.1.1 Temporal variation

Parlow, Vogt and Feigenwinter (2014) found that the daily mean UHI effect is the strongest during spring and early summer with mean values of about 1.3° C. The weakest effect is during winter with mean values of about 0.7° C. Regarding the diurnal cycle, they measured a maximal effect at midnight and a minimum at midday. The daily temporal fluctuation does not exhibit a perfectly sinusoidal curve. The urban-rural temperature difference rapidly increases after sunset until the peak around midnight. During the morning hours, the difference decreases constantly until midday. The UHI effect is relatively stable throughout the afternoon. The temperature difference ranges from around -0.5 to 1.8° C during the day to about 2.8 to 4.3° C during the night (figure 13) (Parlow, Vogt & Feigenwinter 2014).

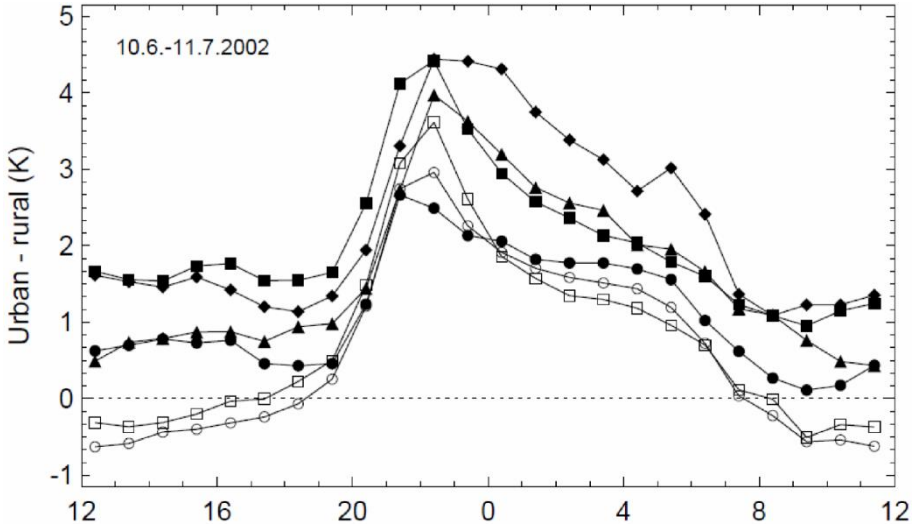

Figure 13: *Mean diurnal courses of the UHI effect in Basel. Two urban stations compared to three rural stations. The x-axis ranges from midday (12) to midday (12) (Parlow, Vogt & Feigenwinter 2014).*

6.1.2 Spatial variation

Investigations of the spatial distribution of the UHI effect in Basel exhibit a very heterogeneous pattern. There are districts which are considerably more affected by high urban temperatures compared to others. Figure 17 shows the measured UHI effect in Basel at four o'clock in the morning (Basel-Stadt 2021b). The following observations are based on the data pictured in figure 17.

In general, a stronger UHI effect closer to the city center as well as along the streets can be measured. With an increasing distance to the center, especially in the more open outer urban districts (e.g. Riehen), the effect is getting weaker. The temperature field is especially heterogeneous within the built-up areas due to large differences in the geometry and orientation of buildings and street canyons (Burmeister, Büter & Trute 2019). The settlement structure (density of developments and land cover classes) strongly influences the emittance of radiation and thus the possibility of hot or cold air to circulate through and escape out of the city (Rahuel et al. 2021). However, regardless of the settlement structure, the UHI effect is exceptionally pronounced in all urban districts during hot and humid nights. The most uncomfortable weather constellation for an enhanced UHI effect occurs in the summer during southwest meteorological conditions (Basel-Stadt 2011).

Hot spots:

The strongest UHI effect in Basel can be measured in the very center (old towns Grossbasel and Kleinbasel), near the railway stations (Basel SBB and Basel Badischer Bahnhof), at the exhibition site, and around the industrial parks of Novartis and Roche. At these places, the vegetation ratio is especially low and the density of tall buildings exceedingly high. Even though high buildings deliver extensive shady areas, the lack of vegetation and the interruption of fresh air currents predominate the local temperature conditions.

Figure 14: *Enclosed court at the exhibition site without vegetation (own image).*

Figure 15: *The lack of vegetation in Kleinbasel leads to an increased UHI effect (own image).*

Regarding the housing estates in Basel, there are mainly three districts which have a distinctively increased UHI effect. Gundeldingen, Dreispitz, and Gotthelf suffer under high temperatures due to their specific block developments. As high buildings in the industrial parks, block developments exhibit a very bad air circulation capability. Especially during hot summer days, air is trapped in the inner courtyards, heats up, and cannot be exchanged with fresh and cool air during the night.

Figure 16: *Confining border of a house front (block development) without sufficient vegetation in Gundeldingen (own image).*

Cool spots:

The coolest districts in Basel can be found in or near green parks (Zoo Basel, Kannenfeldpark, and Schützenmattpark), and along water streams (Rhine, Wiese, and Birs). However, the cool spots along the river are very local. Cool air is not able to penetrate into the city to cool down nearby districts. The increased warming effect of water itself as represented in figure 17 is due to the fact that the UHI effect was measured at four o'clock in the morning. Water, with its high heat capacity, stays relatively warm throughout the night until the morning hours compared to other surfaces. During the day and especially in the late afternoon, when the air temperatures rise to their maximum, however, the cooling effect of water becomes more relevant.

Bruderholz and Gellert are two housing estates which are characterized by low air temperatures compared to other housing estates in the city. The main reason for this is the row development of these areas. Unlike block developments, row developments are not as dense and enclosed from the vicinity which is beneficial for a continuous fresh air supply. Furthermore, Bruderholz and Gellert have a considerably high vegetation ratio. A high vegetation ratio in combination with an open settlement structure are beneficial to mitigate the UHI effect in cities.

Riehen in the northeastern part of the city is generally less affected by a strong UHI effect. The forested hills to the southeast are effective cool air production areas which strongly influence the climatic conditions of the surrounding urban quarters (Burmeister, Büter & Trute 2019, Rahuel et al. 2021,

Basel-Stadt 2021b, Wicki, Parlow & Feigenwinter 2018). Cool air from the forests on the top of the hills flows downhill and cools down the surrounding settlements. Compared to main Basel, Riehen has also a much lower sealing ratio and a lot of vegetation along the streets and between the houses.

Vulnerable facilities:

The spatial pattern of the UHI effect in Basel is not very meaningful if the occupants living in the city are not considered. Some of the aforementioned very hot districts do not pose a huge problem for human health if the population density is considerably low or vulnerable people are not directly affected. On the other hand, a weak UHI effect can already be problematic if sensitive facilities, like health care facilities, nursing homes, hospitals, kindergarten, or schools are affected (Rahuel et al. 2021).

In addition to the spatial distribution of the UHI effect, figures 17 and 18 do also show the location of any nursing home and hospital in Basel. There are noteworthy differences in the thermal situation amongst the nursing homes as well as hospitals in the city. Quite a few nursing homes are located in the hot center of Kleinbasel near the exhibition site. Others are situated near the railway station Basel SBB and thus probably also suffer under hot summer conditions. In contrast to these places, there are health care facilities which are at very comfortable locations regarding the thermal exposure. Especially, locations at the edge of the town and near bigger green parks are very suitable for hospitals and nursing homes. Not only due to the favorable thermal conditions, but also due to a quick accessibility to nearby recreation areas.

Future UHI effect:

Figure 18 includes a map where the differences between the current and 2030 UHI effect are shown. One expects a more or less universal increase of about 0.01-1° C across the city. There are some smaller districts which could experience a slight cooling and others which could warm up stronger than 1° C. However, these changes could potentially originate from model uncertainties or other invariabilities and therefore must be interpreted with caution. Since the future UHI effect in Basel is not only dependent on the expected large-scale climatic conditions, but also on the planned urban developments (growing of the city, implementation of adaptation measures), it is quite difficult to determine small-scale changes for future years.

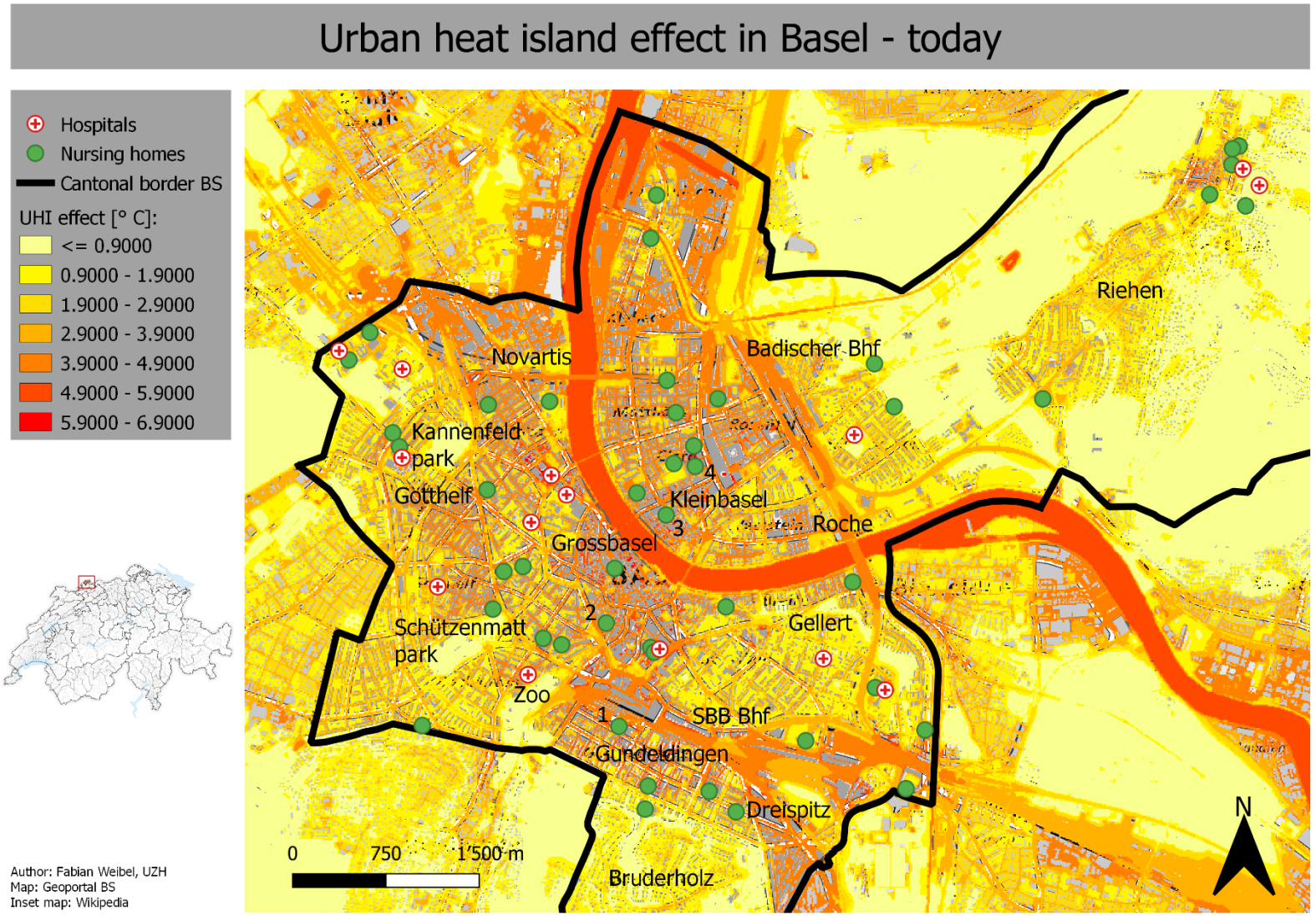

Figure 17: *Current UHI effect in Basel at 4am in ° C. Map includes nursing homes (green dots) and hospitals (red crosses). 1 → Residenz Südpark, 2 → irides AG, 3 → zum Lamm, 4 → Gustav Benz Haus (own figure, based on Basel-Stadt (2021a), created with QGIS Desktop).*

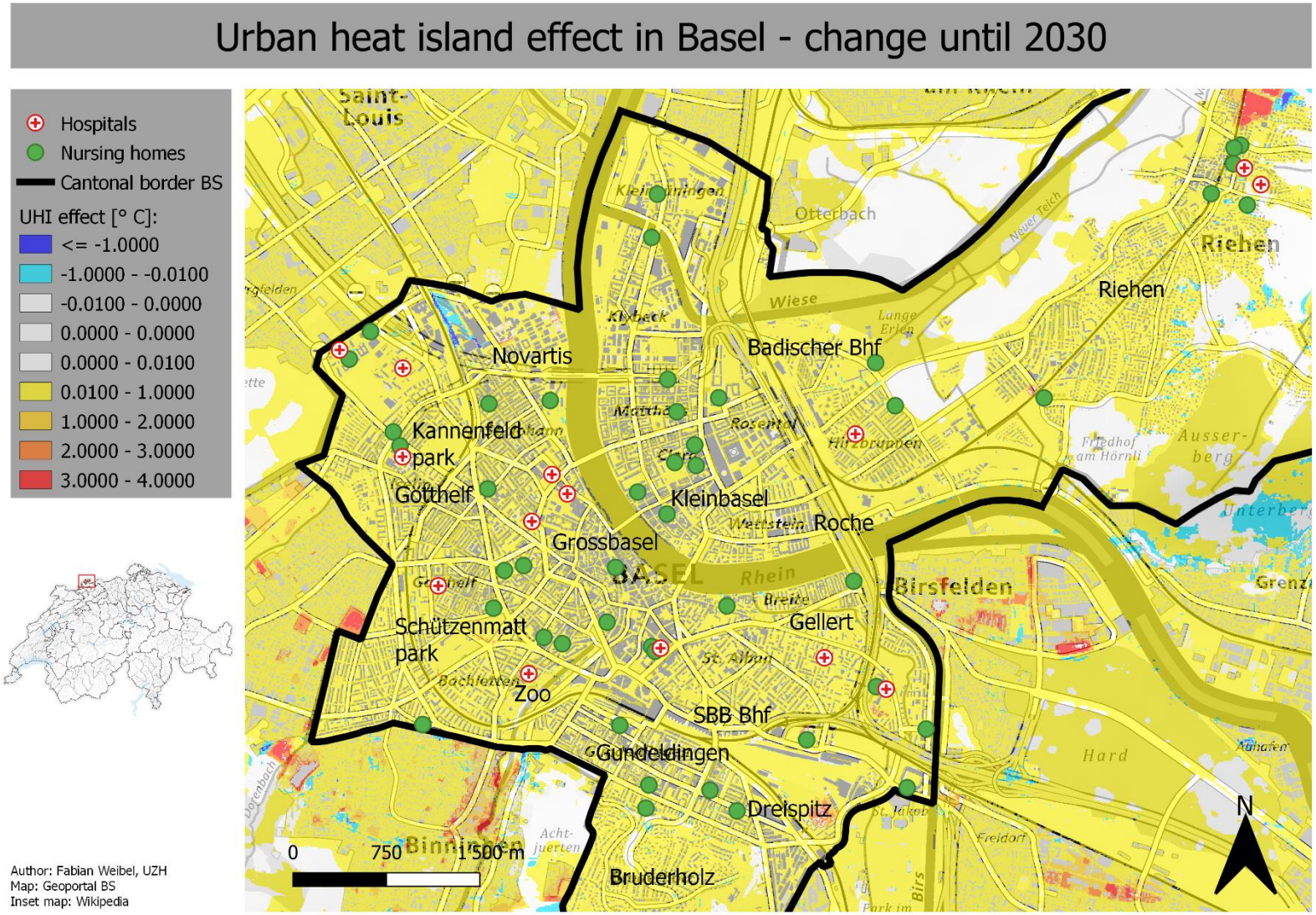

Figure 18: *Projected UHI effect change until 2030 in Basel at 4am in ° C. Map includes nursing homes (green dots) and hospitals (red crosses) (own figure, based on Basel-Stadt (2021a), created with QGIS Desktop).*

6.2 EMA Workbench

The second part of the results section provides an overview of the outcomes of the EMA Workbench. The first section (chapter 6.2.1) presents a comparison between the three WBGT approaches. Raw WBGT values for the observed time period (1981 – 2020) are compared in order to obtain a comprehensive picture of the measured thermal conditions in Basel. Furthermore, the comparison between three different WBGT approaches helped to evaluate which of them is the most suitable for the investigated study areas. This part of the results section does not include any information of policy leavers yet. The data presented in the figures are the outcomes of the climatic analysis (WBGT) without incorporating threshold ranges for extreme days or applying simulated adaptation effects.

The second section (chapters 6.2.2) presents the occurrence of three heat indicators (number of extreme days (NED), number of extreme events (NEE), and average length of extreme events (LEE) per year) in order to show how future climatic conditions could influence the frequency and severity of heat events in Basel. The results in this part include threshold ranges as policy leavers to determine extreme days.

The third section (chapters 6.2.3, 6.2.4, and 6.2.5) presents the sensitivity of the heat indicators to several external factors and policy leavers (threshold ranges for extreme days, simulated adaptation effects).

Chapter 6.2.6 shows how the conditions at the measuring station could compare to potential conditions in the city center and chapter 6.2.7 presents a comparison between Basel and Zurich.

Finally, the last chapter demonstrates potential adaptation measures as well as illustrates results of a DAPP analysis applied for this case study.

The statistics and figures shown in the main part of this chapter are for the location of Basel. Similar figures for Zurich and additional material for Basel are listed in the appendix.

6.2.1 Comparison of WBGT approaches (observations) – Basel

Figure 19 depicts a clear overestimation of the Steadman (1994) approach during the summer season compared to the ones of Bernard (1999) and Ono and Tonouchi (2014). Mean WBGT reached values of over 40° C. Between day 50 and 300 of the year, they greatly exceeded the measured air temperatures. The highest overestimation was during midsummer with a difference of up to 32° C.

Bernard (1999) and Ono and Tonouchi (2014) on the other hand estimated lower WBGT values compared to the air temperature during spring, summer, and autumn. One reason for this could be a stronger integration of the cooling effect of wind gusts.

The difference between the three approaches was much less pronounced during the winter season. Interestingly and unlike in the spring, summer, and autumn, the values of Steadman (1994) were the lowest during winter. They were even lower than the air temperature.

Figure 20, which shows daily maximum WBGT values and air temperatures instead of daily averages of the years 1981 to 2020, depicts even more extreme values for the Steadman (1994) approach. Values of over 60° C were possible whereas the other two approaches and the air temperature had a maximum at about 33° C. Furthermore, the Steadman (1994) approach had a much wider spread, ranging from -15° C up to 65° C.

The mean over the whole observed period of daily maximum WBGT for the Steadman (1994) approach was about 22° C whereas the means for Bernard (1999) and Ono and Tonouchi (2014) were slightly under 14° C.

Table 4 summarizes the most important statistical measures for all three approaches for the observed period between 1981 and 2020.

Table 4: *Statistical analysis of the three WBGT approaches for the observed period between 1981 and 2020 in Basel-Binningen (own table).*

	Steadman (1994)	Bernard (1999)	Ono and Tonouchi (2014)
Mean WBGT	22° C	13.9° C	13.9° C
Max WBGT	65.3 °C	33.2° C	33.4° C
Min WBGT	-15.7° C	-7.9° C	-14.3° C
Annual mean WBGT	22° C	13.9° C	13.9° C
WBGT range	80.1° C	41.1° C	47.7° C
Standard deviation	16° C	7.3° C	8.4° C

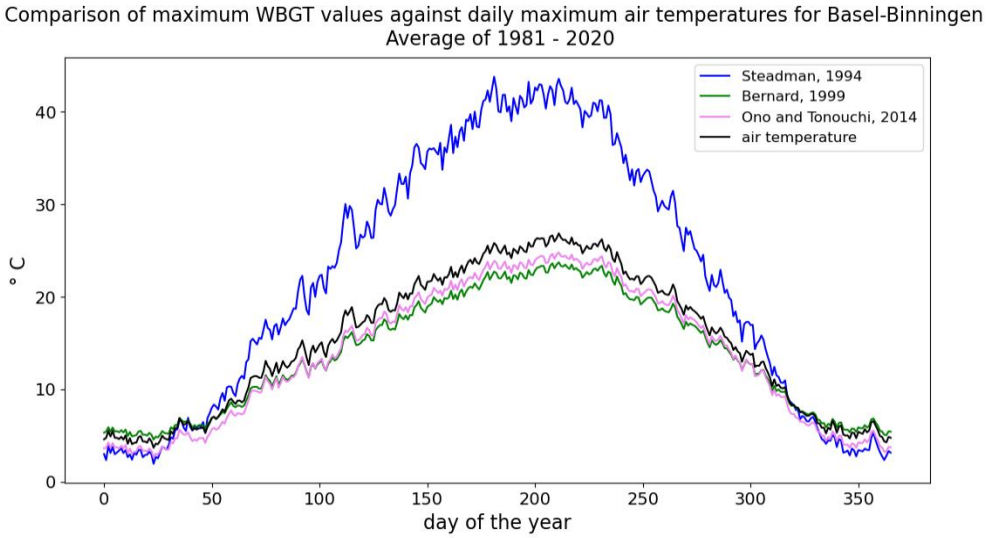

Figure 19: *Comparison of the three WBGT approaches (Steadman (1994) in blue, Bernard (1999) in green, Ono and Tonouchi (2014) in pink) against measured air temperatures (black) for the measurement station in Basel-Binningen. Average of daily maximum air temperatures for the period between 1981 and 2020 (own figure).*

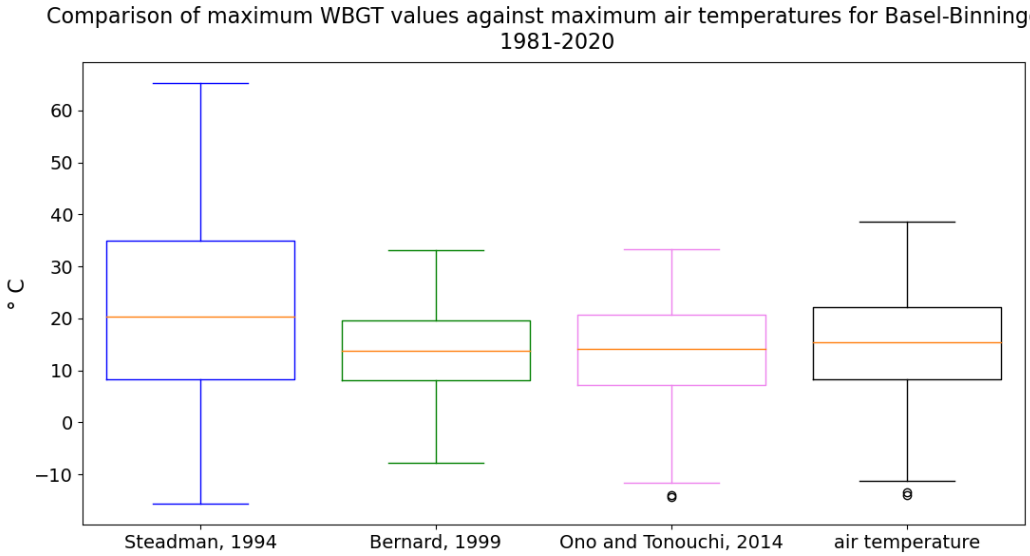

Figure 20: *Comparison of the three WBGT approaches (Steadman (1994) in blue, Bernard (1999) in green, Ono and Tonouchi (2014) in pink) against measured air temperatures (black) for the measurement station in Basel-Binningen. Daily maximum air temperatures for the period between 1981 and 2020. Orange lines show the means (own figure).*

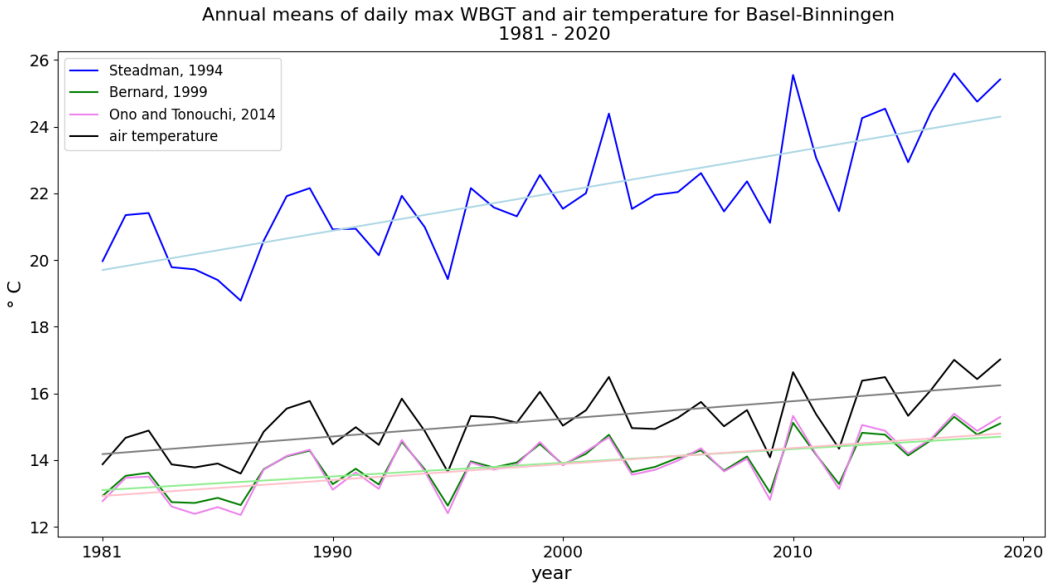

Figure 21: *Comparison of the three WBGT approaches (Steadman (1994) in blue, Bernard (1999) in green, Ono and Tonouchi (2014) in pink) against measured air temperatures (black) for the measurement station in Basel-Binningen. Annual mean of daily maximum air temperatures for the period between 1981 and 2020. Light blue, light green, pink, and grey show the long-term trends for each approach respectively (own figure).*

Figures 19, 20, and 21 as well as the statistical values listed in table 4 prove that the difference between the Bernard (1999) and the Ono and Tonouchi (2014) approach is rather small. Furthermore, it seems that the approach of Steadman (1994) is not suitable for this study. The sometimes quite unrealistic values indicate that either there is an implementation error in the equation, the available data is not suitable for this approach, or the empirical formula is not applicable for this study region. On the basis of these findings, further analyzation steps only employed the approach of Bernard (1999).

6.2.2 Heat indicators – Basel

The figures in the following sections present the results of determined heat indicators (number of extreme days (NED), number of extreme events (NEE), average length of extreme events (LEE) per year) using the raw WBGT. A day is classified as extreme when the maximum WBGT exceeds a certain threshold out of a predefined range. An extreme event is a period of consecutive days during which the maximum WBGT never fell below the defined threshold. The average length of single extreme events was calculated by the sum of consecutive days with extreme WBGT values, averaged over one year.

The figures respectively show the results of 4080 experiments (136 future scenarios * 30 WBGT thresholds) conducted with the EMA Workbench (see chapter 4.1). Each boxplot aggregates all 4080 experiments (or subgroups thereof depending on the RCP scenario), whereas in the line charts, each line represents one single experiment for the whole simulated time period.

Supplementary figures for Basel and Zurich are listed in the appendix.

All three climate scenarios (RCP2.6, RCP4.5, RCP8.5) predict an increase of the total NED per year in Basel, although the incline under RCP2.6 is rather weak. During the observed period between 1980 and 2020, an average of almost 7 extreme days per year could be measured. For the future however, one predicts an increase to over 8, 10, or 17 extreme days per year on average under RCP2.6, RCP4.5, or RCP8.5 respectively. That corresponds to an increase of over 240% by the end of this century for the most extreme scenario (figure 22).

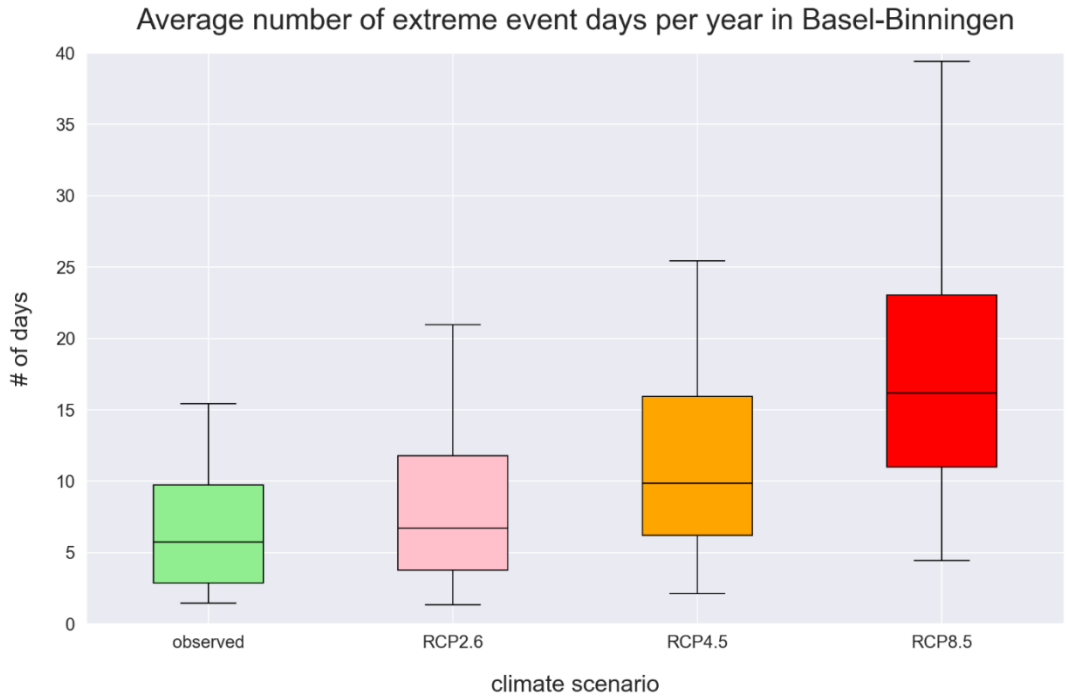

Figure 22: *Average NED per year for the observed period (1981 – 2020, green) and three different future scenarios (1981 – 2099, RCP2.6 in pink, RCP4.5 in orange, RCP8.5 in red). The threshold range for an extreme day is between 26° C and 30° C (own figure).*

Figures 24, 25, 26, and 27 show timeseries of all model runs for the observed time period (figure 24) and for the simulated time periods (figures 25 to 27). Unlike the boxplots in figure 22, where an annual average of all model runs is pictured, the timeseries are useful to analyze inter-annual fluctuations and to compare an expectable range of future projections. Very extreme experiments and how they develop over time can be determined. It becomes evident that the trends are positive, either for NED, NEE, and LEE. However, the steepness of the incline is very different comparing RCP2.6 to RCP4.5 and RCP8.5. For the case of extreme days per year, the annual increase is on average about 0.045 days under RCP2.6 whereas under RCP8.5, it is about 0.333 days per year until 2100. This corresponds to a more than 7 times stronger increase until the end of this century. The total increase of extreme days per year is directly coupled to an increase of extreme events. It can be determined that they will last longer and occur more frequently in the future, independent of the considered future scenario. In quantitative terms, this corresponds to more than a doubling of the annual growth rate for NEE and LEE when comparing RCP8.5 and RCP4.5 with RCP2.6 (figures 26 and 27 and table 6 in the appendix).
The increase of NED, NEE, and LEE per year although is probably anything but linear and differs from RCP to RCP (figures 28, 55, and 56). Under RCP2.6, one can expect a stagnation during the next two decades which holds until the end of this century. Some simulations even predict a very weak decline in the second half of this century. Under RCP4.5, the increase is more or less linear, whereas under RCP8.5, it is predicted that the amount of NED, NEE, and LEE per year will grow faster during the next decades with some simulations even showing an acceleration the further one looks into the future.
The area below the NED = 20 line (blue) in figure 25 shows the years with a moderate heat stress for the population. Simulations where a lot of years are above the NED = 40 line (dark blue) on the other hand depict very extreme years in terms of thermal stress. Under RCP2.6, only a few experiments are above the extreme line (NED = 40). There are some outlier years, however the trend principally stays below the dark blue line. Under the most extreme future scenario, one can expect that about every second year is going to exceed the extreme line by the end of this century.
In figure 26, the NEE = 5 line (blue) shows moderate and the NEE = 8 line (dark blue) extreme heat stress. A similar trend like for NED can be seen for NEE meaning that under RCP2.6, most of the simulations stay below both lines until 2100 whereas under RCP8.5, most of the simulations predict extreme heat stress conditions every year.
In figure 27, an extreme event is defined as particularly extreme if the length exceeds 5 days (LEE = 5 line (blue)). Again, a comparable trend emerges when looking at the increases of LEE until the end of this century. At about 2060 to 2070, the simulations predict that every second year could have multiple extreme events which last for more than one working week under RCP8.5. Under RCP4.5 and RCP2.6, however, most of the extreme events are expected to be shorter than one working week.

The variations between the different experiments are substantial. Even under RCP8.5, the difference between the expected hottest and coolest years is more than 90 extreme days per year. This big variation amongst single experiments once again demonstrates that the climate is a rather non-linear system and the high degree of complexity makes it difficult to calculate clear future predictions.

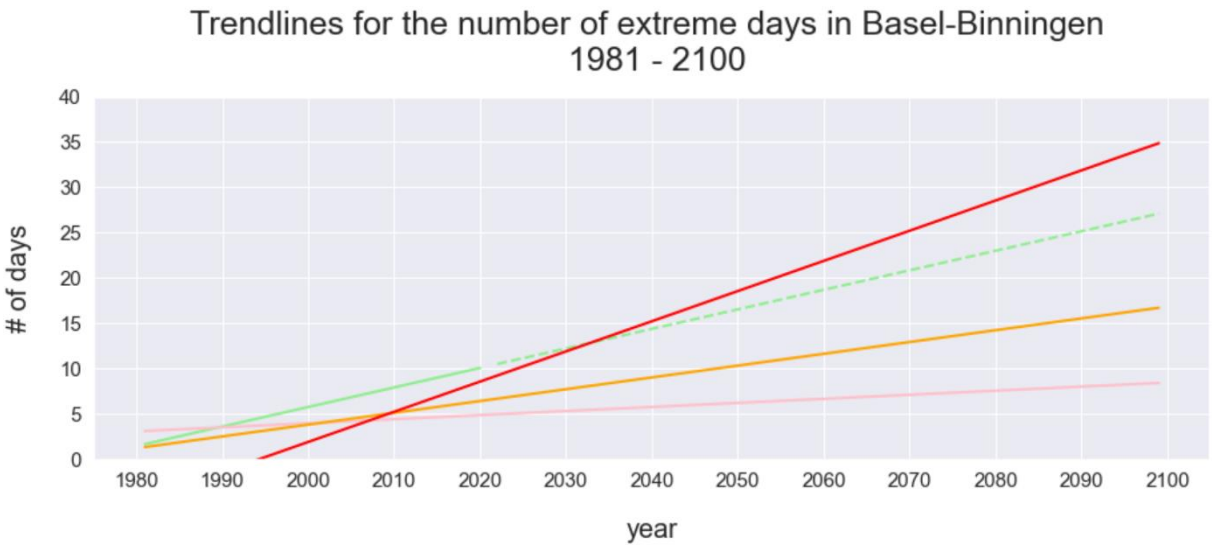

Figure 23: *Trendlines for NED for the observed period (solid green), the extrapolated observed period (dashed green), the RCP2.6 scenario (pink), the RCP4.5 scenario (orange), and the RCP8.5 scenario (red) in Basel-Binningen (own figure).*

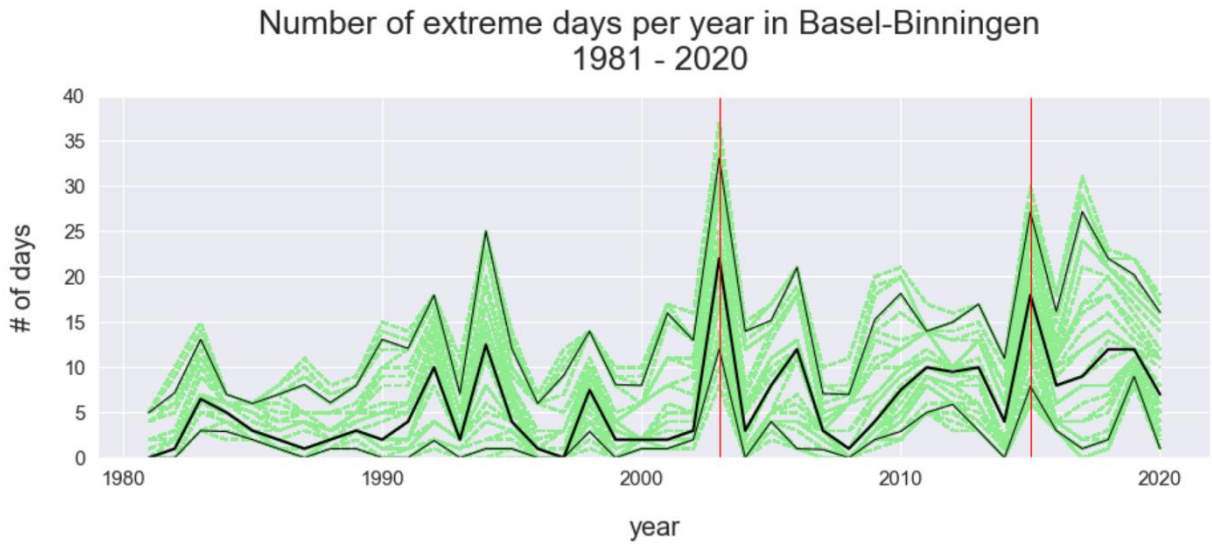

Figure 24: *NED per year for the observed period in Basel-Binningen. The threshold range for an extreme day is between 26° C and 30° C. The green lines show the scenarios. The three black lines show the 10th, 50th, and 90th quantiles respectively. The red vertical lines at 2003 and 2015 indicate the extreme heat waves occurred in Central Europe (own figure).*

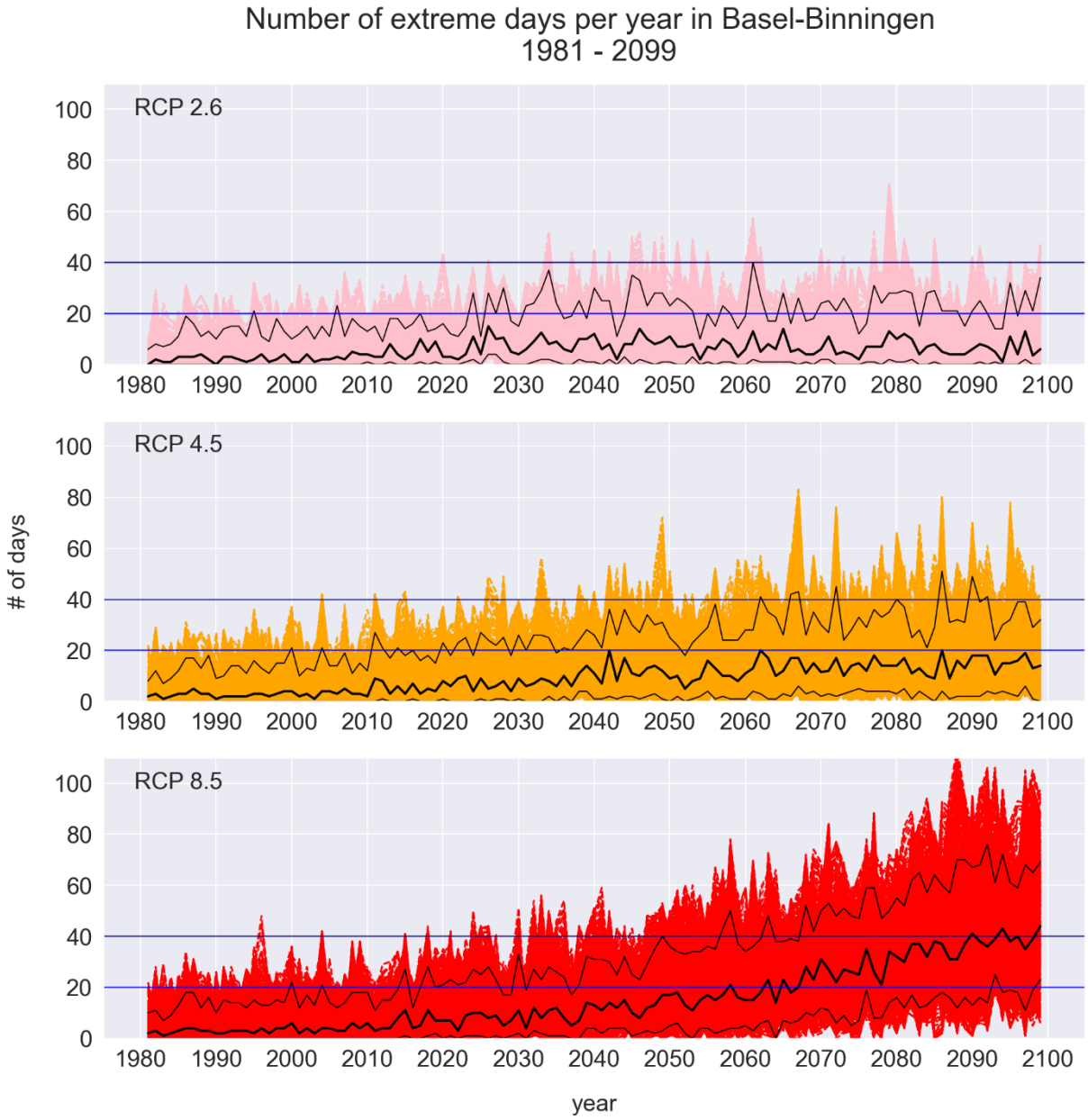

Figure 25: *NED per year for the future simulations in Basel-Binningen. The threshold range for an extreme day is between 26° C and 30° C. The first graph shows the RCP2.6 scenario (pink), the second graph shows the RCP4.5 scenario (orange), and the third graph shows the RCP8.5 scenario (red). The black lines show the 10th, 50th, and 90th quantiles respectively. The blue line marks NED = 20, the dark blue line NED = 40 (own figure).*

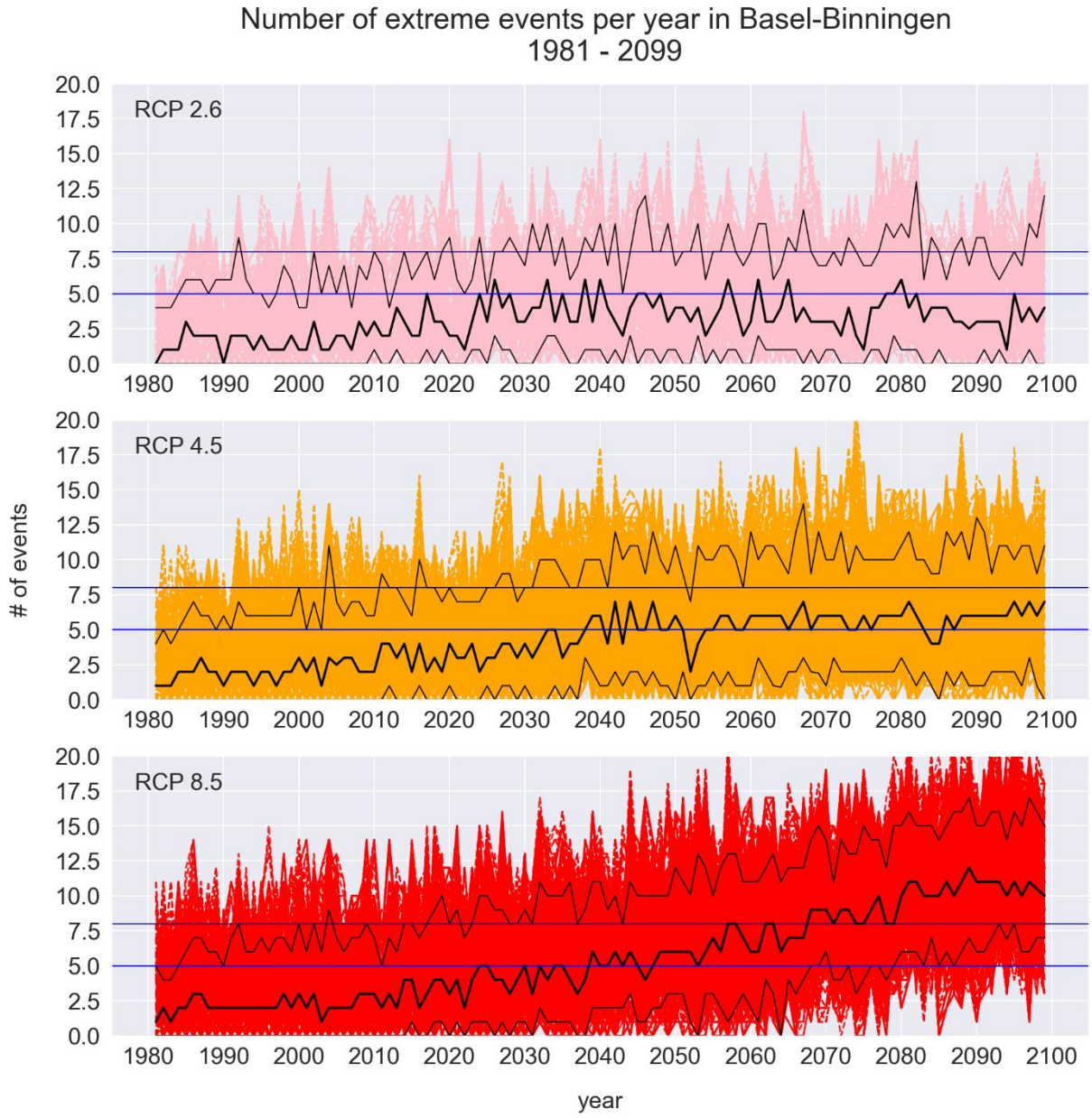

Figure 26: *NEE per year for the future simulations in Basel-Binningen. The threshold range for an extreme day is between 26° C and 30° C. The first graph shows the RCP2.6 scenario (pink), the second graph shows the RCP4.5 scenario (orange), and the third graph shows the RCP8.5 scenario (red). The black lines show the 10th, 50th, and 90th quantiles respectively. The blue line marks NEE = 5, the dark blue line NEE = 8 (own figure).*

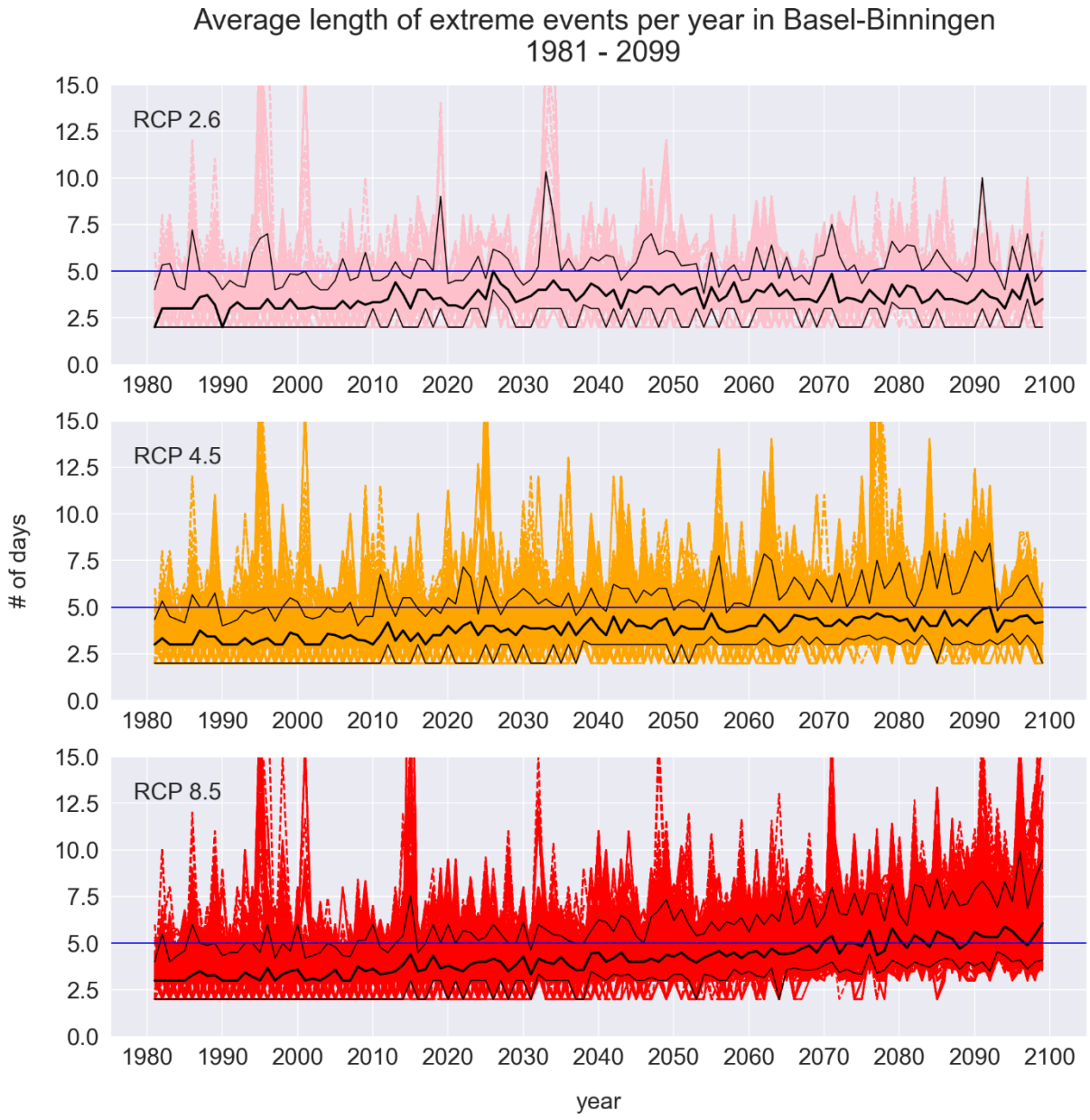

Figure 27: *LEE per year for the future simulations in Basel-Binningen. The threshold range for an extreme day is between 26° C and 30° C. The first graph shows the RCP2.6 scenario (pink), the second graph shows the RCP4.5 scenario (orange), and the third graph shows the RCP8.5 scenario (red). The black lines show the 10th, 50th, and 90th quantiles respectively. The blue line marks LEE = 5 (own figure).*

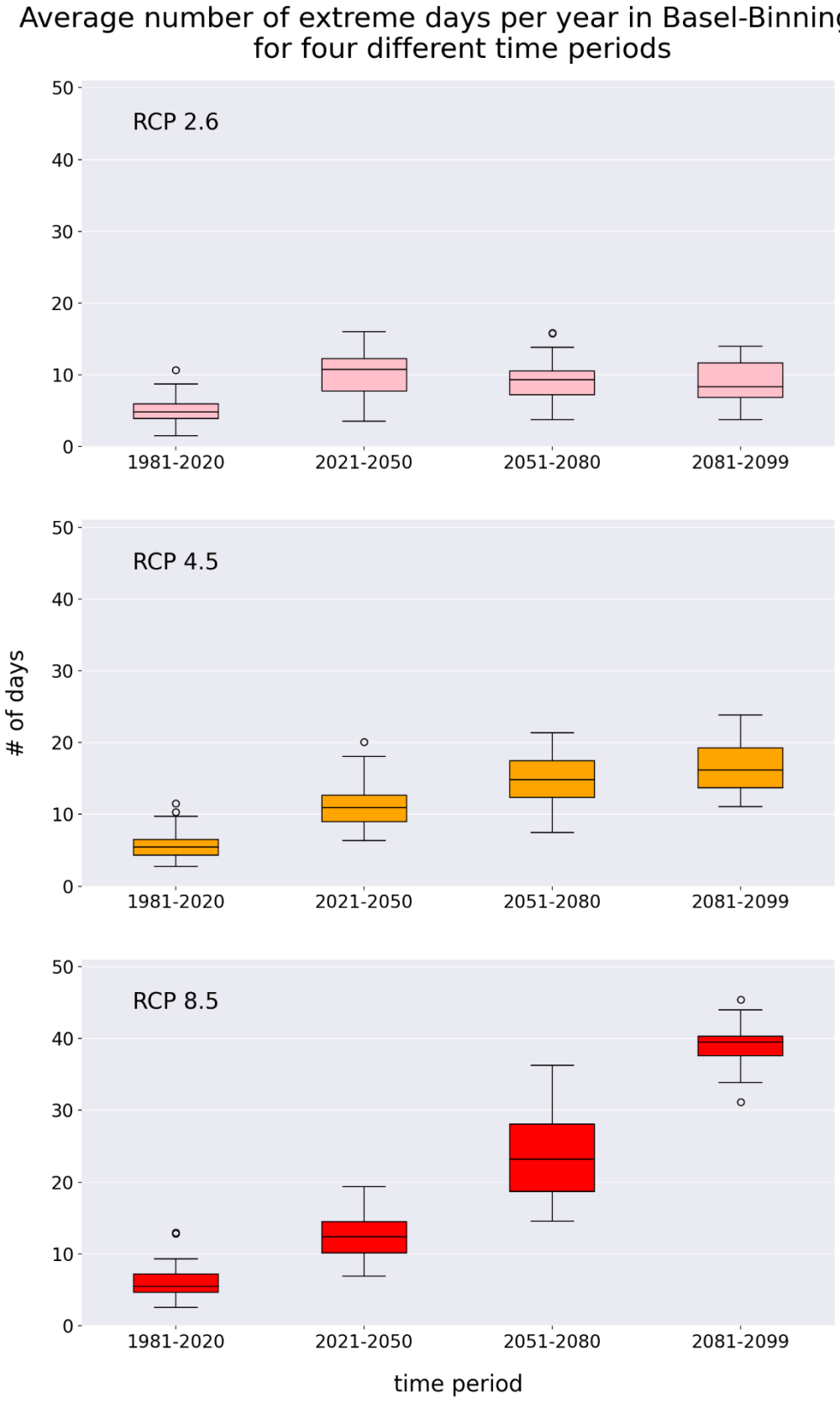

Figure 28: *Average NED for four time periods for the future simulations in Basel-Binningen. The threshold range for an extreme day is between 26° C and 30° C. The first graph shows the RCP2.6 scenario (pink), the second graph shows the RCP4.5 scenario (orange), and the third graph shows the RCP8.5 scenario (red) (own figure).*

6.2.3 Sensitivity analysis of policy leavers and external factors – Basel

Threshold ranges of 26°-30° C vs. 28°-32° C:

Increasing the threshold range for extreme days by 2° C (from 26° - 30° C to 28° - 32° C) has a huge impact on the resulting heat indicators. In the case of the amount of annual extreme days, a reduced mean of 5.5, 7, and 8.5 days per year under RCP2.6, RCP4.5, and RCP8.5 respectively can be measured. These reductions in extreme days clearly bear out that heavy outdoor workers and very vulnerable people (threshold range 26° C to 30° C) do considerably suffer more under heat wave conditions than workers with reduced physical activities or younger people with a healthy thermoregulatory system (threshold range 28° C to 32° C) (figure 29).

A similar comparison between NEE and LEE is presented in the appendix.

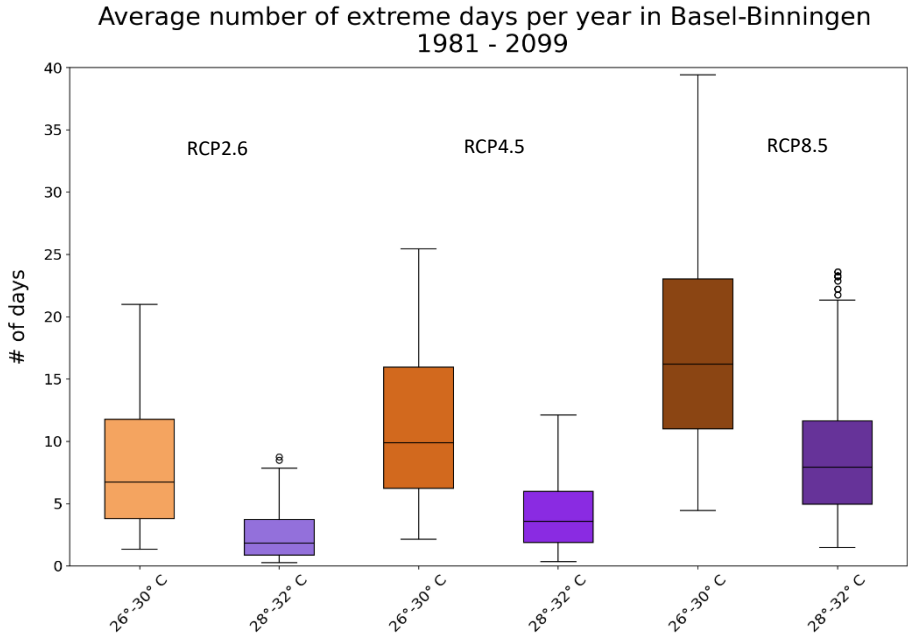

Figure 29: *Average NED per year of the future simulations in Basel-Binningen. Threshold range 26°-30° C in orange/brown and 28°-32° C in violet (own figure).*

Threshold range of 33°-35° C:

Figure 30 shows the results for very extreme hot days. The threshold range was set to 33°-35° C. It is clear that under RCP2.6 and RCP4.5, the chance of such extraordinary extreme days in Basel is rather low. On average, less than 1 day per year is expected until 2100. Under RCP8.5 although, one can expect 1 to 2 very extreme days in Basel.

The moderate (28°-32° C) and the extreme (33°-35° C) increase of the threshold range prove that highly acclimatized (e.g. people who grew up in tropical or subtropical regions), young, and healthy people are able to withstand heat much better than people from colder climatic regions or elderly people with a weak thermoregulatory system.

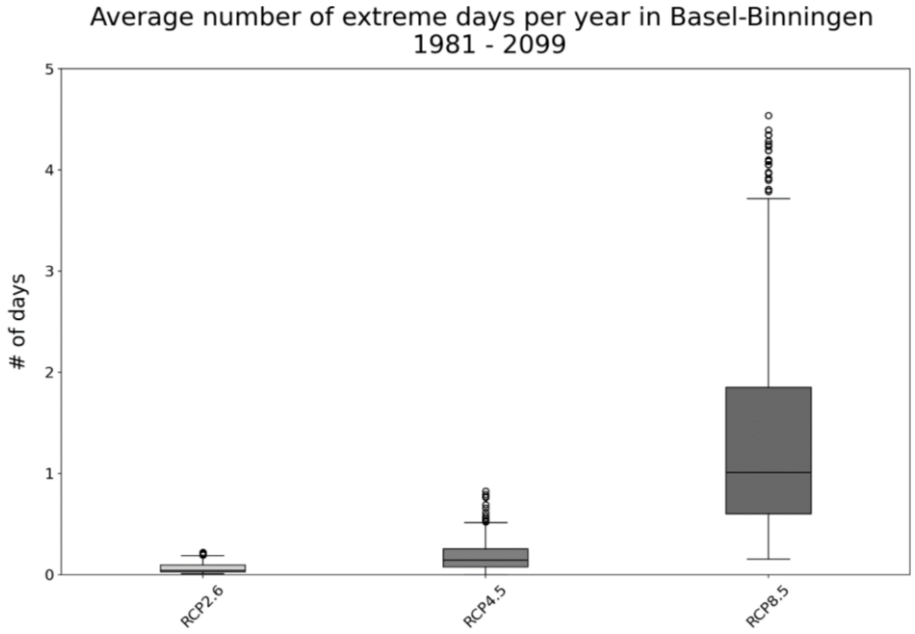

Figure 30: *Average NED per year of the future simulations in Basel-Binningen. Threshold range 33°-35° C. RCP2.6 in light grey, RCP4.5 in grey, and RCP8.5 in dark grey (own figure).*

Feature Scoring:

Figure 31 shows how important certain variables (policy leavers, external factors) are for the model run outcomes. It becomes evident that the choice of the WBGT threshold has the most controlling effect on resulting heat indicators. The selected RCP scenario (RCP2.6, RCP4.5, RCP8.5) is the second most influencing factor. The random choice of a climate model realization of either RCP2.6, RCP4.5, or RCP8.5 however does not influence the model run outcomes.

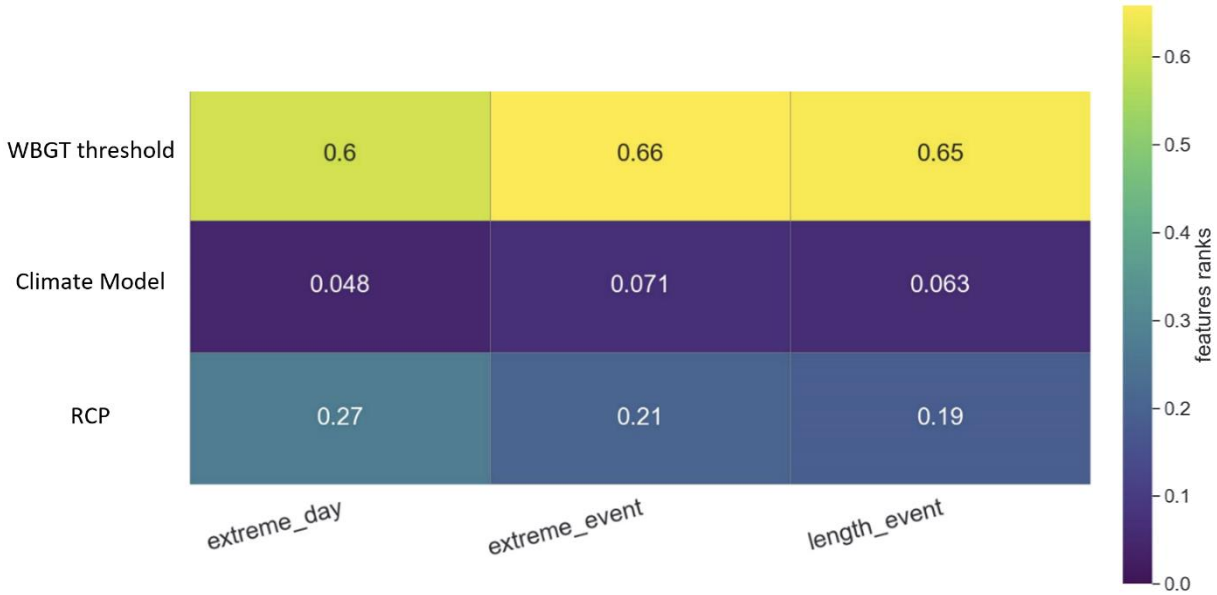

Figure 31: *Feature scoring for Basel-Binningen of the future simulations. Importance of policy leavers (WBGT threshold) and external factors (RCP, climate model) on heat indicators. The higher the feature rank, the more important is the variable (own figure).*

6.2.4 Effects of adaptation measures on heat indicators – Basel

Figures 32 and 33 compare the average NED per year for normal conditions (grey, no simulated adaptation effects) to five different scenarios with simulated adaptation effects (decreased temperatures 3x (blue) in figure 32, increased wind (green), decreased global radiation (yellow) in figure 33). The goal of this analysis was to investigate the potential effects of certain adaptation measures on WBGT and the derived heat indicators.

The grey boxes picture the unchanged conditions for the three different future scenarios (RCP2.6, RCP4.5, RCP8.5).

The blue boxes in figure 32 represent conditions with reduced air temperatures by 1° C (light blue), 3° C (blue), and 5° C (dark blue) during the spring, summer, and autumn months (April to September). Between October and March, no temperature reduction was implemented. This kind of manual reduction of air temperatures could mimic the effects of evaporative cooling and shadowing by an increase of foliated trees in the city. The results show a decrease of the mean average NED per year of about 5 days for the reduction of 1° C, of 10 days for the reduction of 3° C, and of over 10 days for the reduction of 5° C. The reduction of extreme days is especially strong under RCP8.5 and T-5° C where a difference of 15 days can be expected on average.

The orange boxes in figure 33 represent a condition where the incoming global radiation at the Earth's surface was manually reduced to 15% during the spring, summer, and autumn months (April to September) and to 50% during the winter months (October to March). Researchers could estimate in various studies that the transmissivity of global radiation below foliated trees in urban areas can sink to about 15 to 10% and below defoliated trees to about 50% (Cantón, Cortegoso & de Rosa 1994, Konarska et al. 2014, Gay, Knoerr & Braaten 1971). The effect of reducing the global radiation results in a decrease of the mean average NED per year of about 2 days, independent from the chosen RCP scenario.

Finally, the green boxes in figure 33 represent a condition where the wind speed was artificially increased by 1 m/s. Wind plays an important role for the evaporative cooling mechanism in our body and is a necessary part of an efficient urban ventilation. By increasing the simulated wind speeds by 1 m/s, an optimized ventilation in the city can be imitated. Yuan and Ng (2012) did a study where they investigated the ventilation effect of wind on the outdoor thermal comfort in cities. They identified a minimum wind speed of 1 m/s as satisfactory and wind speeds above 1.3 m/s as good urban ventilation in terms of thermal comfort (Yuan & Ng 2012). The results of the simulations indicate that in the case of Basel, only a small reduction of 1 extreme day or less per year can be achieved on average.

A summary of some calculated results can be found in the tables 7 and 8 in the appendix.

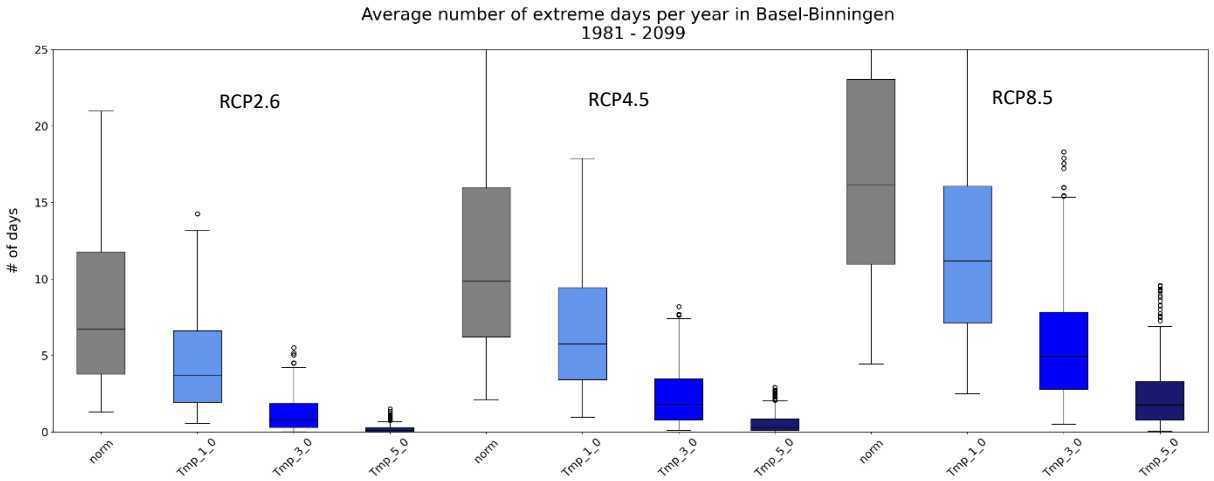

Figure 32: *Average NED per year of the future simulations in Basel-Binningen. No simulated adaptation effects in grey. Reduced air temperature (1° C, 3° C, and 5° C) in light blue, blue and, dark blue. Results for three different climate scenarios (RCP2.6, RCP4.5, RCP8.5) (own figure).*

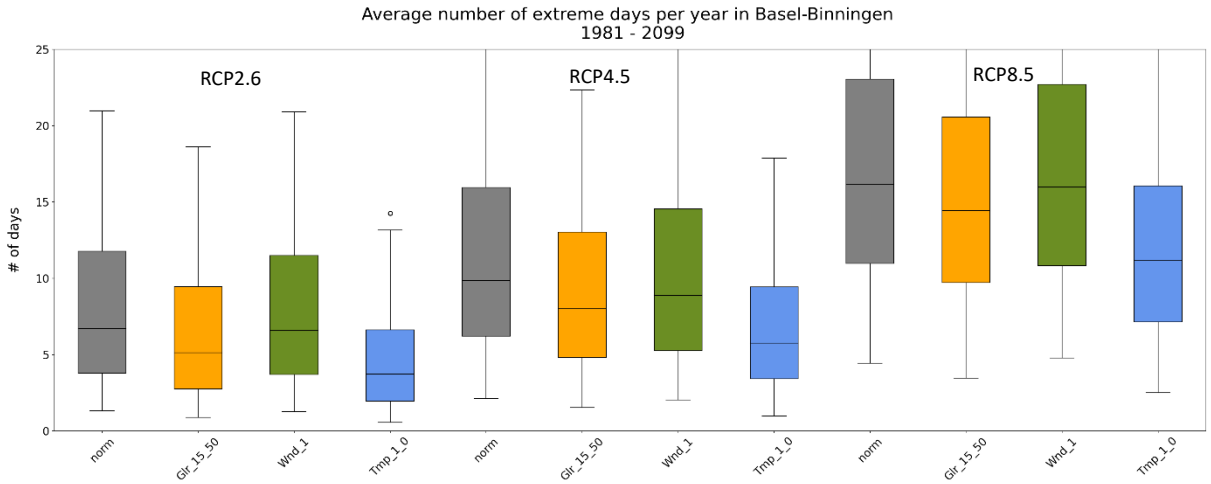

Figure 33: *Average NED per year of the future simulations in Basel-Binningen. No simulated adaptation effects in grey. Reduced global radiation in orange, increased wind speed in green, and decreased air temperature in light blue. Results for three different climate scenarios (RCP2.6, RCP4.5, RCP8.5) (own figure).*

6.2.5 Effects of wind and urban ventilation on heat indicators – Basel

The analysis of the observed wind speeds at the measuring station in Basel-Binningen (figure 8 in chapter 3.1) points out that there is a noticeable wind throughout the year. Since the measuring station is located outside the city center and the wind sensor is attached in a height of 12 m above the ground, it can be expected that the measured values are higher compared to conditions in the city. To get an estimate of the thermal conditions in the city center with more realistic wind speeds, a scenario with manually reduced wind speeds was implemented.

The results of these investigations are presented in the figures 34 and 35. The grey boxes once again represent average NED (figure 34) and LEE (figure 35) per year under unchanged climatic conditions. The green boxes represent conditions with a slightly improved ventilation effect (increased wind speed by 1 m/s), whereas the dark green boxes summarize the results of drastically worsened aerodynamic

conditions (decreased wind speed by 3 m/s when the initial value is greater than 3 m/s, otherwise the wind speed was set to 0 m/s). It clearly becomes evident that wind is very important to keep places in cities cool. The simulations show that a weakened wind pattern can increase total average NED per year by 2 to 3 days, depending on the investigated RCP scenario. Regarding LEE, a similar picture can be observed.

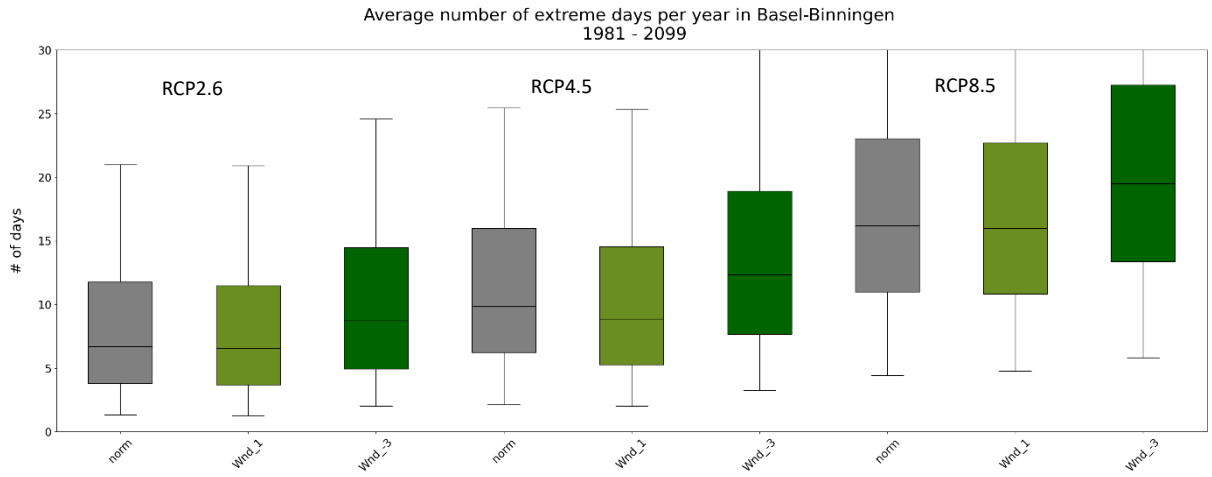

Figure 34: *Average NED per year of the future simulations in Basel-Binningen. No simulated adaptation effects in grey, increased wind speed in green, and reduced wind speed in dark green. Results for three different climate scenarios (RCP2.6, RCP4.5, RCP8.5) (own figure).*

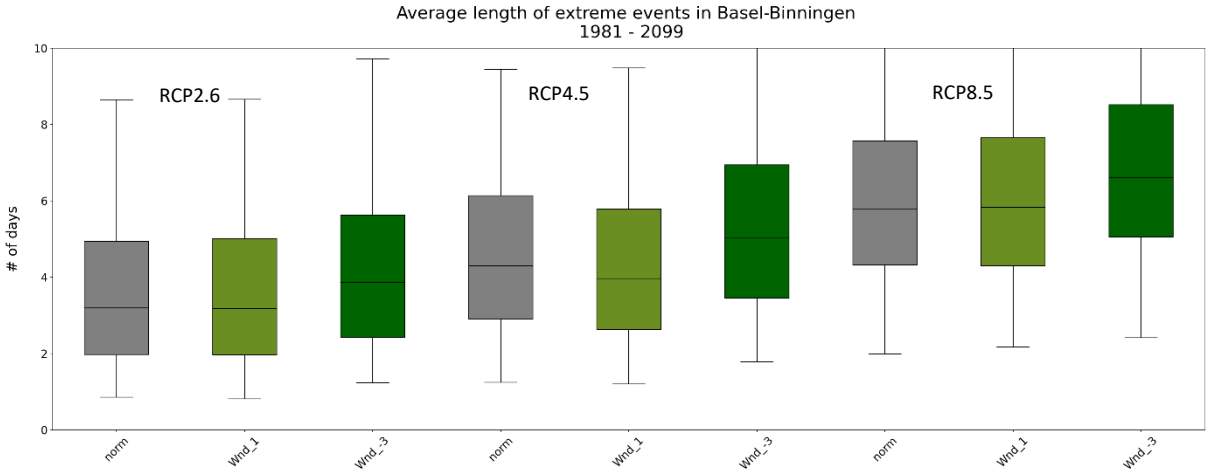

Figure 35: *LEE per year of the future simulations in Basel-Binningen. No simulated adaptation effects in grey, increased wind speed in green, and reduced wind speed in dark green. Results for three different climate scenarios (RCP2.6, RCP4.5, RCP8.5) (own figure).*

According to a two sample Z-test, the means for normal conditions and for a weakened wind field are significantly different (significance level α=0.05). Furthermore, the density plots in figure 36 show that the difference is most noticeable during extreme years (between 21 and 31 extreme days per year (left side) and between a length of 6 to 11 days (right side)).

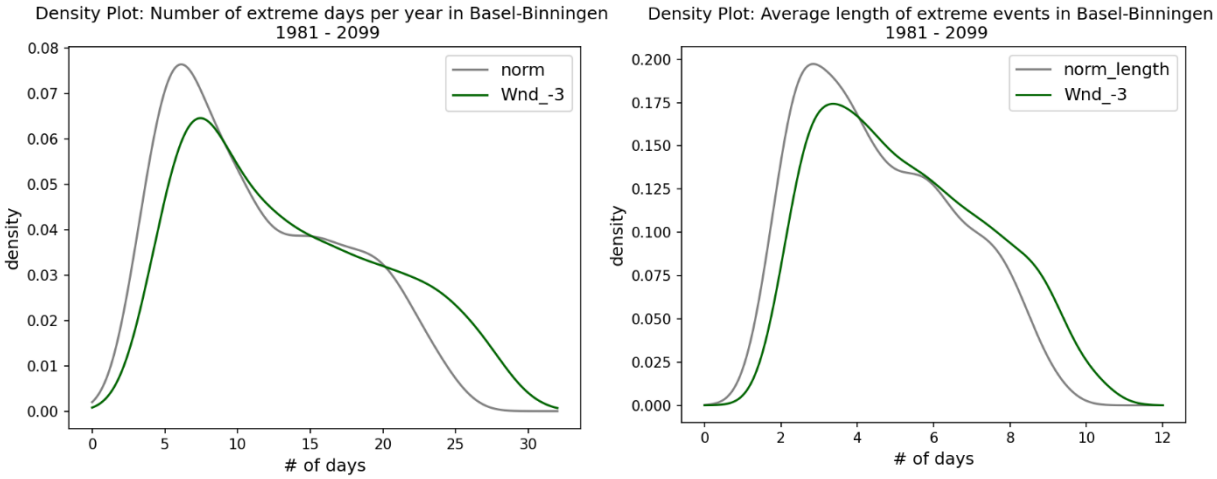

Figure 36: *Density plots of all simulations for NED per year (left) and LEE (right) for the future simulations (RCP4.5) in Basel-Binningen. The grey line represents the climate without simulated adaptation effects whereas the dark green line represents a climatic condition with weakened wind speeds (own figure).*

6.2.6 Difference from the measuring station to the hottest places in the city – Basel

Figure 37 (and figures 65 and 66 in the appendix) unambiguously illustrate that the thermal conditions in the city center can be far more impactful for human health compared to the measured and simulated values at the measuring stations. In the case of Basel, NED per year can be two to three times higher in the hottest districts of the city than simulated for Basel-Binningen. Regarding LEE per year, the difference can reach a factor of 1.5 to 2.

The results for Zurich are pictured in the figures 71, 72, and 73 in the appendix. The outcomes predict an even bigger difference between the measuring station and the city center. For NED per year, a factor of 1.5 to 4 is possible, for LEE per year, a factor of 1.5 to 2.5.

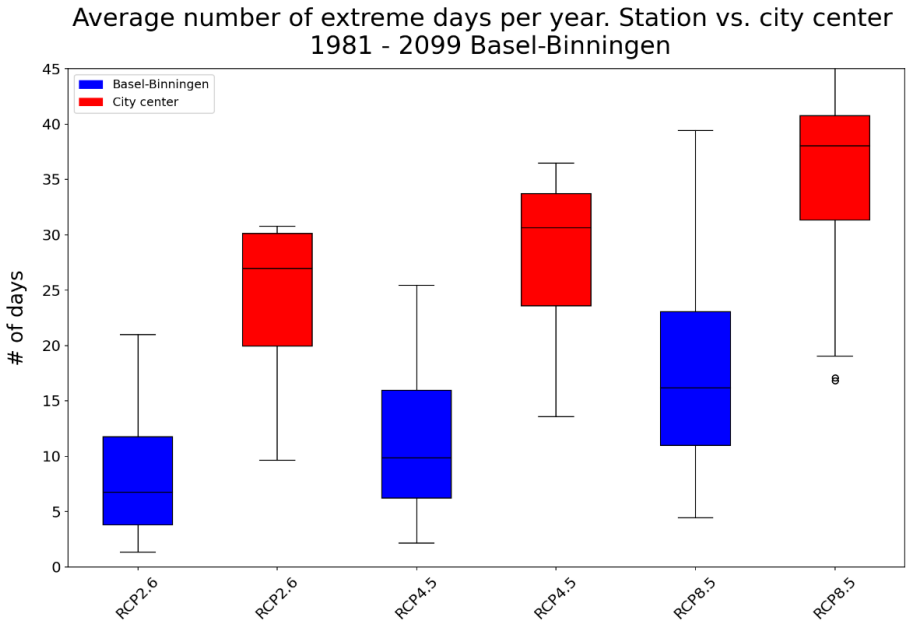

Figure 37: *Simulated NED per year at the measuring station in Basel-Binningen in blue and simulated NED per year for potential heat conditions in the city center in red (adapted WBGT values according to chapter 4.6) for the simulated period (1981-2099). Comparison between RCP2.6, RCP4.5, and RCP8.5 (own figure).*

6.2.7 Basel vs. Zurich

This section of the results chapter shows a rough overview of the differences between the expected thermal conditions in Basel and Zurich. Figure 38 compares the averaged simulated maximum WBGT over the course of one year. Figure 39 distinguishes between the three RCP scenarios and gives insight into the difference of the expected number of extreme days per year until 2100.

Further figures of the comparison between Basel and Zurich (NEE, LEE) can be found in the appendix.

On average, WBGT is higher in Basel compared to Zurich. The simulated annual mean in Basel is about 15.5° C whereas the annual mean in Zurich is slightly higher than 14° C. The difference between these two cities is more or less constant over the course of one year, however, it tends to be somewhat smaller during autumn (figure 38).

Comparing the average NED per year for the three different RCP scenarios reveals a similar picture. Under the most extreme future scenario, one can expect about 7 extreme days per year more in Basel compared to Zurich (figure 39).

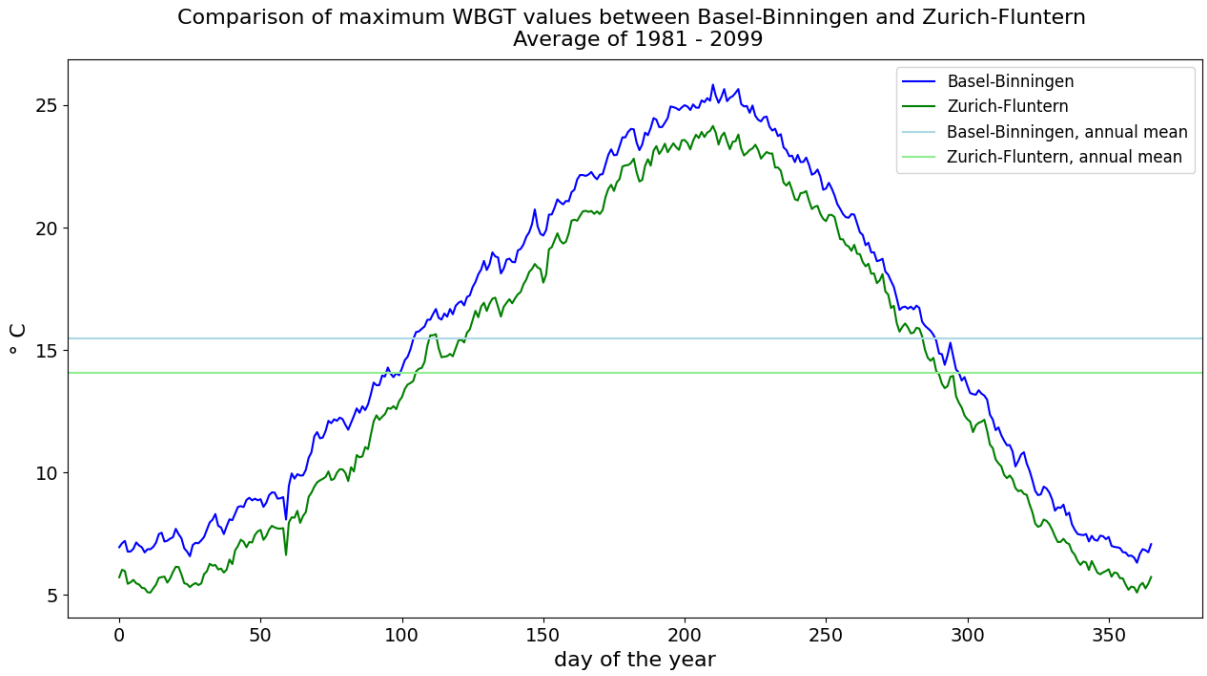

Figure 38: *Comparison of simulated maximum WBGT between Basel-Binningen (blue) and Zurich-Fluntern (green). Light blue and light green show the annual mean for Basel-Binningen and Zurich-Fluntern respectively (own figure).*

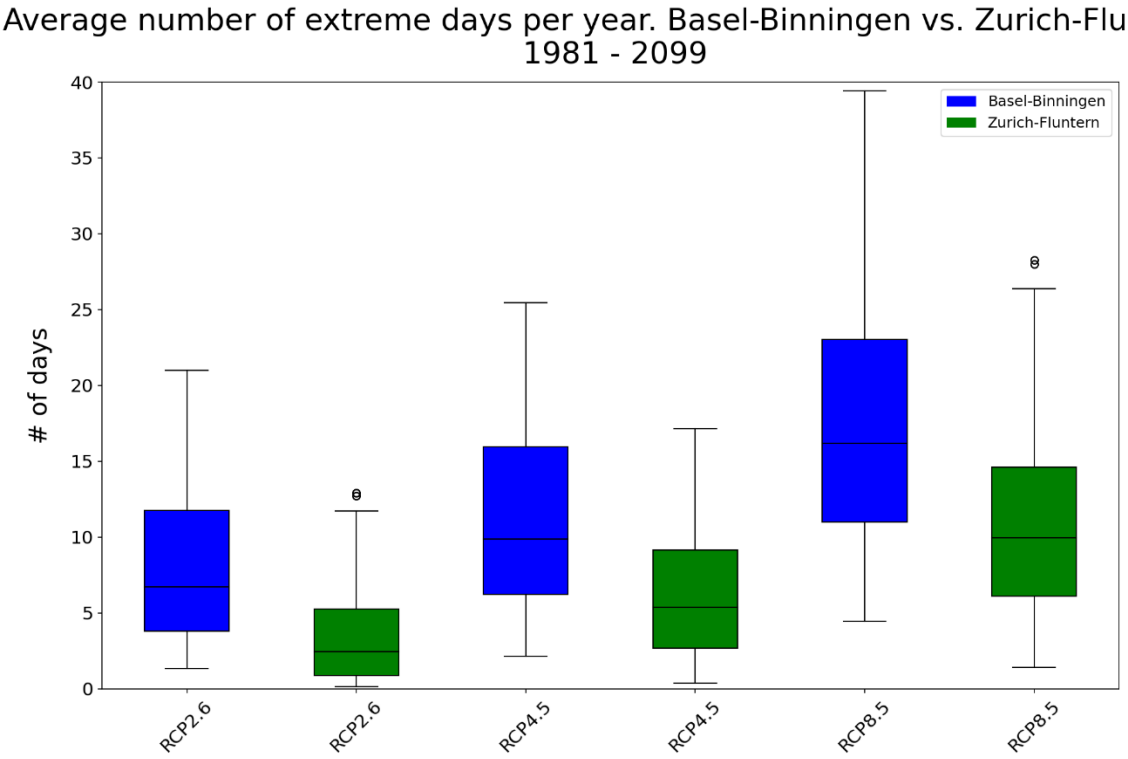

Figure 39: *Comparison of average NED per year between Basel-Binningen and Zurich-Fluntern for three different climate scenarios (RCP2.6, RCP4.5, RCP8.5) (own figure).*

6.2.8 Adaptation measures, metro map, and feasibility-effectiveness diagram

The results off this study as well as off other studies carried out for various regions on Earth clearly point out that climate change heavily influences the everyday life in cities. To protect highly populated regions against severe impacts on human health and comfort, both local adaptation as well as global climate protection measures must be discussed and implemented as soon as possible. Adaptation measures for a city are always site specific and thus cannot be one-to-one copied to and implemented in other cities. They must be individually evaluated and adapted to local weather and climate conditions, demographic compositions, urban characteristics, and legal frameworks. Table 5 summarizes some of the most important adaptation measures and the climatic effects which can be expected (Weber et al. 2018, Burmeister, Büter & Trute 2019, Yow 2007, Gunawardena, Wells & Kershaw 2017).

Table 5: *Possible adaptation measures to mitigate the UHI effect (own table, according to* Yow (2007), Weber et al. (2018), Burmeister, Büter & Trute (2019), Kühnle (2021), Lai et al. (2019), Minor & Unternährer (2022)*).*

Adaptation measure	Effects
Increase **vegetation density**, e.g. urban parks, vegetated facades, rooftop gardens, tree avenues, renaturation of urban streams.	• Altered sensible and latent heat flux (evaporation and transpiration) • Blocked solar radiation, shadowing • Improved air quality • Wildlife habitats (e.g. birds, insects) • Urban flood control • Recreation area
Build or enlarge **water bodies**, e.g. fountains, excavation of urban streams. 'Make use' of existing water bodies, e.g. rivers, lakes.	• Altered air flow patterns and ventilation • Altered latent heat flux (evaporation)
Increase the **albedo** of surfaces and change **construction materials**, e.g. of roofs and facades.	• Increased reflection of solar radiation and thus reduced heat absorption • Altered heat capacities
Reduce the **anthropogenic heat** and the energy consumption, e.g. traffic, air conditioning, industry.	• Reduced sensible heat flux • Improved air quality • Reduced greenhouse gases
Change the layout of house constructions, street orientations, and building heights (**urban geometry**).	• Altered air flow patterns and ventilation • Blocked solar radiation (N-S vs. E-W orientation)
Use **porous materials** with large water storage for underground.	• Reduced sensible heat through evaporation of stored water • Urban flood control
Generate local **artificial clouds**	• Blocked and reflected solar radiation • Evaporation of small water droplets

The three metro maps pictured in figure 40 present possible adaptation pathways for the three future scenarios RCP2.6, RCP4.5, and RCP8.5. The four adaptation groups included in the metro maps are generating green spaces (green path) and blue spaces (blue path), changing, adapting, or optimizing

the urban geometry (red path), and increasing the surface albedo (yellow path). They are defined so that they roughly cover the adaptation measures listed in table 5. The effectiveness of each adaptation group is based on information from the literature as well as the outcomes of the EMA Workbench and the sensitivity analysis. It is important to mention that the year of the adaptation tipping points were determined qualitatively rather than quantitatively. The transition from one path to another over a node (tipping point) must not be considered as immediate since the implementation of every adaptation measure needs a certain lead and implementation time. The tipping points should therefore be regarded as transition periods rather than one single point at a fixed time.

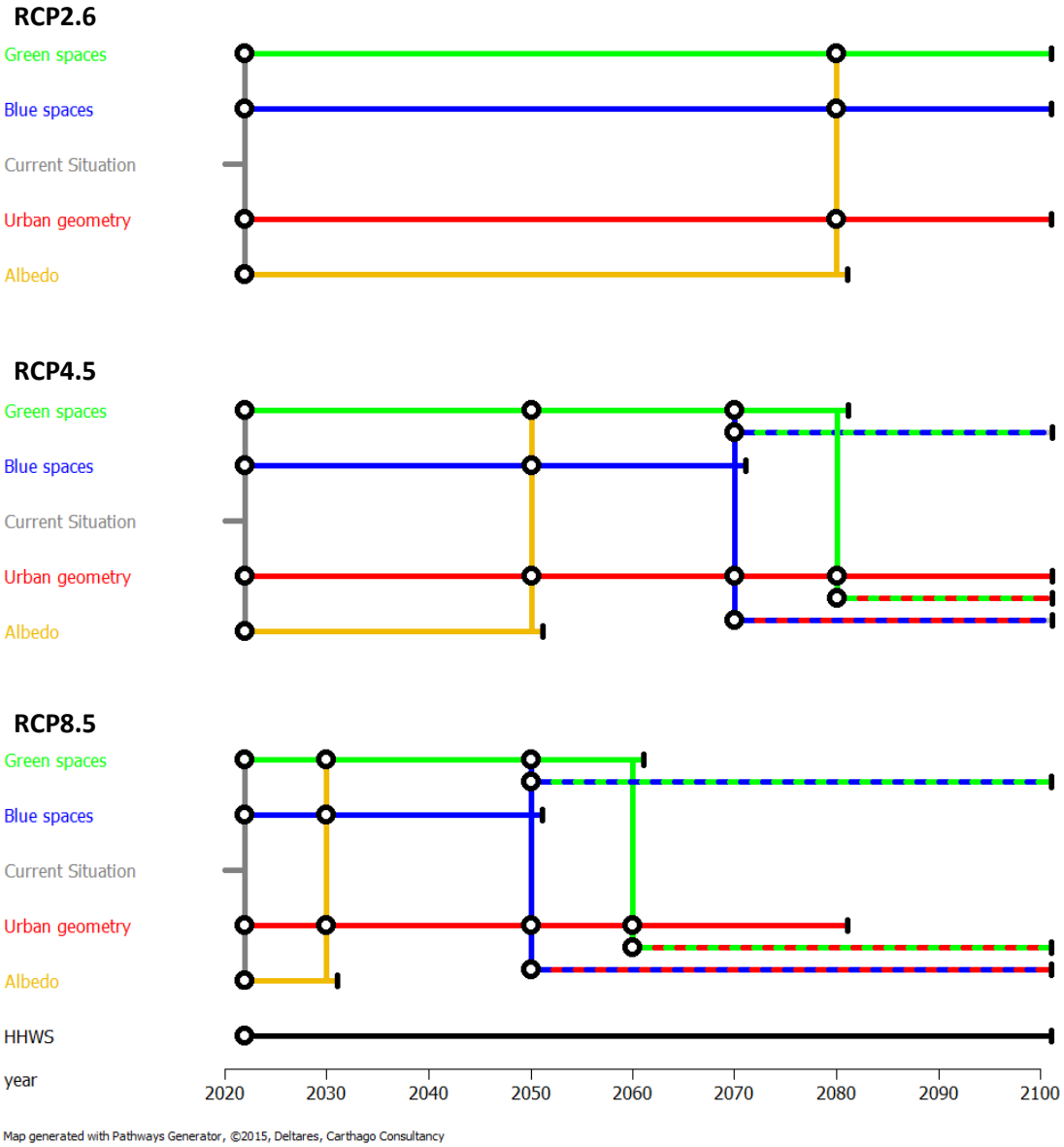

Figure 40: *Metro maps for three different future scenarios (top to bottom: RCP2.6, RCP4.5, RCP8.5). Four groups of adaptation actions, namely green spaces in green (e.g. vegetation), blue spaces in blue (e.g. water bodies, fountains, gravel roads), urban geometry in red (e.g. orientation of street canyons, shape of buildings), and albedo in yellow (bright surfaces). Dashed paths mark combined actions. A separated path for HHWS is mapped at the bottom in black (own figure, metro maps generated with https://publicwiki.deltares.nl/display/AP/Pathways+Generator).*

The classification of each adaptation group in the diagram in figure 41 is based on the results of the sensitivity analysis and on a study conducted by Lai *et al.* (2019). As the adaptation pathways, the classification is just qualitative and can vary significantly between cities and between districts within a city. Since technologies are constantly developing and probably will drop in cost in the future, the placement of each measure in the diagram can change over time and should not be regarded as absolute (Haasnoot, Warren & Kwakkel 2019).

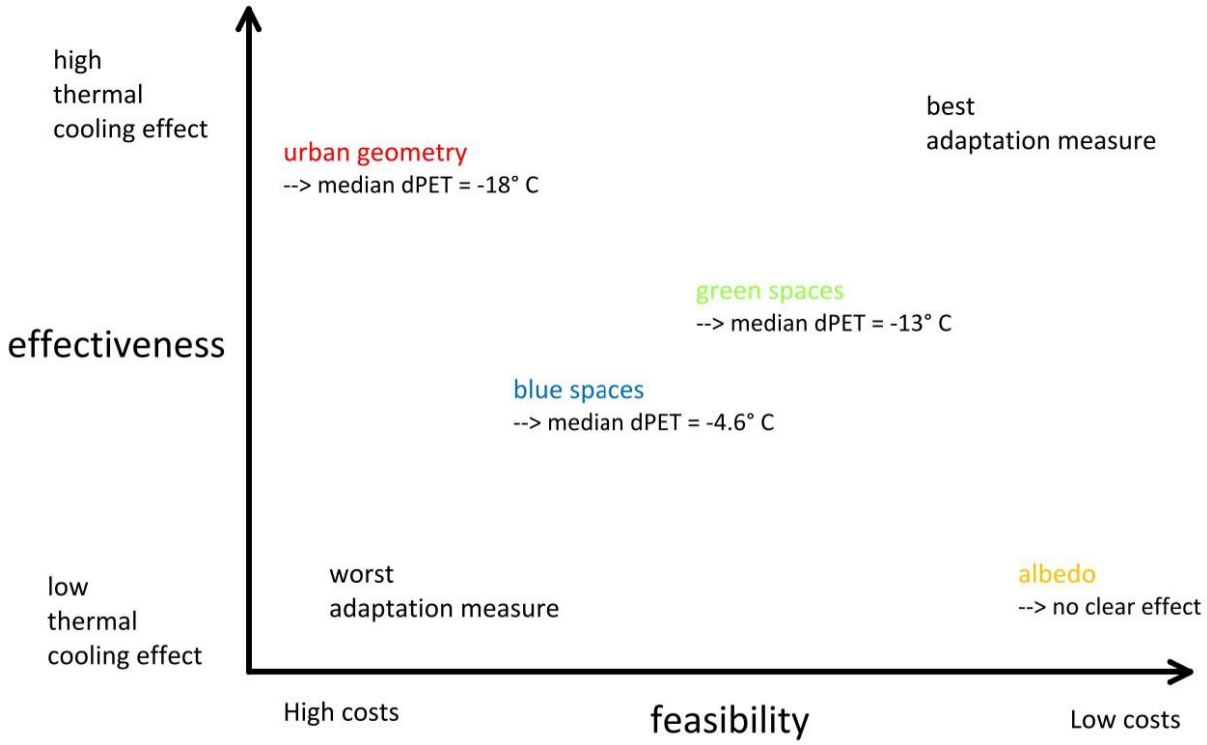

Figure 41: *Feasibility-effectiveness diagram including the four main groups of adaptation options. The feasibility is rated according to the costs (money, time, realizability) and the effectiveness according to the effect on thermal stress. The best adaptation action would be in the top right, the worst in the bottom left corner (own figure, according to Lai et al. (2019)).*

7 Discussion

7.1 The right choice of a WBGT approach

As seen in chapter 6.2.1, there are huge differences amongst the calculated WBGT values in Basel. The Steadman (1994) approach has considerably higher values during the spring, summer, and autumn seasons compared to the Bernard (1999) and Ono and Tonouchi (2014) approaches. During the winter season on the other hand, the Steadman (1994) approach slightly underestimates WBGT. However, the differences between all three investigated approaches are negligible during winter.

There is no clear reason for this huge cap between the Steadman (1994) and the other two approaches. One explanation could be that all three equations were empirically derived and thus base on input data of a specific region. The Steadman (1994) approach was initially developed for an application in Australia, the Bernard (1999) approach was used for a study in Central Alabama, and the Ono and Tonouchi (2014) approach was implemented to evaluate heat waves in South Korea. Depending on the predominant climatic conditions at each region, the resulting equations could be quite different. In order to get the most accurate data as possible for a specific city or region, it would be necessary to develop a local specific WBGT approach. To improve this approximation, a WBGT measuring station could be used to calibrate and evaluate the results.

If developing a region specific WBGT approach or the maintenance of a WBGT measuring station is not possible, it is especially important to rethink the choice of an already existing approach, as it is done in this thesis. The incorporation of more than one approach helped making the heat stress analysis more robust. The differences amongst the three WBGT approaches made clear that the use of an empirically derived formula has limitations. The choice of a specific approach had a considerable influence on the resulting heat stress indices and thus on the actions decision-makers would develop. If the Steadman (1994) approach would be applied, very stringent adaptation measures would be required since the simulated heat stress massively overestimates the expected climatic development in the future. However, a comparison to the other two approaches as well as raw air temperatures shows that the values are unrealistic and thus lead to the choice of another, more appropriate approach (Bernard 1999).

7.2 Projected impacts of climate change on human health in Basel

All executed simulations predict a gradually increasing thermal stress in Basel until the end of this century, regardless of the investigated RCP scenario. However, the differences between the three future scenarios are substantial. In the case of NED per year, the annual increase is more than seven times higher under RCP8.5 compared to RCP2.6 (table 6 in the appendix). The difference in the annual

increase of NEE and LEE is less significant (4.35 times and 3.5 times respectively, table 6), although still substantial.

A closer look at the trendlines of the observations and the three simulations highlights that currently, we are on a path which is worse than under RCP4.5 and RCP2.6, but the increase is less steep compared to RCP8.5. These results on the one hand point out that stringent climate protection measures could have a massive positive effect on how future thermal conditions will develop in Basel. Trying to follow RCP2.6 instead of RCP4.5 or RCP8.5 makes a huge difference in the future in terms of the frequency, severity, and duration of heat waves. On the other hand, the results also make clear that regardless of the future scenario, specific adaptation measures to cool down urban heat islands are inevitable.

In this master's thesis, the focus is primarily on daytime conditions. However, to get a thorough understanding of health impacts due to heat in urban areas, heat exposure during the night should be considered as well. Murage, Hajat and Kovats (2017) particularly looked at nighttime thermal conditions in the city of London. They state that under certain conditions and especially for people of younger age groups (below the age of 65 years), elevated nighttime temperatures can be as impactful or even worse compared to abnormally high daytime temperatures. The results of their study exhibited that elevated nighttime temperatures were particularly impactful when a hot day was preceded by a hot night or vice versa. The reasons for these findings are not fully discovered yet. A plausible explanation could be that hot temperatures during the night could interfere with physiological processes which are important for the regulation of the sleep-wake cycle as well as the body's internal thermoregulation (Murage, Hajat & Kovats 2017).

A first assessment of how consecutive hot days and warm nights could develop in the future in Basel can be drawn from the NEE and LEE simulations. More extreme events are expected in the future and the longer they last, the more nighttime temperatures will gradually increase. As the future simulations show that NEE and LEE will increase under all discovered future scenarios, the number of tropical nights ($T_{min} \geq 20°$ C) can be expected to increase accordingly. Important to consider here however is the cloud cover over the city during the nights. If the nights are cloud-free, heat can easily escape to space. Refreshing morning hours will counteract the heat stress during the day to a certain degree. Clouds on the other hand act as an impervious cover for warm air (thermal radiation). Thus, temperatures do not much fluctuate over the course of one day and therefore gradually increase from night to night (Global radiation balance --> Schneider (1972), Wild *et al.* (2015)). The worst weather conditions in terms of heat stress are therefore a cloud-free sky and very hot air during the day followed by a cloud-covered night with little wind.

For a deeper analysis of the UHI effect and the impacts of climate change on human health in Basel, further research about specific nighttime conditions is needed. The results of the daytime and

nighttime studies could then be compared and combined to gain an extensive understanding of potential impacts of increasing urban temperatures on human health.

The trendlines for all scenarios show an unequivocal picture for the future. WBGT will increase and accordingly do NED, NEE, and LEE. However, the differences amongst the experiments are quite substantial. This shows that it is not straight forward to make a clear prediction of how thermal stress will affect the population in Basel in the next 50 to 80 years. Furthermore, it is unclear at which speed the thermal stress will intensify in the upcoming years. It is possible that a more or less linear trend will occur until the end of this century. Another possibility could be that a period of a weak increase will be followed by a very strong increase, or vice versa. A third imaginable development could be characterized by alternating periods of short cooling and longer warming phases. Which one of these scenarios is finally turning into reality is hard to predict. It certainly depends on the applied global climate protection measures. Figure 28 illustrates that under strict mitigation measures (RCP2.6), the rising trend will stagnate in the upcoming decades. If no climate protection measures are implemented (RCP8.5), however, the increase is going to speed up until the end of this century.

These findings once again emphasize that the complexity of the climate system notably impedes the process of developing appropriate adaptation measures.

7.3 Adaptation measures

In the following sections, some of the listed adaptation measures in table 5 in chapter 6.2.8 are discussed in detail and applied to the conditions found in Basel.

7.3.1 Urban geometry and air ventilation

The analysis of the effect of wind on the felt temperature clearly demonstrates that a pronounced ventilation and supply of fresh and cool air in a city efficiently enhances the thermal comfort in urban places. The EM simulations with decreased wind speeds lead to higher WBGT values and therefore to more and longer-lasting heat events whereas the simulations with slightly increased wind speeds only lead to minor changes in the derived heat indicators. One reason for this result can be attributed to the fact that rather high wind speeds were observed at the location of the measuring station. The wind speeds are higher most of the time than the proposed threshold for 'good urban ventilation' of 1.3 m/s (Yuan & Ng 2012). Simulating an increase of 1 m/s has therefore no decisive effect to further improve the thermal conditions. Since the location of the measuring station is outside the city center and the wind sensor is attached to a mast in a height of 12 m, natural breezes are not blocked by any obstacles and therefore directly noticeable.

Water bodies are able to induce a local ventilation effect and thus can have a huge impact on local air temperatures. Especially during cold nights, lakes and rivers are warmer compared to their direct vicinity and thus pull cold air from surrounding areas. This ventilation effect results in a minor cooling.

The cooling effect is especially strong during hot summer days. Chen *et al.* (2014) found that rivers in urban places can reduce the temperature of their direct vicinity by about 10° to 15° C. However, without efficient and perfectly aligned air canals to remote districts, this cooling effect diminished rapidly within a distance of only 100 m.

In Basel, the river Rhine has the potential to cool down the city through evaporation and ventilation. Especially in combination with nearby vegetated places. However, the implementation of effective ventilation channels which transport cool air to districts further away from the river is not straight forward. It is difficult to change existing building geometries and arrangements along the river in a way that they support the air flow through the street canyons. Huge construction measures would need to be undertaken. In Basel, rows of buildings along the waterfront of the Rhine actually prevent a cool air flow from entering into the inner areas of both old towns (Grossbasel, Kleinbasel) (figure 42). The sole sections where air is potentially able to flow from the river into the city centers are at big road bridges. Wide roads create a gap between continuous building fronts. Changing the building geometry at other sections alongside the river would be associated with massive cost and construction efforts. Furthermore, most of the buildings in the old towns and alongside the river are under preservation order. Implementing construction changes are therefore not possible or associated with strict constructional requirements (Basel-Stadt 2022a, Rahuel et al. 2021).

Figure 42: *Row of houses along the Rhine which blocks cool air to enter the city (own image).*

Changing the urban geometry must therefore be approached differently for existing districts and for districts which are not realized yet.

Analyzing the spatial distribution of the UHI effect in Basel (figure 17) reveals that block developments are far worse for an active ventilation in the city compared to row developments. The thermal comfort in block developments like Gotthelf, Gundeldingen, or Dreispitz is by far worse than in the row developments Bruderholz or Gellert. To improve the thermal comfort in the whole city, a very effective measure would thus be to plan and build open row developments in the outer parts of the city instead of enclosed block developments. The openings of the rows should point towards the city in order to maintain a fresh air supply. An optimized urban geometry should contain long and open canals (e.g.

street canyons) which range from the town boundaries into as many inner districts as possible. Well aligned row developments combined with the usage of bright construction materials for roofs, facades, and other big open places are key points to consider when planning new districts in the peripheral parts of the city. Open places and broad street canals allow fresh air to circulate through the city and provide ample places for vegetation. Figure 43 shows an example of an opening along a house front in Gundeldingen. However, this example only reaches about 100 m into the block development. For an improved cooling in the whole district, the opening should be much deeper to reach the innermost areas.

Figure 43: *Opening in the house front of the block development Gundeldingen. The cooling effect is enhanced with a small cluster of trees (own image).*

7.3.2 Green spaces and water bodies

The Rhine as well as the surrounding topography (Vosges, Black Forest, Jura Mountains) in Basel and the Lake Zurich, the Limmat, the Shil, and the Üetliberg in Zurich play a major role in regulating the local climate. Whereas surrounding mountains in general are the reason for diurnal variations of air supply through mountain and valley winds, large water bodies on the other hand essentially influence the air temperature variations within cities. Water acts as a perfect heat storage. Through its high heat capacity, it warms up less quickly during very hot periods compared to for example asphalt or meadows. During colder periods, water can hold the stored heat longer and thus releases it slower to the near surrounding. Due to these specific properties, water bodies act as heat sink during heat waves and as warming body during cold snaps. Chen *et al.* (2014) investigated the role of water bodies in urban places as regulators of local temperature variations. They found that urban rivers in general have a measurable effect, however, it is less strong compared to rivers in rural areas or highly vegetated places. Oftentimes, high buildings block horizontal dispersions of air masses and thus prevent large-scale cooling or warming effects within cities (Burmeister, Büter & Trute 2019, Chen et al. 2014).

As discussed in the previous chapter, changing the orientation, geometry, and arrangement of existing buildings like for example converting a block into a row development or realizing openings in the house fronts of block developments is very elaborate and therefore associated with huge financial and constructional investments. Hence, less expensive and complex solutions to minimize heat stress are needed, especially in existing districts of the city. The most effective and economically as well as

ecologically friendly measure would probably be the creation of green spaces in combination with open water surfaces. The image in figure 44 shows an example of an open place with a lot of trees and a small central fountain.

Figure 44: *Combination of trees and an open fountain in the Margarethenpark leads to a strong cooling effect (own image).*

A study published by Wende, Rößler and Krüger (2014) investigated the potential effects of green spaces on air temperatures. The scientists concluded that an amount of about 30% green space in a city could lead to a reduction of 1° C on average (Wende, Rößler & Krüger 2014). The higher the amount of green space, the stronger the cooling effect. In extreme cases, a cooling of up to 7° C could be measured (combined effects of evapotranspiration and shadowing) (Weber et al. 2018).

In the case of Basel, potential places for vegetation are along railways and the railway stations (figure 45), inside of the exhibition area (figure 46), or in the courtyards of block developments (e.g. Gundeldingen, Dreispitz, or Gotthelf). However, at places where planting trees or other vegetation types are not possible due to a lack of space or safety restrictions (e.g. along narrow lanes in the city center, in or near historic districts (Kleinbasel and Grossbasel), at heavy traffic loads, or at sealed places), other solutions are necessary. One possible solution would be to unseal surfaces and make use of a porous material. Percolation surfaces like gravel have the benefit that rainwater can infiltrate into the pores and be stored for several days. During hot periods, the stored water can evaporate and

Figure 45: *An open water body near the railway station Basel SBB with some small trees (own image).*

Figure 46: *Sealed and open place in the exhibition area. The existing water fountain on the left side could be combined with a cluster of trees to enhance the cooling effect (own image).*

cool down the streets. Additional advantages of a well implemented rainwater management in a city are the minimization of the risk of floods, the support for refilling of groundwater acquifers (Rahuel et al. 2021), and an improved situation for the irrigation of vegetation. Another possible solution would be local installations which generate artificial clouds a few meters above the ground. The mist in the air is able to reflect shortwave radiation to a certain extent before it hits the surface as well as cools down the atmosphere through evaporation of small water droplets. This specific adaptation measure is currently being tested in Zurich at the Turbinenplatz in order to check whether the cooling effect justifies a heightened water consumption (Minor & Unternährer 2022).

Tree species and planting configurations:

So far, vegetation was viewed in a general way without a differentiation between vegetation types (e.g. different tree species) or possible planting configurations (e.g. trees in a cluster, in a row, or as isolated plants). The cooling effect of trees in urban areas can significantly be enhanced by choosing the right tree species and an optimal planting configuration. For a sustainable development of urban trees, they need to be as long-lived as possible and experience a healthy process of growth. Furthermore, they should not need too much water to grow. It is difficult to select the right tree species and apply good growing conditions in urban environments. Hot temperatures, the lack of water in the soil, a restricted rooting space, a bad growth substrate, and diseases inhibit an optimal growth (Sjöman et al. 2012).

Zhao *et al.* (2020) investigated the effect of different trees on the microclimate in urban places. They differentiated between deciduous and evergreen (conifer) trees as well as between three different planting configurations, namely group, linear, and individual planting. They concluded that deciduous trees clearly outperformed evergreen trees in terms of transpiration rates and stomatal conductance. Therefore, they stronger influenced urban air temperatures. Furthermore, they found that grouping was much more efficient than linear planting. Individual trees had the weakest effects on the microclimate. According to these findings, it is recommended to plant deciduous trees (e.g. beeches or buckeyes) instead of coniferous trees, whenever possible in groups or clusters of several trees. However, the scientists also mentioned that too dense planting is not favorable either (Zhao et al. 2020).

Further information about the selection of optimal tree species for urban environments can be found in Sjöman *et al.* (2012). They conducted two case studies, one in central China and the other in Romania, in order to propose a selection of tree species which is optimal for urban environments.

Stream excavation and renaturation:

Beside of the Rhine as main stream through Basel, there are three smaller streams which wind through the city. The Birs flows along the southeastern border of Basel-Stadt and Basel-Landschaft and enters

the Rhine just above the industry park of Roche. The Birsig and the Wiese enter the Rhine a little bit further downstream (figure 47).

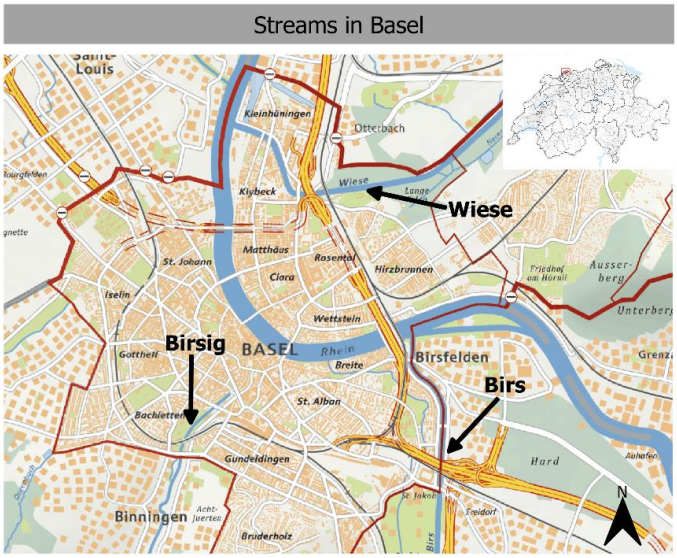

Figure 47: *Overview of three streams in Basel which have the potential to be excavated and/or renatured (own figure, based on Basel-Stadt (2021a)).*

According to the findings of two studies conducted by Kim *et al.* (2009) and Kim *et al.* (2008), the potential of excavating and restoring urban streams to affect the local climatological environment is significantly noticeable. Both studies exhibited a so-called 'oasis effect' through a reduction of air temperatures and a modification of the sensible heat flux along the stream and in its vicinity. They measured a decrease of the ratio of the sensible heat flux to the net radiative flux which indicates a heightened use of energy for evaporation instead of heating the surrounding air. Measurements showed that the cooling effect was stronger, the higher the air temperatures were before the excavation. However, as already mentioned in a previous chapter, the climatological effect of a stream on surrounding air temperatures and humidities is spatially confined, especially when the surrounding configuration of buildings prevent the cool air to be transported away from the stream. A statistical test conducted by Kim *et al.* (2009) indeed classified the drop in the air temperature more than 300 m away from the stream as not significant anymore (Kim et al. 2009, Kim et al. 2008).

After the correction of the Birs in the nineteenth century, several renaturation projects during the last decades put the river course in a more natural environment again. The established nature reserve is on the one hand beneficial for a vast number of plants and animals living in or near the water. On the other hand, enhanced thermal conditions as well as a regained local recreation area are huge ecological upgrades for the residents and the whole city (Basel-Stadt n.d., Küry 2002, Küry 2010).

There are also several ongoing and planned renaturation projects for the Wiese west of Riehen (e.g. WieseVital and WieseVital Plus). Beside of the positive ecological and climatological effects, it is hoped that the flood and groundwater protections are going to be enhanced as well (Basel-Stadt 2022b, WieseVital n.d.).

Figure 48: *Renaturation of the Birs in Birsfelden in 2002 (Küry 2002).*

Figure 49: *Restored Birs in Birsfelden in 2010 (Küry 2010).*

7.3.3 Demographic distribution

Developing and planning suitable adaptation measures demands to not only look at climatic conditions in a city. It also includes considering the demographic distribution. Special attention hereby should be given to the distribution of health care facilities, hospitals, kindergarten, and schools. Figures 17 and 18 in chapter 6.1.2 present an overview map of all hospitals and nursing homes in Basel. The distribution of the facilities indicates that there are huge differences in the exposure to heat discomfort. Facilities closer to the city center are in general more affected by an increased UHI effect than those in the peripheral districts. The Residenz Südpark (number 1 in figure 17) for example is located in the block development Gundeldingen right next to the railway station Basel SBB. A strong UHI effect in this area therefore demands putting particular efforts in this district to protect the occupants from threatening thermal conditions. The same is true for the nursing homes Irides AG (number 2 in figure 17) near the old town Grossbasel and Zum Lamm (number 3 in figure 17) and Gustav Benz Haus (number 4 in figure 17) in the old town Kleinbasel. Due to preservation orders, it is difficult to realize geometry changes at existing buildings to improve the thermal conditions. The courtyards of these buildings, however, provide the opportunity to plant trees and other vegetation and to combine it with open water surfaces like fountains. Such small, encapsulated courtyards inspired by nature ensure local oases with significantly lower air temperatures. These idyllic green gardens not only enhance the thermal comfort but also support the general well-being of the inhabitants.

7.4 Heat-Health Warning System (HHWS)

Instead of developing and implementing adaptation measures directly in the city to cool down hot spot areas or working on global climate change mitigation measures, another solution would be to devise strategies to caution the population from an upcoming hot spell as early and reliable as possible in order to plan appropriate preventive conduct recommendations. It is clear that the amount and

severity of heat waves will increase in the future, even if some of the abovementioned adaptation measures or global mitigation plans are implemented. Therefore, so called Heat-Health Warning Systems (HHWS) in order to warn the population are in demand. They are not meant to replace adaptation measures but rather should act as complementary tools.

The results from the feature scoring analysis clearly demonstrated that the choice of an optimal threshold range for extreme days is much more important and therefore has a stronger influence on the estimated heat indicator than the choice of a climate scenario or a climate model. Whether for the prediction of NED, NEE, or LEE per year, the choice of the threshold was more than two times more decisive for the outcomes than the RCP or the climate model. The outcome of this analysis is consistent for both Basel and Zurich. This finding helps decision-makers to develop appropriate and effective HHWSs. However, the development of a general HHWS which holds for the whole population in a city is associated with many trade-offs. It is difficult to treat the population in a city as one unite, especially in the field of preventative health care measures. Morabito *et al.* (2019) therefore recommended developing personalized warning systems which take into account several individualizations: The age of a person, the physical activity, the clothing, the behavioral characteristics, the working environment, or the heat acclimatization (Morabito et al. 2019). Especially the latter factor is important to consider since the feeling of and the physiological reaction to very hot temperatures is individual. On the one hand, people originating from hot climatic regions are generally better adapted to high temperatures compared to people who grew up in higher latitudinal regions. On the other hand, heat acclimatization can also relatively easy be trained. The adaption to increased temperatures may take several weeks, however, the effect is clearly measurable. Acclimatized people exhibit adjusted cardiovascular, endocrine, and renal systems. The sweat rate in general is increased which leads to a massively improved thermal regulation in the body (McGregor et al. 2015). A study conducted by Tian et al. (2011) confirmed these biological adaptions in the body after systematic acclimatization trainings. The scientists determined significant physiological changes in the body ranging from an increased sweat rate over dilated blood vessels in order to increase the heat loss of the body to slightly adapted heart rates (Tian et al. 2011). Due to these findings, the threshold for extreme events should be adjusted appropriately and applied for various groups of people.

A detailed example of a personalized HHWS can be found in Morabito et al. (2019). They determined tailored WBGT thresholds for various groups of workers and simultaneously included behavioral recommendations and an overview for an optimal water consumption (Morabito et al. 2019).

A second very important aspect to consider when developing a HHWS is the choice of a thermal comfort index. The effectiveness of a HHWS is directly controlled by the selection of an appropriate index. As discussed in chapter 7.1, the resulting WBGT values can be quite different. Consequently, the number of heat wave days and the severity of those extreme events could potentially be predicted

incorrectly (Heo, Bell & Lee 2019). For that reason, it is recommended to evaluate thermal comfort indices that are best suited for the region of interest.

7.5 Metro map and feasibility-effectiveness diagram

Since the UHI effect, the urban structure, and the demographic distribution are very heterogeneous in cities, it is not possible to apply the metro maps in figure 40 in chapter 6.2.8 one-to-one to the whole city of Basel or Zurich. The effectivities of certain adaptation measures are therefore rather location-dependent. Furthermore, at some places, certain adaptation measures are not realizable due to specific restrictions or a lack of space. Therefore, these metro maps are meant as an overview of one among many possible solutions. The proposed pathways can be used as baseline, the adaptation tipping points, however, should be evaluated specifically for different districts in the city (Ashraf Vaghefi et al. 2021, Lawrence & Haasnoot 2017, Haasnoot, Warren & Kwakkel 2019, Haasnoot et al. 2013).

The efficacy of an adaptation measure to alter WBGT is very dependent on where and how it is implemented in the city. For example, if trees are planted in areas where, due to an optimized urban geometry, already a lot of shady places exist, the cooling effect is much less pronounced compared to the effect in open areas. Or, if water bodies are constructed while taking into consideration the local street orientation, it is possible to improve the cooling effect through an enhanced channeling of cool air. These two examples affirm that it is important to not implement the adaptation measures independently from each other but to try to develop strategies where various measures are implemented together (complementarily). Such combinations of adaptation measures are marked with dashed lines in the metro maps (figure 40).

Changing, adapting, or optimizing the urban geometry are rather cost and time intensive actions. As discussed in a previous section, there are conflicts with the guidelines of the preservation order. Increasing the surface albedo or planting trees on the other hand is much easier to realize. According to studies, the urban geometry measure in return is much more efficient compared to for example the albedo measure. It is therefore recommended to start following the yellow, green, and blue paths of the metro maps in the near term, depending on the highest feasibility and lowest costs. This gives some time in the long term to develop effective plans for changing and adapting the urban geometry, either for existing or for projected districts.

Following the yellow path, however, requires well thought out plans where to implement reflective surfaces. Studies have shown that a cooling effect could be negligible if the measure is implemented incorrectly. Some findings even calculated a reduced thermal comfort for people walking through the streets or sitting on a bench due to an increased solar re-radiation to the pedestrians (Lai et al. 2019, Yang et al. 2016, Taleghani & Berardi 2018).

The metro maps for RCP4.5 and RCP8.5 include some dashed paths which indicate options of combined adaptation actions. Basically, it is possible to combine any adaptation action with any other in order to improve the cooling effect. However, it is important to carefully rethink which combination is applied and how the measures interact with each other. Probably the most efficient combinations are those which include either the green, blue, or red paths. The interaction of shadowing, evapotranspiration, and urban ventilation can significantly enhance the thermal comfort in the city (Weber et al. 2018). The combined paths in the metro maps therefore do not end where the paths of single actions end but rather go on until the end of this century or even beyond.

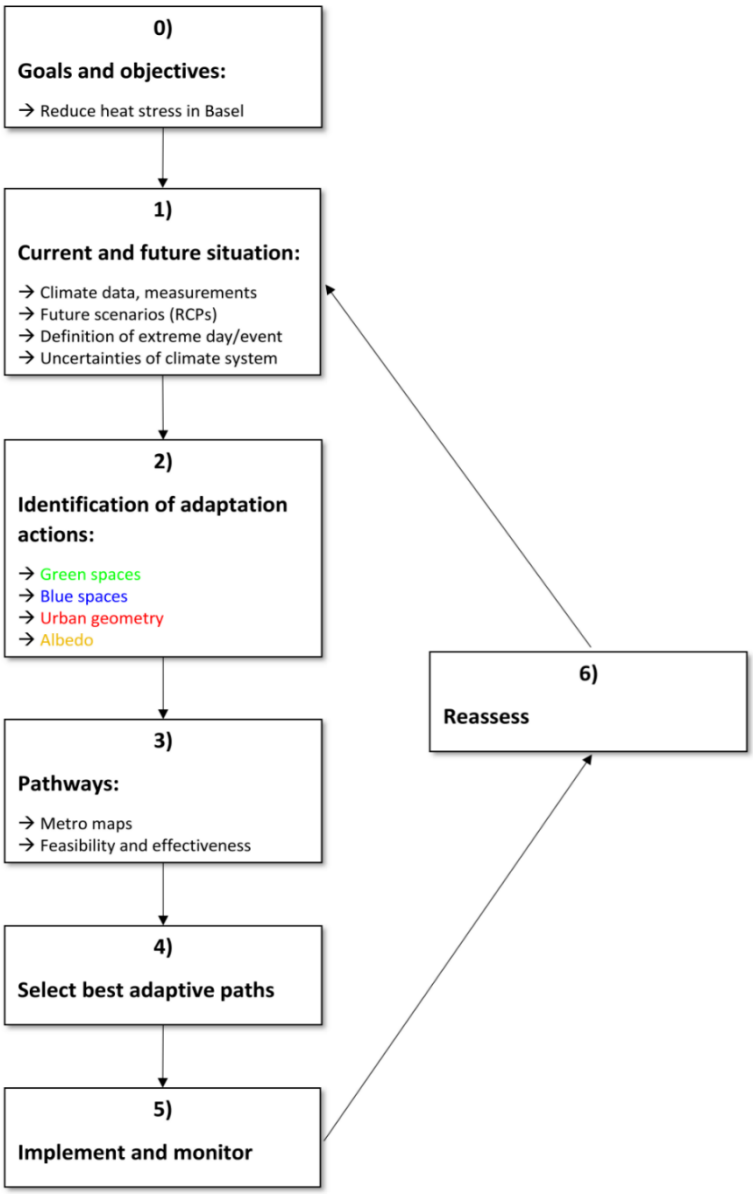

Figure 50: *Steps of the DAPP approach applied for the heat stress study in Basel (own figure, according to Haasnoot et al. (2013), Haasnoot, Warren & Kwakkel (2019)).*

Both the metro maps as well as the feasibility-effectiveness diagram are an essential part of DMDU and DAPP. Figure 50 summarizes all important steps of DAPP according to Haasnoot *et al.* (2013) and Haasnoot, Warren and Kwakkel (2019). The DAPP approach is an iterative process. After every step, the current situation must be reassessed and newly evaluated.

7.6 Climatic differences between Basel and Zurich

The results reveal that Basel is stronger affected by uncomfortable thermal conditions than Zurich in the future. The main reason for this difference is due to different macroclimatic conditions. The measuring station in Zurich is located 556 m a.s.l. whereas the station in Basel is positioned at an altitude of 316 m a.s.l. Using the moist adiabatic lapse rate (-0.6° C per 100 m height gain), the height difference of 240 m would correspond to a temperature difference of 1.44° C. This difference matches quite good with the results of the WBGT and heat indicator analysis.

A second cause for the difference can be found in topographic circumstances. The measuring station in Zurich is situated on a small hill. The vicinity to a small forest and thus to a local cold air production area leads to decreased temperatures compared to conditions measured in the city. Although the station in Basel is located at the periphery as well, it is probably still more affected by the urban climate than the station in Zurich.

These findings emphasize the importance to always consider the environment of the measuring station and to compare it to the situation in the city. The measured values at the station can be quite different compared to actual conditions in the city center. To get a more realistic picture about the thermal conditions in a city and potential future changes, a widespread network of measuring stations should be installed. As done for the measuring station in Basel-Binningen, future simulations should then be calculated based on the observations collected with the measuring network. A comparison of the results between the measurement network in Basel and Zurich would be much more reliable than simply comparing two standalone measuring stations.

7.7 Potential sources of errors

As discussed in the previous sections, the climate is a highly complex and non-linear system. A lot of processes are happening randomly and thus cannot be described properly yet. Combined with uncertainties of socio-economic developments, making reliable predictions for the future is difficult. In order to make future calculations, simplifications in all involved systems had to be made. Every simplification of a system, however, implicates a potential source of error.

A second source of error arose from the data (observations and future simulations). The measuring stations are not completely accurate. Without a periodic maintenance and proper calibration, measurement errors could arise. There are two types of measurement errors, namely data inaccuracy and data imprecision. Whereas the former describes how close the observations are to virtual true values, the latter describes the closeness of the observations to each other (Wikipedia 2022b).

In the case of the measuring stations used for this study, a further aspect had to be considered. Since the locations of both stations are not directly in the city center but rather slightly elevated in a peripheral region, it is important to take into account potential differences in the climatic conditions.

The difference in altitude has a potential influence on the measured air temperatures (see chapter 7.6) whereas the proximity to nearby green spaces and the exposition of the wind sensor could influence the measured humidity and wind speeds (see chapters 6.2.4 and 6.2.5). Figure 37 and figures 65, 66, 71, 72, and 73 in in the appendix show results of simulated increased urban heat conditions. It is clear that this approach is a strong simplification of the reality. However, it gives a first overview of potential differences between the location of the measuring station and the city centers. The results suggest that the difference could reach a factor between 1.5 and 4 (depending on the RCP scenario, the considered heat indicator, and the city under investigation). This is a quite substantial variance which clearly points out that the heat conditions in some places in a city could be far more impactful for human health than those in the peripheral regions.

Another possible solution to handle the height difference of the measuring station to the city center is to apply a standard lapse rate of e.g. -0.6° C per 100 m height gain (Wicki, Parlow & Feigenwinter 2018). This technique allows to convert the measured and simulated air temperatures at the measuring station to different altitudes. However, the conversion of the relative air humidity, global radiation, and wind speed is more difficult.

Finally, a third potential source of error lies in the empirical formula used to calculate WBGT. Since it is an empirically developed equation for a specific region on Earth, the calculated values for Basel or Zurich could be slightly different to real WBGT values which would be measured with a proper measuring station.

8 Conclusion

An increasing number of severe heat waves and long-lasting droughts all over the world impressively demonstrate that climate change is real and hitting us with great force. Extreme climate events are becoming more frequent and long-lasting. The appearance of spatially and temporally combined extreme events makes the situation even more threatening. The impacts on nature and humanity are already huge and according to various studies expected to become even worse in the future.

The aim of this master's thesis was to investigate how climate change, and in particular an intensifying Urban Heat Island (UHI) effect in urban places, will develop in Switzerland, what impacts on human health are to be expected in the future, and what adaptation measures are the most suitable to reduce the threat of thermal stress. As case studies, the cities of Basel and Zurich were examined.

In the first part of this thesis, the UHI effect in Basel was analyzed. The UHI effect basically describes the temperature difference between urban and rural landscapes in comparable macro-climatic conditions (Burgstall 2019, Parlow, Vogt & Feigenwinter 2014). The example of Basel showed that the UHI effect is very heterogeneous. There are clearly distinguishable hot spots in which the thermal comfort is particularly bad. In Basel, these places are, among others, the railway stations (Basel SBB, Basel Badischer Bahnhof), the exhibition site, both old towns (Grossbasel, Kleinbasel), and in general block developments (Gundeldingen, Gotthelf, Dreispitz). Cool spaces on the other hand are primarily in open districts with a pronounced air circulation (row developments like Bruderholz and Gellert) and parks with a lot of vegetation and open water bodies (Zoo Basel, Kannenfeldpark, Schützenmattpark).

In order to get an improved understanding of the potential heat stress in Basel and Zurich, a special heat index was needed. The wet-bulb globe temperature (WBGT) is a weighted temperature measure which brings together the air temperature, relative air humidity, radiation, and wind speed into one single value. WBGT is a commonly used measure to quantify heat stress in various applications (Lemke & Kjellstrom 2012). In this thesis, empirically derived mathematical formulas were used to calculate the daily WBGT for a historic time period (1981-2020) as well as for future simulations (1981-2099). Based on the obtained results, three heat indicators were determined (number of extreme days per year, number of extreme events per year, average length of extreme events per year) in order to predict the potential impacts of heat on human health.

Since the climate is a very complex and highly non-linear system with many uncertainties, theories of Decision Making under Deep Uncertainties (DMDU) were applied in this study (Exploratory Modeling (EM), Dynamic Adaptive Policy Pathways (DAPP)). A wide range of possible future states for three different scenarios (RCP2.6, RCP4.5, RCP8.5) were calculated using an exploratory modelling approach (EMA Workbench (Kwakkel 2017)). Each model run represents the result of a randomly chosen combination of external factors and policies.

The findings of the EMA Workbench unambiguously pointed out that thermal stress is already pronounced in Basel and Zurich and will further enhance in the next decades. The future trends however are very different depending on the chosen RCP scenario. Whereas under RCP8.5, one has to expect more than a doubling of the number of extreme days and of the average length of extreme events in Basel per year until the end of this century, RCP2.6 rather predicts a stagnation and under some circumstances even a decrease in the upcoming years. The future trends for Zurich are very similar, though the heat stress in general is slightly lower compared to Basel.

The current heat stress in Basel and the predictions for the future proved that global mitigation measures against climate change and site-specific adaptation actions must be developed and implemented as soon as possible. A deep literature review as well as a sensitivity analysis pointed out that optimizing the urban geometry (e.g. orientation of street canyons, shape of buildings), increasing the amount of green spaces, and building open water bodies are the most effective measures to cool down very hot places (Lai et al. 2019). A thought-out combination of multiple actions further enhances the cooling effects. Increasing the surface albedo, even though comparatively easy and low in costs to implement, probably leads to rather small changes in the thermal situation (Taleghani & Berardi 2018). It can be implemented as transitional solution, however in the long term, other actions are much more effective.

Complementary to adaptation actions, Heat-Health Warning Systems (HHWS) could help to specifically caution vulnerable groups of people against upcoming heat waves and to declare situative conduct recommendations (Morabito et al. 2019).

This study demonstrated that developing suitable adaptation measures is not straightforward and needs detailed knowledge about site-specific circumstances. They must be individually evaluated and adapted to local weather/climate conditions, demographic compositions, urban characteristics, and legal frameworks. Building regulations in old towns and the lack of space in dense districts oftentimes further restrain the feasibility of efficient actions. It is therefore crucial that for the process of decision-making, all affected participants should be included (inhabitants, politicians, private sector) in order to achieve the most effective and sustainable solutions.

Further research on this topic is certainly needed since this thesis only explored the current and future heat stress in Basel and Zurich during daytime. It would be interesting to also investigate nighttime thermal conditions to get a complete understanding of potential impacts of heat waves on human health in cities. In addition, investigating other heat indices besides WBGT and the usage of improved technologies (measurements, measurement networks, models) could help decision-makers to develop more efficient strategies to fight against the increasing heat stress in urban areas.

9 Bibliography

Abram, Nerilie J, Henley, Benjamin J, Sen Gupta, Alex, Lippmann, Tanya JR, Clarke, Hamish, Dowdy, Andrew J, et al. 2021, 'Connections of climate change and variability to large and extreme forest fires in southeast Australia', *Communications Earth & Environment*, vol. 2, pp. 1–17, DOI: 10.1038/s43247-020-00065-8.

Ashraf Vaghefi, Saeid, Muccione, Veruska, van Ginkel, Kees CH, & Haasnoot, Marjolijn 2021, 'Using Decision Making under Deep Uncertainty (DMDU) approaches to support climate change adaptation of Swiss Ski Resorts', *Environmental Science and Policy*, vol. 126, pp. 65–78, DOI: 10.1016/j.envsci.2021.09.005.

Basel-Stadt n.d., *Die Birs - gestern und heute*, *Erhiehungsdepartement des Kantons Basel-Stadt, Gymnasium Kirschgarten*, viewed 10 July 2022, <https://www.gkgbs.ch/obsolet/schulleben/oekowoche/1998-2003/landschaftswandel/unterer-birslauf/die-birs-gestern-und-heute>.

Basel-Stadt 2011, 'Bericht über die Folgen des Klimawandels im Kanton Basel-Stadt', *Kanton Basel-Stadt*, pp. 1–118, <https://www.bs.ch/publikationen/aue/Bericht-Folgen-Klimawandels-Kanton-Basel-Stadt.html>.

Basel-Stadt 2021a, 'Anpassung an den Klimawandel im Kanton Basel-Stadt', *Departement für Wirtschaft, Soziales und Umwelt*, pp. 1–150.

Basel-Stadt 2021b, *Geoportal MapBS, Karten Klimaanalyse*, *Kanton Basel-Stadt*, viewed 22 January 2022, <https://map.geo.bs.ch/?lang=de&baselayer_ref=Grundkarte grau&map_x=2611940&map_y=1267813&map_zoom=2&tree_group_layers_Stadtklima Basel-Stadt=KL_Stadtklima_Waermeinseleffekt&tree_groups=Stadtklima Basel-Stadt>.

Basel-Stadt 2022a, *Willkommen bei Städtebau & Architektur - Kantonale Denkmalpflege*, *Kanton Basel-Stadt*, viewed 12 May 2022, <https://www.denkmalpflege.bs.ch/>.

Basel-Stadt 2022b, *'WieseVital': Die Revitalisierung der Wiese wird konkret*, *Bau- und Verkehrdepartement*, viewed 7 October 2022, <https://www.bs.ch/nm/2022-wiesevital-die-revitalisierung-der-wiese-wird-konkret-bd.html>.

Bernard, Thomas E 1999, 'Prediction of Workplace Wet Bulb Global Temperature', *Applied Occupational and Environmental Hygiene*, vol. 14, no. 2, pp. 126–134, DOI: https://doi.org/10.1080/104732299303296.

Bi, Peng, Williams, Susan, Loughnan, Margaret, Lloyd, Glenis, Hansen, Alana, Kjellstrom, Tord, et al. 2011, 'The Effects of Extreme Heat on Human Mortality and Morbidity in Australia: Implications for Public Health', *Asia-Pacific Journal of Public Health*, vol. 23, no. 2, pp. 27S-36S, DOI: 10.1177/1010539510391644.

Boer, Matthias M, de Dios, Victor Resco, & Bradstock, Ross A 2020, 'Unprecedented burn area of Australian mega forest fires', *Nature Climate Change*, vol. 10, pp. 171–172, DOI: https://doi.org/10.1038/s41558-020-0716-1.

De Bono, Andréa, Peduzzi, Pascal, Kluser, Stéphane, & Giuliani, Gregory 2003, 'Impacts of Summer 2003 Heat Wave in Europe', *United Nations Environment Programme, Environment Alert Bulletin*, vol. 2, pp. 1–4, <https://archive-ouverte.unige.ch/unige:32255>.

Bowman, David MJS, Williamson, Grant J, Gibson, Rebecca K, Bradstock, Ross A, & Keenan, Rodney J 2021, 'The severity and extent of the Australia 2019–20 Eucalyptus forest fires are not the legacy of forest management', *Nature Ecology and Evolution*, vol. 5, pp. 1003–1010, DOI: 10.1038/s41559-021-01464-6.

Budd, Grahame M 2008, 'Wet-bulb globe temperature (WBGT)-its history and its limitations', *Journal of Science and Medicine in Sport*, vol. 11, pp. 20–32, DOI: 10.1016/j.jsams.2007.07.003.

Burgstall, Annkatrin 2019, 'Representing the Urban Heat Island Effect in Future Climates', *Scientific Report MeteoSwiss*, vol. 105, p. 92.

Burgstall, Annkatrin, Casanueva, Ana, Kotlarski, Sven, & Schwierz, Cornelia 2019, 'Heat warnings in Switzerland: Reassessing the choice of the current heat stress index', *International Journal of Environmental Research and Public Health*, vol. 16, pp. 1–19, DOI: 10.3390/ijerph16152684.

Burke, Marshall, Hsiang, Solomon M, & Miguel, Edward 2015, 'Global non-linear effect of temperature on economic production', *Nature*, vol. 527, pp. 235–239, DOI: 10.1038/nature15725.

Burmeister, Cornelia, Büter, Björn, & Trute, Peter 2019, *Stadtklimaanalyse Kanton Basel-Stadt 2019. Grundlagen, Methoden, Ergebnisse*, GEO-NET Umweltconsulting GmbH, Hannover/Dresden.

Byrne, Michael 2020, *Guest post: Why does land warm up faster than the oceans?*, *Carbon Brief. Clear on climate*, viewed 2 January 2022, <https://www.carbonbrief.org/guest-post-why-does-land-warm-up-faster-than-the-oceans>.

Cantón, MA, Cortegoso, JL, & de Rosa, C 1994, 'Solar permeability of urban trees in cities of western Argentina', *Energy and Buildings*, vol. 20, no. 3, pp. 219–230.

Carter, Anabel W, Zaitchik, Benjamin F, Gohlke, Julia M, Wang, Suwei, & Richardson, Molly B 2020, 'Methods for Estimating Wet Bulb Globe Temperature From Remote and Low-Cost Data: A Comparative Study in Central Alabama', *GeoHealth*, vol. 4, pp. 1–16, DOI: 10.1029/2019GH000231.

Casanueva, Ana, Kotlarski, Sven, Fischer, Andreas M, Flouris, Andreas D, Kjellstrom, Tord, Lemke, Bruno, et al. 2020, 'Escalating environmental summer heat exposure — a future threat for the European workforce', *Regional Environmental Change*, vol. 20, no. 40, pp. 1–14, DOI: https://doi.org/10.1007/s10113-020-01625-6.

CH2018 2018, *CH2018 - Climate Scenarios for Switzerland, Technical Report, National Centre for Climate Services*, Zurich.

Chapman, DS & Davis, MG 2010, 'Climate Change: Past, Present, and Future', *Eos*, vol. 91, no. 37, pp. 325–332.

Chen, Yen-chang, Tan, Chih-hung, Wei, Chiang, & Su, Zi-wen 2014, 'Cooling Effect of Rivers on Metropolitan Taipei Using Remote Sensing', *International Journal of Environmental Research and Public Health*, vol. 11, pp. 1195–1210, DOI: 10.3390/ijerph110201195.

Cissé, Guéladio, McLeman, Robert, Adams, Helen, Aldunce, Paulina, Bowen, Kathryn, Campbell-Lendrum, Diarmid, et al. 2022,'Health, Wellbeing, and the Changing Structure of Communities', in, *Climate Change 2022: Impacts, Adaptation, and Vulnerability. Contribution of Working Group II to the Sixth Assessment Report of the Intergovernmental Panel on Climate Change*, Cambridge University Press, Cambridge (UK), New York (USA), pp.1041–

1170, DOI: doi:10.1017/9781009325844.009.

Clark, Jordan 2018, *Comparing the Relationships Between Heat Stress Indices and Mortality in North Carolina*, *master's thesis at Department of Geography, UNC-Chapel Hill*, pp. 1–22, viewed 3 May 2022, <https://www.cisa.sc.edu/ccrc/pdfs/Presentations_2018/Clark_Jordan.pdf>.

Deser, Clara, Phillips, Adam, Bourdette, Vincent, & Teng, Haiyan 2012, 'Uncertainty in climate change projections: The role of internal variability', *Climate Dynamics*, vol. 38, pp. 527–546, DOI: 10.1007/s00382-010-0977-x.

Dodman, David, Hayward, Bronwyn, Pelling, Mark, Broto, Vanesa Castan, Chow, Winston, Chu, Eric, et al. 2022,'Cities, Settlements and Key Infrastructures', in, *Climate Change 2022: Impacts, Adaptation, and Vulnerability. Contribution of Working Group II to the Sixth Assessment Report of the Intergovernmental Panel on Climate Change*, Cambridge University Press, pp.1–183.

Dong, Buwen, Sutton, Rowan, Shaffrey, Len, & Wilcox, Laura 2016, 'EXPLAINING EXTREME EVENTS OF 2015 From A Climate Perspective', *Bulletin of the American Meteorological Society*, vol. 97, no. 12, pp. 557–562, <https://www.jstor.org/stable/10.2307/26265435?seq=1&cid=pdfreference#references_tab_contents>.

Fendt, Lindsay & Schlosser, Adam 2021, *Which parts of the planet are warming the fastest, and why?*, *MIT Climate Portal*, viewed 2 January 2022, <https://climate.mit.edu/ask-mit/which-parts-planet-are-warming-fastest-and-why>.

Filkov, Alexander I, Ngo, Tuan, Matthews, Stuart, Telfer, Simeon, & Penman, Trent D 2020, 'Impact of Australia's catastrophic 2019/20 bushfire season on communities and environment. Retrospective analysis and current trends', *Journal of Safety Science and Resilience*, vol. 1, pp. 44–56, DOI: 10.1016/j.jnlssr.2020.06.009.

Fischer, Paul H, Brunekreef, Bert, & Lebret, Erik 2004, 'Air pollution related deaths during the 2003 heat wave in the Netherlands', *Atmospheric Environment*, vol. 38, pp. 1083–1085, DOI: 10.1016/j.atmosenv.2003.11.010.

Fountain, Henry 2022, *Climate Change Fuels Heat Wave in India and Pakistan, Scientists Find*, *The New York Times*, viewed 12 June 2022, <https://www.nytimes.com/2022/05/23/climate/india-pakistan-heat-wave-global-warming.html>.

Gay, LW, Knoerr, KR, & Braaten, MO 1971, 'Solar radiation variability on the floor of a pine plantation', *Agricultural Meteorology*, vol. 8, pp. 39–50.

Gebhardt, Hans, Glaser, Rüdiger, Radtke, Ulrich, & Reuber, Paul 2016,'Strahlungs- und Wärmehaushalt der Erde', in, *Geographie. Physische Geographie und Humangeographie*, Springer Spektrum, Berlin Heidelberg, pp.240–248.

Gunawardena, KR, Wells, MJ, & Kershaw, T 2017, 'Utilising green and bluespace to mitigate urban heat island intensity', *Science of the Total Environment*, vol. 584–585, pp. 1040–1055, DOI: 10.1016/j.scitotenv.2017.01.158.

Haasnoot, Marjolijn, van 't Klooster, Susan, & van Alphen, Jos 2018, 'Designing a monitoring system to detect signals to adapt to uncertain climate change', *Global Environmental Change*, vol. 52, pp. 273–285, DOI: 10.1016/j.gloenvcha.2018.08.003.

Haasnoot, Marjolijn, Kwakkel, Jan H, Walker, Warren E, & ter Maat, Judith 2013, 'Dynamic adaptive policy pathways: A method for crafting robust decisions for a deeply uncertain world', *Global Environmental Change*, vol. 23, pp. 485–498, DOI: 10.1016/j.gloenvcha.2012.12.006.

Haasnoot, Marjolijn, Warren, Andrew, & Kwakkel, Jan H 2019,'Chapter 4 - Dynamic Adaptive Policy Pathways (DAPP)', in Vincent AWJ Marchau, Warren E Walker, JTM Bloemen, Pieter, & Steven W Popper (eds.), *Decision Making under Deep Uncertainty. From Theory to Practice*, Springer Nature Switzerland AG, Cham, Switzerland, pp.71–92, DOI: https://doi.org/10.1007/978-3-030-05252-2.

Hall, Jim W, Lempert, Robert J, Keller, Klaus, Hackbarth, Andrew, Mijere, Christophe, & Mcinerney, David J 2012, 'Robust Climate Policies Under Uncertainty : A Comparison of Robust Decision Making and Info-Gap Methods', *Risk Analysis*, vol. 32, no. 10, pp. 1657–1672, DOI: 10.1111/j.1539-6924.2012.01802.x.

Hansen, James, Sato, Makiko, Ruedy, Reto, Lo, Ken, Lea, David W, & Medina-Elizade, Martin 2006, 'Global temperature change', *Proceedings of the National Academy of Sciences of the United States of America*, vol. 103, no. 39, pp. 14288–14293, DOI: 10.1073/pnas.0606291103.

Heo, Seulkee, Bell, Michelle L, & Lee, Jong-Tae 2019, 'Comparison of health risks by heat wave definition: Applicability of wet- bulb globe temperature for heat wave criteria', *Environmental Research*, vol. 168, pp. 158–170, DOI: 10.1016/j.envres.2018.09.032.

IPCC 2014, *Climate Change 2014: Synthesis Report. Contribution of Working Groups I, II and III to the Fifth Assessment Report of the Intergovernmental Panel on Climate Change*, Geneva.

IPCC 2018, 'Summary for Policymakers', *Global Warming of 1.5° C. An IPCC Special Report on the impacts of global warming of 1.5° C above pre-industrial levels and related global greenhouse gas emission pathways, in the context of strenghtening the global response to the threat of climate chang*.

IPCC 2021a, 'Technical Summary', *The Physical Science Basis. Contribution of Working Group I to the Sixth Assessment Report of the Intergovernmental Panel on Climate Change*, pp. 33–144, DOI: 10.1017/9781009157896.002.

IPCC 2021b, 'Headline Statements from the Summary for Policymakers', *Sixth Assessment Report - Working Group I - The Physical Science Basis*.

IPCC 2022, 'Headline Statements from the Summary for Policymakers', *Sixth Assessment Report - Working Group II - Impacts, Adaptation and Vulnerability*.

Jacklitsch, Brenda, Williams, W Jon, Musolin, Kristin, Coca, Aitor, Kim, Jung-Hyun, & Turner, Nina 2016, *Occupational Exposure to Heat and Hot Environments*, Department of Health and Human Services. Centers for Disease Control and Prevention. National Institute for Occupational Safety and Health, DHHS (NIOSH), Cincinnati, OH.

Kanton Basel-Stadt 2021a, *Dynamischer Wirtschaftsstandort*, viewed 6 December 2021, <https://www.bs.ch/Portrait/wirtschaftsstandort.html>.

Kanton Basel-Stadt 2021b, *Beliebt bei Touristen*, viewed 7 December 2021, <https://www.bs.ch/Portrait/Tourismus.html>.

Kim, Kyu Rang, Kwon, Tae Heon, Kim, Yeon-hee, Koo, Hae-jung, Choi, Byoung-cheol, & Choi, Chee-young 2009, 'Restoration of an Inner-City Stream and Its Impact on Air Temperature and

Humidity Based on Long-Term Monitoring Data', *Advances in Atmospheric Sciences*, vol. 26, no. 2, pp. 283–292, DOI: 10.1007/s00376-009-0283-x.1.Introduction.

Kim, YH, Ryoo, SB, Baik, JJ, Park, IS, Koo, HJ, & Nam, JC 2008, 'Does the restoration of an inner-city stream in Seoul affect local thermal environment?', *Theoretical and Applied Climatology*, vol. 92, pp. 239–248, DOI: 10.1007/s00704-007-0319-z.

Kjellstrom, Tord 2016, 'Impact of Climate Conditions on Occupational Health and Related Economic Losses : A New Feature of Global and Urban Health in the Context of Climate Change', *Asia Pacific Journal of Public Health*, vol. 28, pp. 28S-37S, DOI: 10.1177/1010539514568711.

Konarska, Janina, Lindberg, Fredrik, Larsson, Annika, Thorsson, Sofia, & Holmer, Björn 2014, 'Transmissivity of solar radiation through crowns of single urban trees - application for outdoor thermal comfort modelling', *Theoretical and Applied Climatology*, vol. 117, pp. 363–376, DOI: 10.1007/s00704-013-1000-3.

Kotlarski, Sven & Rajczak, Jan 2018, 'Documentation of the localized CH2018 datasets. Transient daily time series at the local scale: DAILY-LOCAL, DAILY-GRIDDED', *MeteoSwiss, National Centre for Climate Services NCCS*, pp. 1–10.

Kovats, R Sari & Hajat, Shakoor 2008, 'Heat Stress and Public Health: A Critical Review', *Annual Review of Public Health*, vol. 29, pp. 41–55, DOI: 10.1146/annurev.publhealth.29.020907.090843.

Kühnle, Helena 2021, 'Improving Urban Climate', *Polykum*, vol. 3, pp. 24–25.

Küry, Daniel 2002, *Revitalisierung der Birs I*, *Natur und Landschaft der Region Basel, regionatur.ch*, viewed 18 July 2022, <https://www.regionatur.ch/Orte/Naturschutzgebiete/Birsrevitalisierung?a=image&bild_id=6476>.

Küry, Daniel 2010, *Revitalisierung der Birs II*, *Natur und Landschaft der Region Basel, regionatur.ch*, viewed 18 July 2022, <https://www.regionatur.ch/Orte/Naturschutzgebiete/Birsrevitalisierung?a=image&bild_id=6542>.

Kwakkel, Jan H 2017, 'The Exploratory Modeling Workbench: An open source toolkit for exploratory modeling, scenario discovery, and (multi-objective) robust decision making', *Environmental Modelling and Software*, vol. 96, pp. 239–250, DOI: 10.1016/j.envsoft.2017.06.054.

Kwakkel, Jan H 2018, *EMA Workbench documentation*, *2018*, viewed 15 October 2021, <https://emaworkbench.readthedocs.io/en/latest/>.

Kwakkel, Jan H, Auping, Willem L, & Pruyt, Erik 2013, 'Dynamic scenario discovery under deep uncertainty: The future of copper', *Technological Forecasting and Social Change*, vol. 80, pp. 789–800, DOI: 10.1016/j.techfore.2012.09.012.

Kwakkel, Jan H & Haasnoot, Marjolijn 2019,'Chapter 15 - Supporting DMDU: A Taxonomy of Approaches and Tools', in Vincent AWJ Marchau, Warren E Walker, JTM Bloemen, Pieter, & Steven W Popper (eds.), *Decision Making under Deep Uncertainty. From Theory to Practice*, Springer Nature Switzerland AG, Cham, Switzerland, pp.355–392, DOI: https://doi.org/10.1007/978-3-030-05252-2Ma.

Lai, Dayi, Liu, Wenyu, Gan, Tingting, Liu, Kuixing, & Chen, Qingyan 2019, 'A Review of Mitigating

Strategies to Improve the Thermal Environment and Thermal Comfort in Urban Outdoor Spaces', *Science of the Total Environment*, vol. 661, no. April, pp. 337–353, DOI: 10.1016/j.scitotenv.2019.01.062.

Lawrence, Judy & Haasnoot, Marjolijn 2017, 'What it took to catalyse uptake of dynamic adaptive pathways planning to address climate change uncertainty', *Environmental Science and Policy*, vol. 68, pp. 47–57, DOI: 10.1016/j.envsci.2016.12.003.

Lee, June-Yi, Marotzke, Jochem, Bala, Govindasamy, Cao, Long, Corti, Susanna, Dunne, John P, et al. 2021,'Future Global Climate: Scenario-based Projections and Near-term Information', in, *Climate Change 2021: The Physical Science Basis. Contribution of Working Group I to the Sixth Assessment Report of the Intergovernmental Panel on Climate Change*, Cambridge University Press, Cambridge (UK), New York (USA), pp.553–672, DOI: 10.1017/9781009157896.006.553.

Lemke, Bruno & Kjellstrom, Tord 2012, 'Calculating Workplace WBGT from Meteorological Data : A Tool for Climate Change Assessment', *Industrial Health*, vol. 50, pp. 267–278.

Lempert, RJ 2019,'Chapter 2 - Robust Decision Making (RDM)', in Vincent AWJ Marchau, Warren E Walker, JTM Bloemen, Pieter, & Steven W Popper (eds.), *Decision Making under Deep Uncertainty. From Theory to Practice*, Springer Nature Switzerland AG, Cham, Switzerland, pp.23–51, DOI: https://doi.org/10.1007/978-3-030-05252-2_2.

Li, Mengyao, Ferreira, Susana, & Smith, Travis A 2020, 'Temperature and self-reported mental health in the United States', *PLoS ONE*, vol. 15, no. 3, pp. 1–20, DOI: 10.1371/journal.pone.0230316.

Li, Xueqin, Stringer, Lindsay C, & Dallimer, Martin 2021, 'The Spatial and Temporal Characteristics of Urban Heat Island Intensity: Implications for East Africa's Urban Development', *Climate*, vol. 9, no. 51, pp. 1–19, DOI: 10.3390/cli9040051.

Liljegren, James C, Carhart, Richard A, Lawday, Philip, Tschopp, Stephen, & Sharp, Robert 2008, 'Modeling the Wet Bulb Globe Temperature Using Standard Meteorological Measurements', *Journal of Occupational and Environmental Hygiene*, vol. 5, no. 10, pp. 645–655, DOI: 10.1080/15459620802310770.

Lokoshchenko, MA 2014, 'Urban "heat island" in Moscow', *Urban Climate*, vol. 10, pp. 550–562, DOI: 10.1016/j.uclim.2014.01.008.

Manoli, Gabriele, Fatichi, Simone, Schläpfer, Markus, Yu, Kailiang, Crowther, Thomas W, Meili, Naika, et al. 2019, 'Magnitude of urban heat islands largely explained by climate and population', *Nature*, vol. 573, pp. 55–60, DOI: 10.1038/s41586-019-1512-9.

Marchau, Vincent AWJ, Walker, Warren E, Bloemen, Pieter, JTM, & Popper, Steven W 2019a,'Chapter 1 - Introduction', in Vincent AWJ Marchau, Warren E Walker, JTM Bloemen, Pieter, & Steven W Popper (eds.), *Decision Making under Deep Uncertainty. From Theory to Practice*, Springer Nature Switzerland AG, Cham, Switzerland, pp.1–20, DOI: https://doi.org/10.1007/978-3-030-05252-2.

Marchau, Vincent AWJ, Walker, Warren E, Bloemen, Pieter, JTM, & Popper, Steven W 2019b, *Decision Making Under Deep Uncertainty. From Theory to Practice*, Vincent AWJ Marchau, Warren E Walker, Pieter JTM Bloemen, & Steven W Popper (eds.), Springer Nature Switzerland AG, DOI: 10.1093/oxfordhb/9780190455811.013.50.

Matzarakis, Andreas & Amelung, Bas 2008, 'Physiological Equivalent Temperature as Indicator for Impacts of Climate Change on Thermal Comfort of Humans', *Seasonal Forecasts, Climatic*

Change and Human Health, pp. 161–172, DOI: 10.1007/978-1-4020-6877-5_10.

McGregor, GR, Bessemoulin, P, Ebi, K, & Menne, B 2015, *Heatwaves and Health: Guidance on Warning-System Development*, World Meteorological Organization (WMO) and World Health Organization (WHO), Geneva.

MeteoSwiss 2018, 'SwissMetNet : The MeteoSwiss reference monitoring network', *Federal Office of Meteorology and Climatology MeteoSwiss*, pp. 1–2.

MeteoSwiss 2020, *Automatic monitoring network*, viewed 25 December 2021, <https://www.meteoswiss.admin.ch/home/measurement-and-forecasting-systems/land-based-stations/automatisches-messnetz.html>.

MeteoSwiss 2021, *Measurement values. Basel / Binningen*, viewed 31 December 2021, <https://www.meteoswiss.admin.ch/home/measurement-values.html?param=messnetz-automatisch&station=BAS&chart=hour>.

MeteoSwiss 2022, *Measurement values. Zürich / Fluntern*, viewed 18 August 2022, <https://www.meteoswiss.admin.ch/home/measurement-values.html?param=messnetz-automatisch&station=SMA&chart=hour>.

Minor, Liliane & Unternährer, Pascal 2022, *Ab Juli kühlt eine künstliche Wolke den Turbinenplatz*, *Tagesanzeiger*, viewed 9 September 2022, <https://www.tagesanzeiger.ch/ab-juli-kuehlt-eine-kuenstliche-wolke-den-turbinenplatz-886258428590>.

Moallemi, Enayat A, Kwakkel, Jan, de Haan, Fjalar J, & Bryan, Brett A 2020, 'Exploratory modeling for analyzing coupled human-natural systems under uncertainty', *Global Environmental Change*, vol. 65, no. November, pp. 1–18, DOI: 10.1016/j.gloenvcha.2020.102186.

Morabito, Marco, Crisci, Alfonso, Moriondo, Marco, Profili, Francesco, Francesconi, Paolo, Trombi, Giacomo, et al. 2012, 'Air temperature-related human health outcomes: Current impact and estimations of future risks in Central Italy', *Science of the Total Environment*, vol. 441, pp. 28–40, DOI: 10.1016/j.scitotenv.2012.09.056.

Morabito, Marco, Messeri, Alessandro, Noti, Pascal, Casanueva, Ana, Crisci, Alfonso, Kotlarski, Sven, et al. 2019, 'An occupational heat–health warning system for Europe: The HEAT-SHIELD platform', *International Journal of Environmental Research and Public Health*, vol. 16, no. 2890, pp. 1–21, DOI: 10.3390/ijerph16162890.

Murage, Peninah, Hajat, Shakoor, & Kovats, R Sari 2017, 'Effect of night-time temperatures on cause and age-specific mortality in London', *Environmental Epidemiology*, vol. 2, no. e005, pp. 1–7, DOI: 10.1097/ee9.0000000000000005.

Niggli, Laura, Huggel, Christian, Muccione, Veruska, Neukom, Raphael, & Salzmann, Nadine 2022, 'Towards improved understanding of cascading and interconnected risks from compound weather extremes: Analysis of historical heat and drought extreme events', *PLOS Climate*, vol. 8, pp. 1–34, DOI: https://doi.org/10.1371/journal.pclm.0000057.

O'Neill, Brian C, Tebaldi, Claudia, Van Vuuren, Detlef P, Eyring, Veronika, Friedlingstein, Pierre, Hurtt, George, et al. 2016, 'The Scenario Model Intercomparison Project (ScenarioMIP) for CMIP6', *Geoscientific Model Development*, vol. 9, pp. 3461–3482, DOI: 10.5194/gmd-9-3461-2016.

Obradovich, Nick & Fowler, James H 2017, 'Climate change may alter human physical activity patterns', *Nature Human Behaviour*, vol. 1, no. 97, DOI: 10.1038/s41562-017-0097.

Ono, Masaji & Tonouchi, Michihiko 2014, 'Estimation of wet-bulb globe temperature using generally measured meteorological indices', *Japanese Journal of Biometeorology*, vol. 50, no. 4, pp. 147–157, DOI: 10.11227/seikisho.50.147.

OSHA 2017, *Technical Manual (OTM) Section III: Chapter 4. Heat Stress*, *United States Department of Labor*, viewed 16 January 2022, <https://www.osha.gov/otm/section-3-health-hazards/chapter-4>.

Parlow, Eberhard, Vogt, Roland, & Feigenwinter, Christian 2014, 'The urban heat island of Basel - seen from different perspectives', *Die Erde*, vol. 145, no. 1–2, pp. 96–110, DOI: 10.12854/erde-145-8.

Patel, Tejash, Mullen, Stephen P, & Santee, William R 2013, 'Comparison of Methods for Estimating Wet-Bulb Globe Temperature Index From Standard Meteorological Measurements', *Military Medicine*, vol. 178, no. 8, pp. 926–933, DOI: 10.7205/MILMED-D-13-00117.

Previdi, Michael, Smith, Karen L, & Polvani, Lorenzo M 2021, 'Arctic amplification of climate change: A review of underlying mechanisms', *Environmental Research Letters*, vol. 16, pp. 1–25, DOI: 10.1088/1748-9326/ac1c29.

Ragettli, Martina S, Vicedo-Cabrera, Ana M, Flückiger, Benjamin, & Röösli, Martin 2019, 'Impact of the warm summer 2015 on emergency hospital admissions in Switzerland', *Environmental Health*, vol. 18, no. 66, pp. 1–10, DOI: 10.1186/s12940-019-0507-1.

Ragettli, Martina S, Vicedo-Cabrera, Ana M, Schindler, Christian, & Röösli, Martin 2017, 'Exploring the association between heat and mortality in Switzerland between 1995 and 2013', *Environmental Research*, vol. 158, pp. 703–709, DOI: 10.1016/j.envres.2017.07.021.

Rahuel, Bettina, Afheldt, Julia, Block, Silke, Heinzer, Catherine, Hofmann, Martin, Leugger, Salomé, et al. 2021, *Stadtklima-Konzept zur klimaangepassten Siedlungsentwicklung im Kanton Basel-Stadt*, Steudler Press, Basel.

Royé, Dominic, Sera, Francesco, Tobías, Aurelio, Lowe, Rachel, Gasparrini, Antonio, Pascal, Mathilde, et al. 2021, 'Effects of Hot Nights on Mortality in Southern Europe', *Epidemiology*, vol. 32, no. 4, pp. 487–498, DOI: 10.1097/EDE.0000000000001359.

Rumsfeld, Donald 2021, *There are known knowns*, *Wikipedia*, viewed 28 December 2021, <https://en.wikipedia.org/wiki/There_are_known_knowns>.

Schneider, Stephen H 1972, 'Cloudiness as a Global Climatic Feedback Mechanism: The Effects on the Radiation Balance and Surface Temperature of Variations in Cloudiness', *Journal of the atmospheric sciences*, vol. 29, pp. 1413–1422.

Schneider, Stephen H, Turner, BL, & Garriga, Holly Morehouse 1998, 'Imaginable surprise in global change science', *Journal of Risk Research*, vol. 1, no. 2, pp. 165–185, DOI: 10.1080/136698798377240.

Sjöman, Henrik, Gunnarsson, Allan, Pauleit, Stephan, & Bothmer, Roland 2012, 'Selection Approach of Urban Trees for Inner-city Environments : Learning from Nature', *Arboriculture & Urban Forestry*, vol. 38, no. 5, pp. 194–204.

Stadt-Zürich 2022, *Stadt Zürich*, viewed 26 March 2022, <https://www.stadt-zuerich.ch/portal/de/index.html>.

Stanton, Muriel C Bonjea & Roelich, Katy 2021, 'Decision making under deep uncertainties: A review of the applicability of methods in practice', *Technological Forecasting and Social Change*, vol. 171, pp. 1–12, DOI: 10.1016/j.techfore.2021.120939.

Steadman, Robert G 1994, 'Norms of apparent temperature in Australia', *Australian Meteorological Magazine*, vol. 43, pp. 1–16.

Sutton, Rowan T, Dong, Buwen, & Gregory, Jonathan M 2007, 'Land/sea warming ratio in response to climate change: IPCC AR4 model results and comparison with observations', *Geophysical Research Letters*, vol. 34, pp. 1–5, DOI: 10.1029/2006GL028164.

Taleghani, Mohammad & Berardi, Umberto 2018, 'The effect of pavement characteristics on pedestrians' thermal comfort in Toronto', *Urban Climate*, vol. 24, pp. 449–459, DOI: 10.1016/j.uclim.2017.05.007.

Theeuwes, Natalie E, Steeneveld, Gert Jan, Ronda, Reinder J, Rotach, Mathias W, & Holtslag, Albert AM 2015, 'Cool city mornings by urban heat', *Environmental Research Letters*, vol. 10, pp. 1–9, DOI: 10.1088/1748-9326/10/11/114022.

Thompson, JMT & Sieber, Jan 2012, 'Climate predictions: The influence of nonlinearity and randomness', *Philosophical Transactions of the Royal Society A: Mathematical, Physical and Engineering Sciences*, vol. 370, pp. 1007–1011, DOI: 10.1098/rsta.2011.0423.

Tian, Zhe, Zhu, Neng, Zheng, Guozhong, & Wei, Huijiao 2011, 'Experimental study on physiological and psychological effects of heat acclimatization in extreme hot environments', *Building and Environment*, vol. 46, pp. 2033–2041, DOI: 10.1016/j.buildenv.2011.04.027.

Tuholske, Cascade, Caylor, Kelly, Funk, Chris, Verdin, Andrew, Sweeney, Stuart, Grace, Kathryn, et al. 2021, 'Global urban population exposure to extreme heat', *Proceedings of the National Academy of Sciences of the United States of America*, vol. 118, no. 41, pp. 1–9, DOI: 10.1073/pnas.2024792118.

Vautard, Robert, Gobiet, Andreas, Sobolowski, Stefan, Kjellström, Erik, Stegehuis, Annemiek, Watkiss, Paul, et al. 2014, 'The European climate under a 2 °C global warming', *Environmental Research Letters*, vol. 9, pp. 1–11, DOI: 10.1088/1748-9326/9/3/034006.

Vicedo-Cabrera, AM, Scovronick, N, Sera, F, Royé, D, Schneider, R, Tobias, A, et al. 2021, 'The burden of heat-related mortality attributable to recent human-induced climate change', *Nature Climate Change*, vol. 11, no. 6, pp. 492–500, DOI: 10.1038/s41558-021-01058-x.

Voogt, JA & Oke, TR 2003, 'Thermal remote sensing of urban climates', *Remote Sensing of Environment*, vol. 86, pp. 370–384, DOI: 10.1016/S0034-4257(03)00079-8.

Watts, Nick, Amann, Markus, Arnell, Nigel, Ayeb-Karlsson, Sonja, Belesova, Kristine, Boykoff, Max, et al. 2019, 'The 2019 report of The Lancet Countdown on health and climate change: ensuring that the health of a child born today is not defined by a changing climate', *The Lancet*, vol. 394, pp. 1836–1878, DOI: 10.1016/S0140-6736(19)32596-6.

Weber, Cordula, Keller, Daniel, Berchtold, Martin, Krass, Philipp, Dragaj, Poliksen Qorri, Trute, Peter, et al. 2018, 'Hitze in Städten. Grundlage für eine klimaangepasste Siedlungsentwicklung', *BAFU, Umwelt-Wissen*, vol. 1812, pp. 1–108, <https://www.bafu.admin.ch/bafu/de/home/themen/klima/publikationen-studien/publikationen/hitze-in-staedten.html>.

Wende, Wolfgang, Rößler, Stefanie, & Krüger, Tobias 2014, *Grundlagen für eine klimawandelangepasste Stadt- und Freiraumplanung*, 6th edn, Rhombos-Verlag, Berlin.

Wicki, Andreas, Parlow, Eberhard, & Feigenwinter, Christian 2018, 'Evaluation and modeling of urban heat island intensity in Basel, Switzerland', *Climate*, vol. 6, no. 55, pp. 1–25, DOI: 10.3390/cli6030055.

WieseVital n.d., *WieseVital*, *WieseVital*, viewed 7 October 2022, <https://www.landschaftsparkwiese.info/wiesevital>.

Wikipedia 2006, *Alpenrelief*, viewed 21 December 2021, <https://de.wikipedia.org/wiki/Datei:Alpenrelief_01.jpg>.

Wikipedia 2021, *Kanton Basel-Stadt*, viewed 6 December 2021, <https://de.wikipedia.org/wiki/Kanton_Basel-Stadt>.

Wikipedia 2022a, *Kontinentalklima*, viewed 17 February 2022, <https://de.wikipedia.org/wiki/Kontinentalklima>.

Wikipedia 2022b, *Accuracy and precision*, viewed 23 June 2022, <https://en.wikipedia.org/wiki/Accuracy_and_precision>.

Wild, Martin, Folini, Doris, Hakuba, Maria Z, Schär, Christoph, Seneviratne, Sonia I, Kato, Seiji, et al. 2015, 'The energy balance over land and oceans: an assessment based on direct observations and CMIP5 climate models', *Climate Dynamics*, vol. 44, pp. 3393–3429, DOI: 10.1007/s00382-014-2430-z.

Yang, Jiachuan, Wang, Zhi Hua, Kaloush, Kamil E, & Dylla, Heather 2016, 'Effect of pavement thermal properties on mitigating urban heat islands: A multi-scale modeling case study in Phoenix', *Building and Environment*, vol. 108, pp. 110–121, DOI: 10.1016/j.buildenv.2016.08.021.

Yow, Donald M 2007, 'Urban Heat Islands: Observations, Impacts, and Adaptation', *Geography Compass*, vol. 1, no. 6, pp. 1227–1251, DOI: 10.1111/j.1749-8198.2007.00063.x.

Yuan, Chao & Ng, Edward 2012, 'Building porosity for better urban ventilation in high-density cities - A computational parametric study', *Building and Environment*, vol. 50, pp. 176–189, DOI: 10.1016/j.buildenv.2011.10.023.

Zhao, Dan, Lei, Quanhuan, Shi, Yajie, Wang, Mengdi, Chen, Sibo, Shah, Kamran, et al. 2020, 'Role of species and planting configuration on transpiration and microclimate for urban trees', *Forests*, vol. 11, no. 825, pp. 1–18, DOI: 10.3390/f11080825.

Appendix

Climate data – Zurich

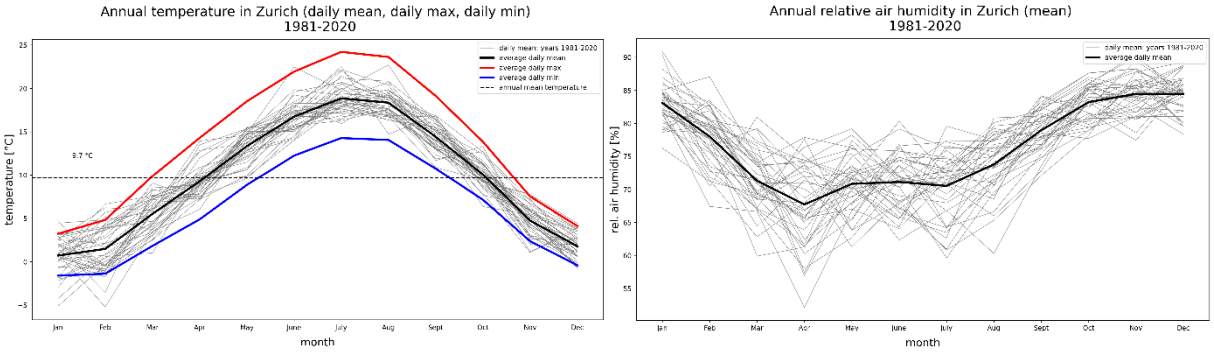

Figure 51: *Left: Annual temperature in Zurich-Fluntern. Daily means of each year (grey), averaged daily mean (black), averaged daily max (red), and averaged daily min (blue). Annual mean temperature (dashed line). Right: Annual relative air humidity in Zurich-Fluntern. Daily means of each year (grey) and averaged daily mean (black) (own figure, based on data from MeteoSwiss (2018) and (2020)).*

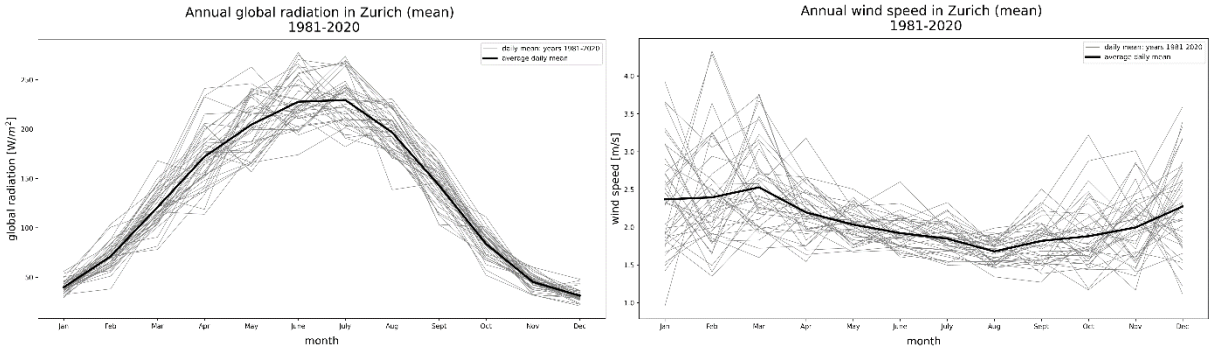

Figure 52: *Left: Annual global radiation in Zurich-Fluntern. Daily means of each year (grey) and averaged daily mean (black). Right: Annual wind speed in Zurich-Fluntern. Daily means of each year (grey) and averaged daily mean (black) (own figure, based on data from MeteoSwiss (2018) and (2020)).*

Heat indicators (observations) – Basel

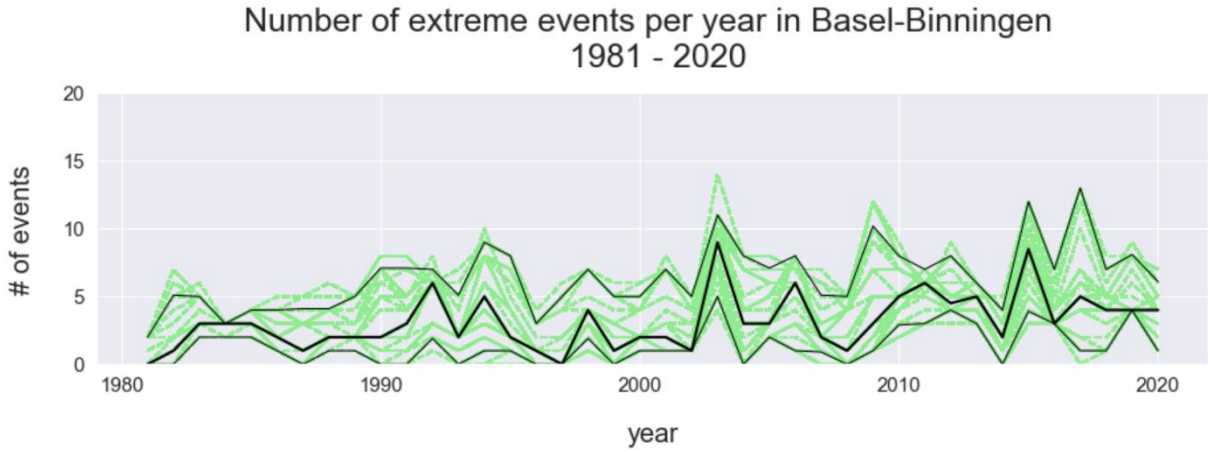

Figure 53: *NEE per year for the observed period in Basel-Binningen. The threshold range for an extreme day is between 26° C and 30° C. The green lines show the scenarios. The three black lines show the 10th, 50th, and 90th quantile respectively (own figure).*

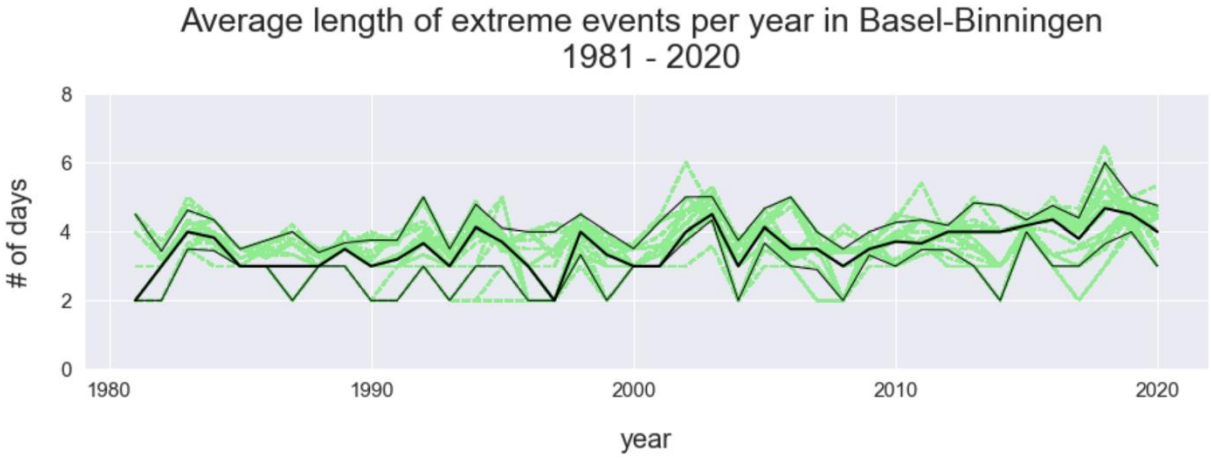

Figure 54: *LEE per year for the observed period in Basel-Binningen. The threshold range for an extreme day is between 26° C and 30° C. The green lines show the scenarios. The three black lines show the 10th, 50th, and 90th quantile respectively (own figure).*

Heat indicators, summary of statistical numbers (simulations) – Basel

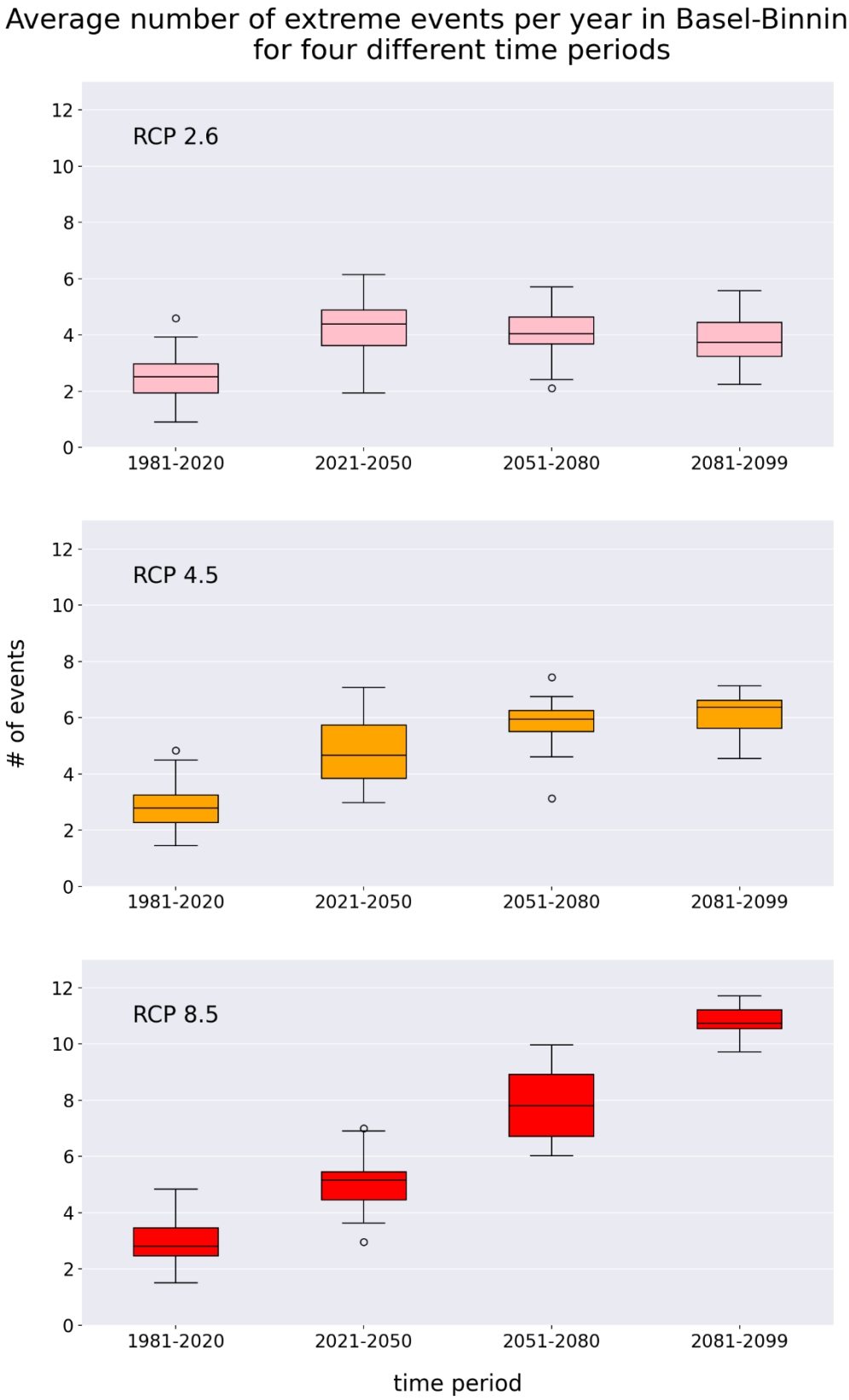

Figure 55: *Average NEE for four time periods for the future simulations in Basel-Binningen. The threshold range for an extreme day is between 26° C and 30° C. The first graph shows the RCP2.6 scenario (pink), the second graph shows the RCP4.5 scenario (orange), and the third graph shows the RCP8.5 scenario (red) (own figure).*

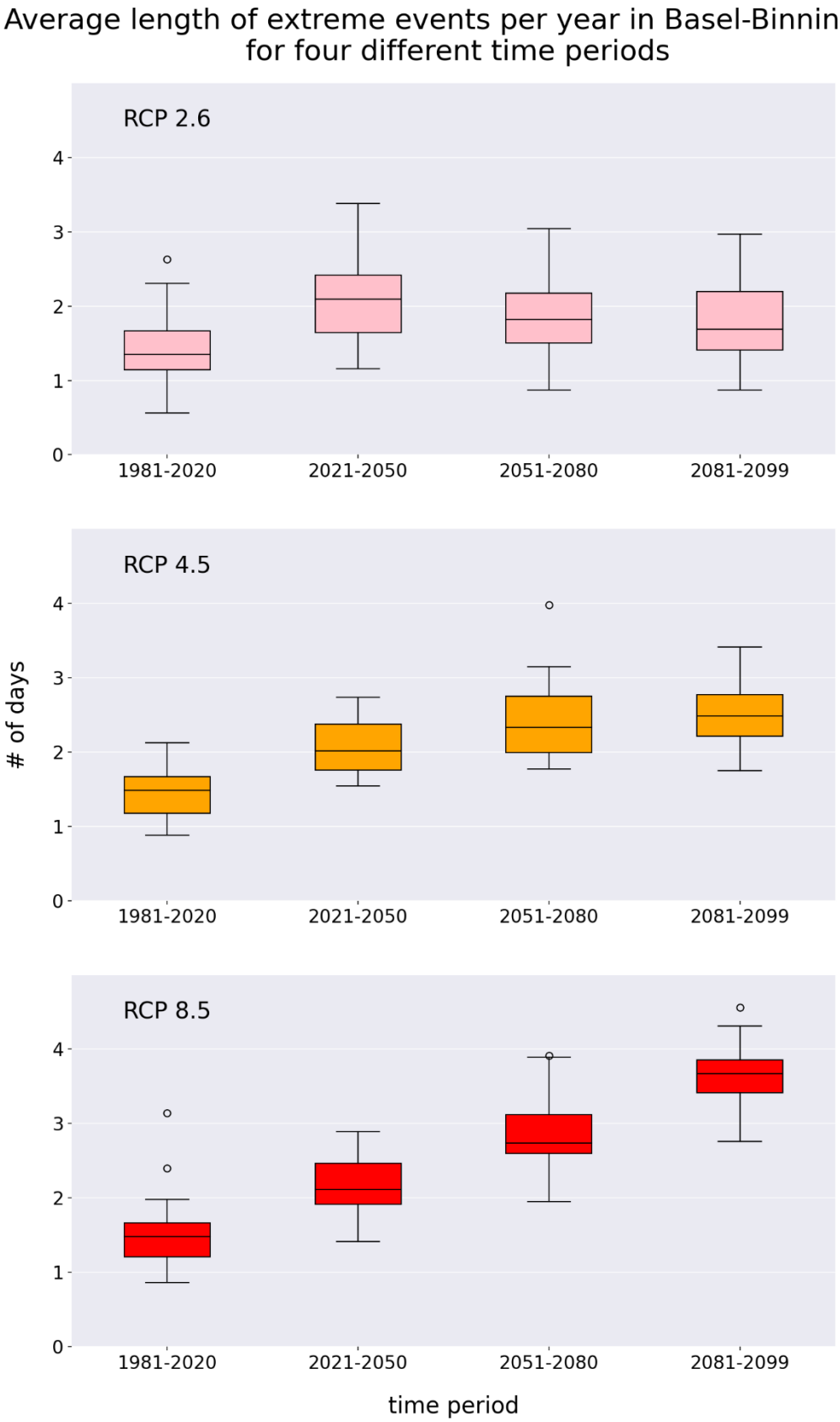

Figure 56: *LEE for four time periods for the future simulations in Basel-Binningen. The threshold range for an extreme day is between 26° C and 30° C. The first graph shows the RCP2.6 scenario (pink), the second graph shows the RCP4.5 scenario (orange), and the third graph shows the RCP8.5 scenario (red) (own figure).*

Table 6: *Annual growth rate of NED, NEE, and LEE for three different future scenarios (RCP2.6, RCP4.5, RCP8.5) in Basel-Binningen for the simulated time period (1981-2099). Values in brackets show by how much RCP4.5 and RCP8.5 stronger increase compared to RCP2.6 until the end of this century (own table).*

	NED (figure 25)		NEE (figure 26)		LEE (figure 27)	
RCP2.6	0.045	(1)	0.020	(1)	0.006	(1)
RCP4.5	0.130	(2.89)	0.044	(2.2)	0.012	(2)
RCP8.5	0.333	(7.4)	0.087	(4.35)	0.021	(3.5)

Table 7: *Average NED per year for the future simulation in Basel-Binningen. Statistical analysis of the adaptation options analysis. Normal conditions in grey and reduced air temperature in blue (-1° C, -3° C, and -5° C during spring, summer, and autumn, no change during winter) (own table).*

	Normal			T - 1			T - 3			T - 5		
	RCP2.6	RCP4.5	RCP8.5	RCP2.6	RCP4.5	RCP8.5	RCP2.6	RCP4.5	RCP8.5	RCP2.6	RCP4.5	RCP8.5
Mean	8	11.3	17.3	4.6	6.6	12.1	1.2	2.3	5.7	0.2	0.6	2.3
Max	21	25.4	39.4	14.3	17.9	31.3	5.5	8.2	18.3	1.5	2.9	9.6
Min	1.3	2.1	4.4	0.6	1	2.5	0	0.1	0.5	0	0	0.1
Range	19.7	23.3	35	13.7	16.9	28.8	5.5	8.1	17.8	1.5	2.9	9.5

Table 8: *Average NED per year for the future simulation in Basel-Binningen. Statistical analysis of the adaptation options analysis. Normal conditions in grey, reduced global radiation in orange (0.15*GlR during summer, 0.5*GlR during winter) and increased wind speed in green (+1 m/s) (own table).*

	Normal			Global radiation			Wind		
	RCP2.6	RCP4.5	RCP8.5	RCP2.6	RCP4.5	RCP8.5	RCP2.6	RCP4.5	RCP8.5
Mean	8	11.3	17.3	6.3	9.2	15.5	7.9	10.1	17.1
Max	21	25.4	39.4	18.6	22.3	36.7	20.9	25.3	39.4
Min	1.3	2.1	4.4	0.9	1.5	3.5	1.3	2	4.8
Range	19.7	23.3	35	17.7	20.8	33.2	19.6	23.3	34.6

Heat indicators – Zurich

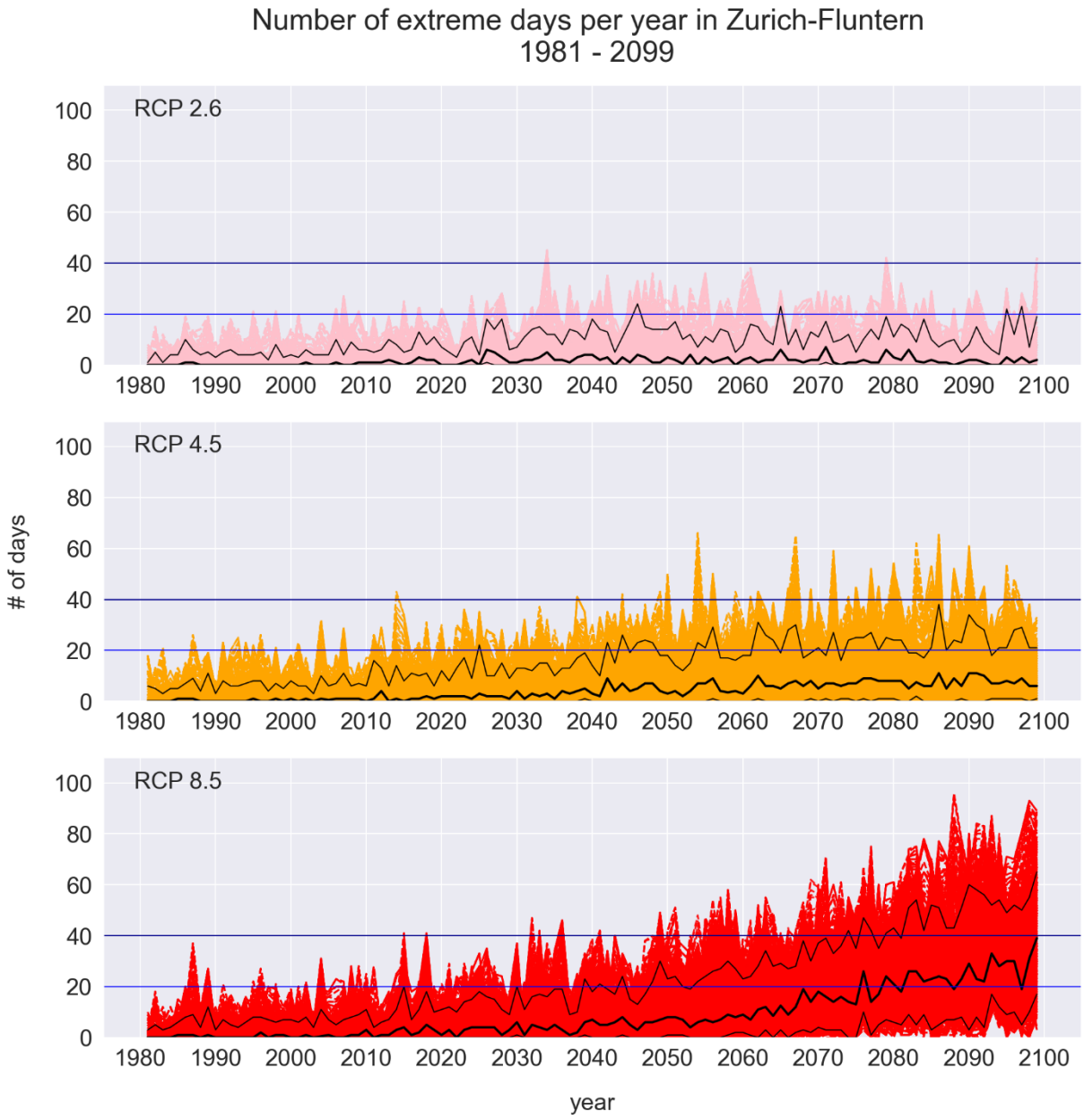

Figure 57: *NED per year for the future simulations in Zurich-Fluntern. The threshold range for an extreme day is between 26° C and 30° C. The first graph shows the RCP2.6 scenario (pink), the second graph shows the RCP4.5 scenario (orange), and the third graph shows the RCP8.5 scenario (red). The black lines show the 10th, 50th, and 90th quantile respectively (own figure).*

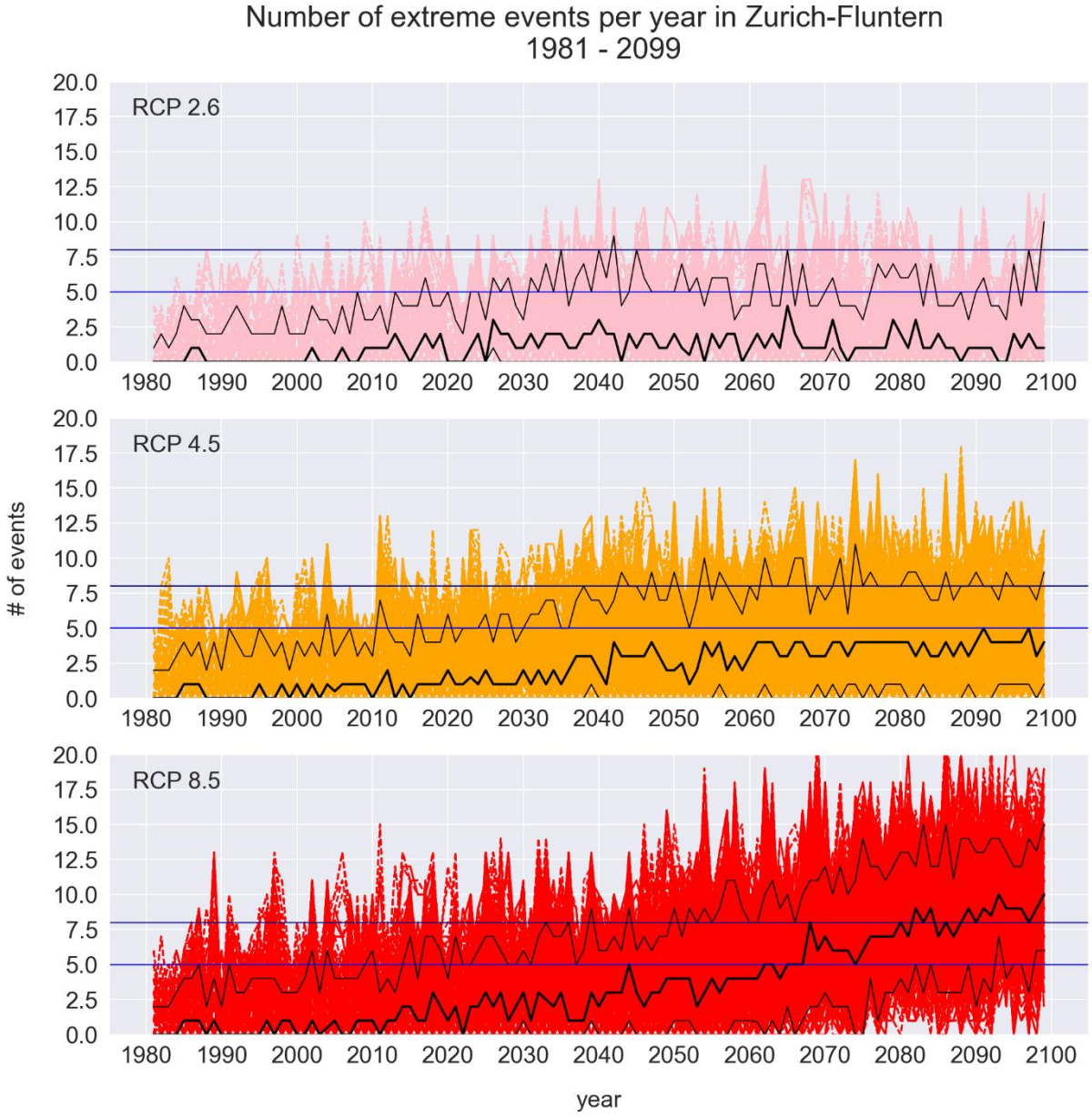

Figure 58: *NEE per year for the future simulations in Zurich-Fluntern. The threshold range for an extreme day is between 26° C and 30° C. The first graph shows the RCP2.6 scenario (pink), the second graph shows the RCP4.5 scenario (orange), and the third graph shows the RCP8.5 scenario (red). The black lines show the 10th, 50th, and 90th quantile respectively (own figure).*

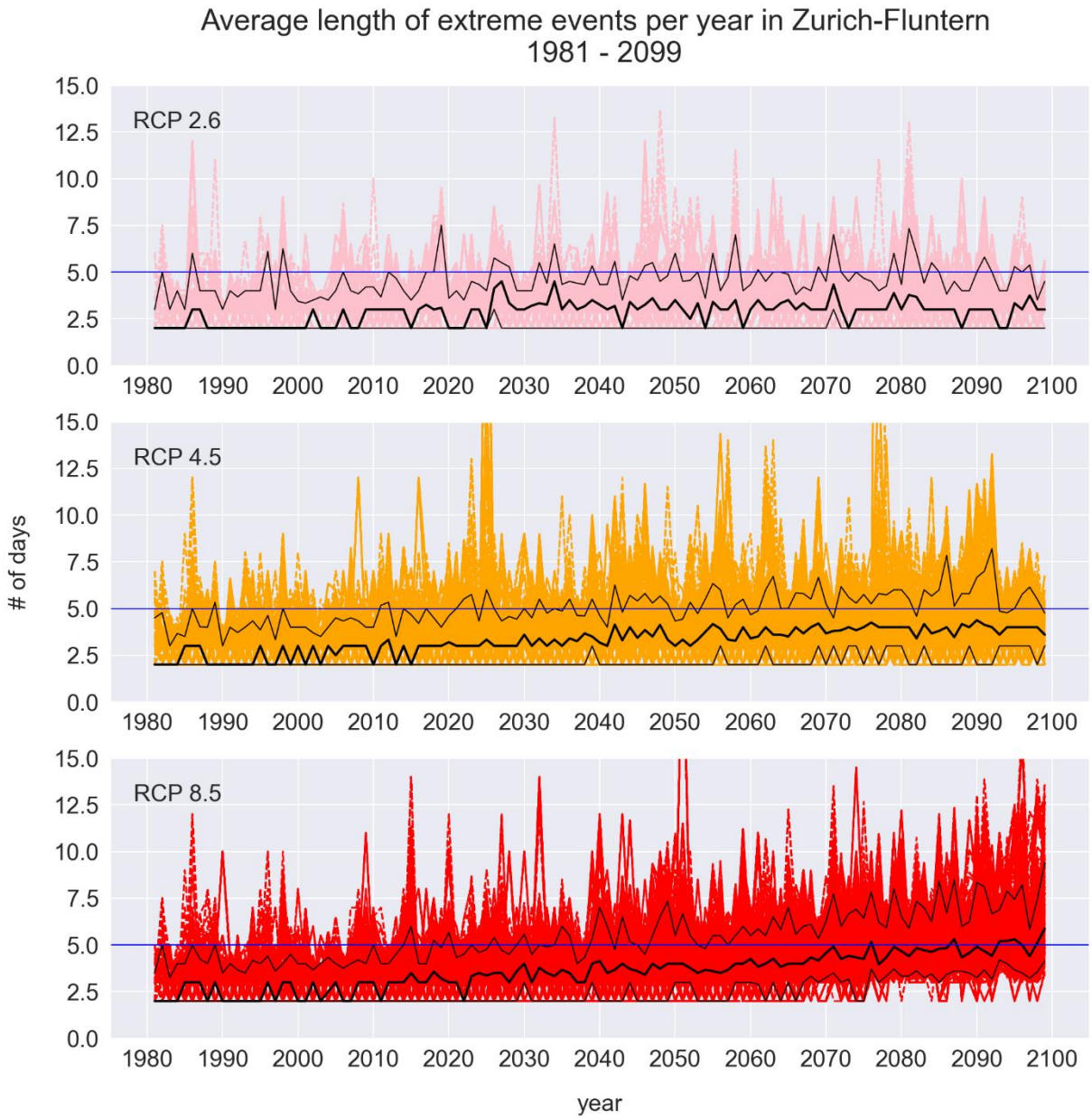

Figure 59: *LEE per year for the future simulations in Zurich-Fluntern. The threshold range for an extreme day is between 26° C and 30° C. The first graph shows the RCP2.6 scenario (pink), the second graph shows the RCP4.5 scenario (orange), and the third graph shows the RCP8.5 scenario (red). The black lines show the 10th, 50th, and 90th quantile respectively (own figure).*

Table 9: *Annual growth rate of NED, NEE, and LEE for three different future scenarios (RCP2.6, RCP4.5, RCP8.5) in Zurich-Fluntern for the simulated time period (1981-2099). Values in brackets show by how much RCP4.5 and RCP8.5 stronger increase compared to RCP2.6 until the end of this century (own table).*

	NED (figure 57)		NEE (figure 58)		LEE (figure 59)	
RCP2.6	0.017	(1)	0.010	(1)	0.008	(1)
RCP4.5	0.082	(4.8)	0.039	(3.9)	0.017	(2.1)
RCP8.5	0.242	(14.2)	0.081	(8.1)	0.025	(3.1)

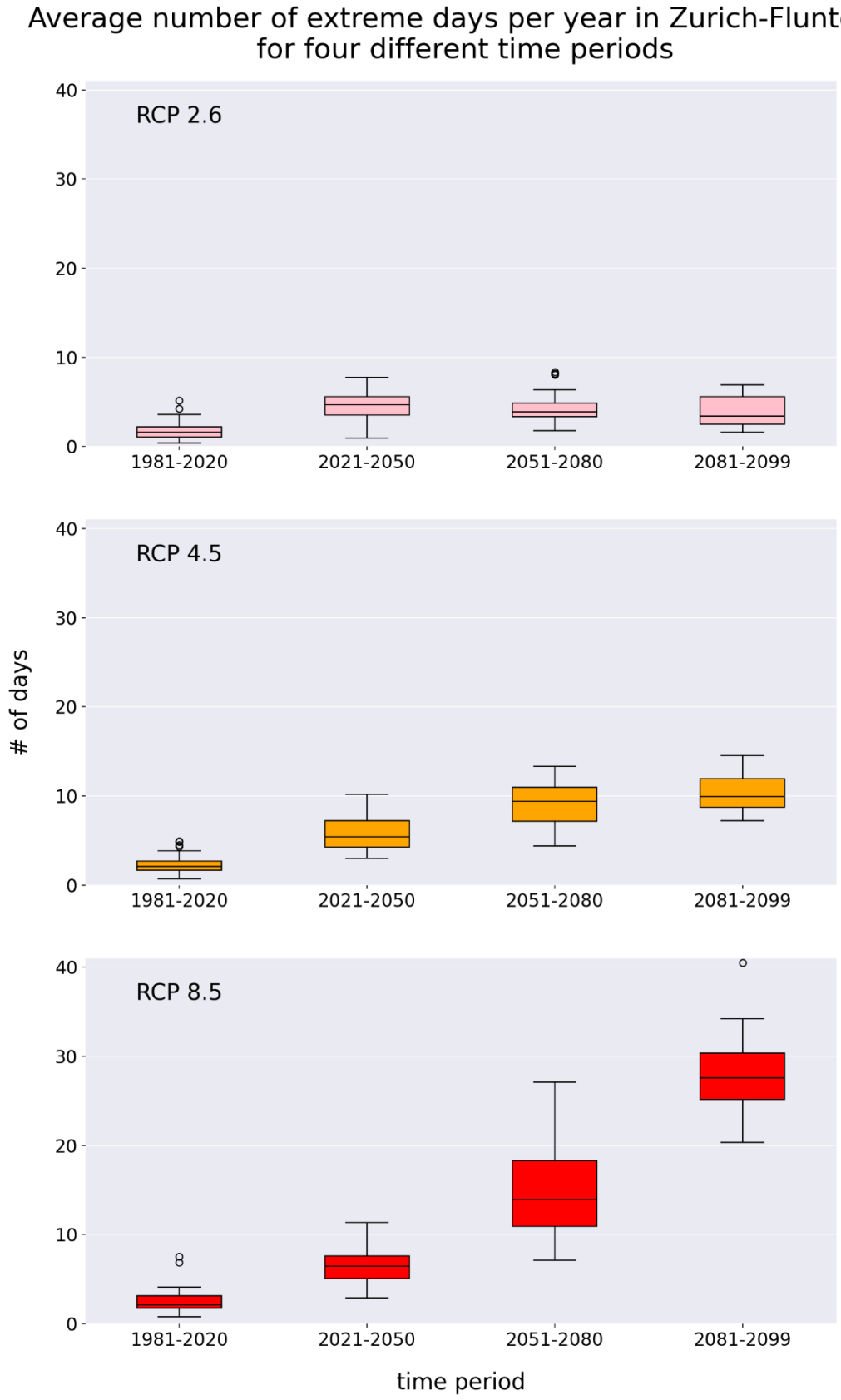

Figure 60: *Average NED for four time periods for the future simulations in Zurich-Fluntern. The threshold range for an extreme day is between 26° C and 30° C. The first graph shows the RCP2.6 scenario (pink), the second graph shows the RCP4.5 scenario (orange), and the third graph shows the RCP8.5 scenario (red) (own figure).*

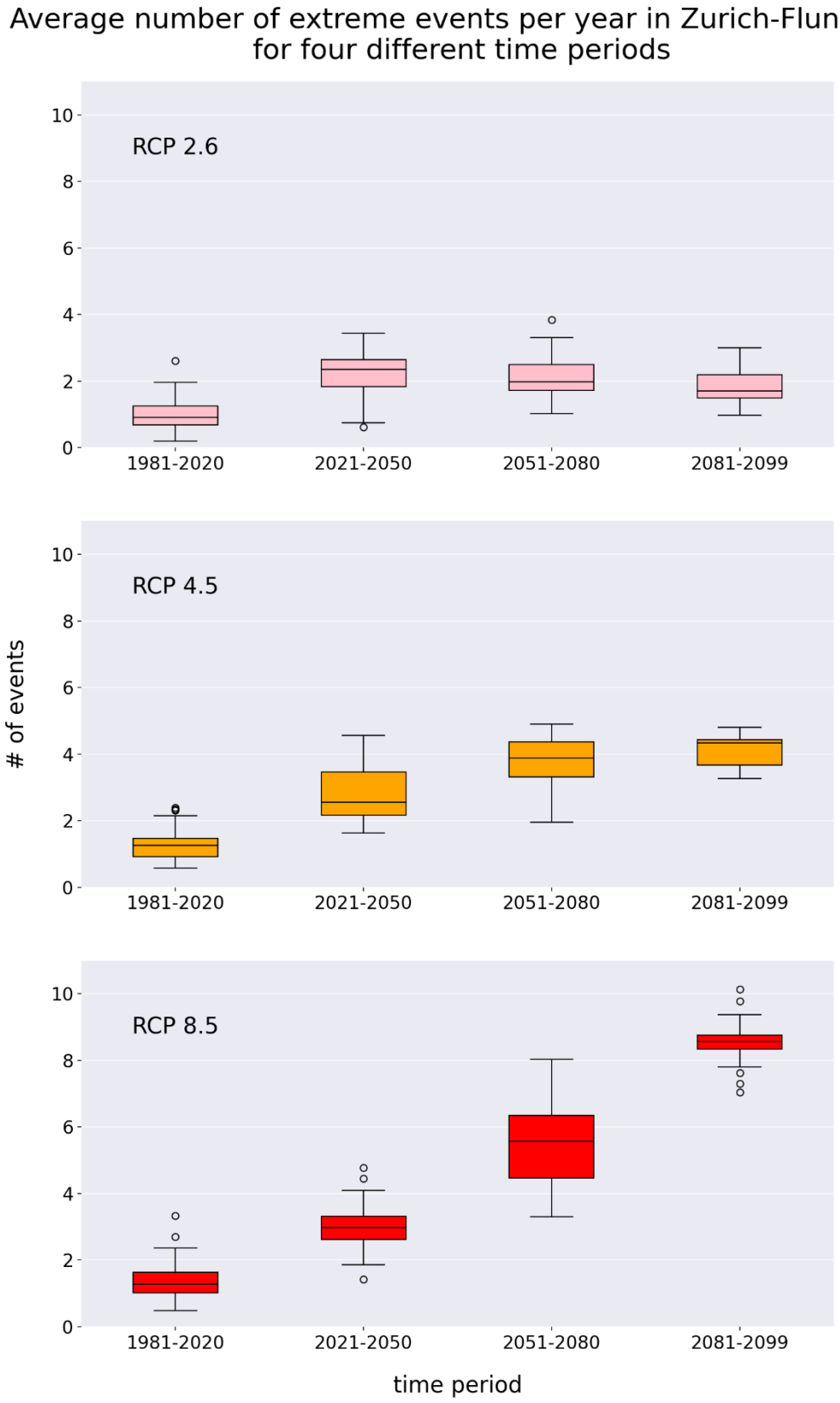

Figure 61: *Average NEE for four time periods for the future simulations in Zurich-Fluntern. The threshold range for an extreme day is between 26° C and 30° C. The first graph shows the RCP2.6 scenario (pink), the second graph shows the RCP4.5 scenario (orange), and the third graph shows the RCP8.5 scenario (red) (own figure).*

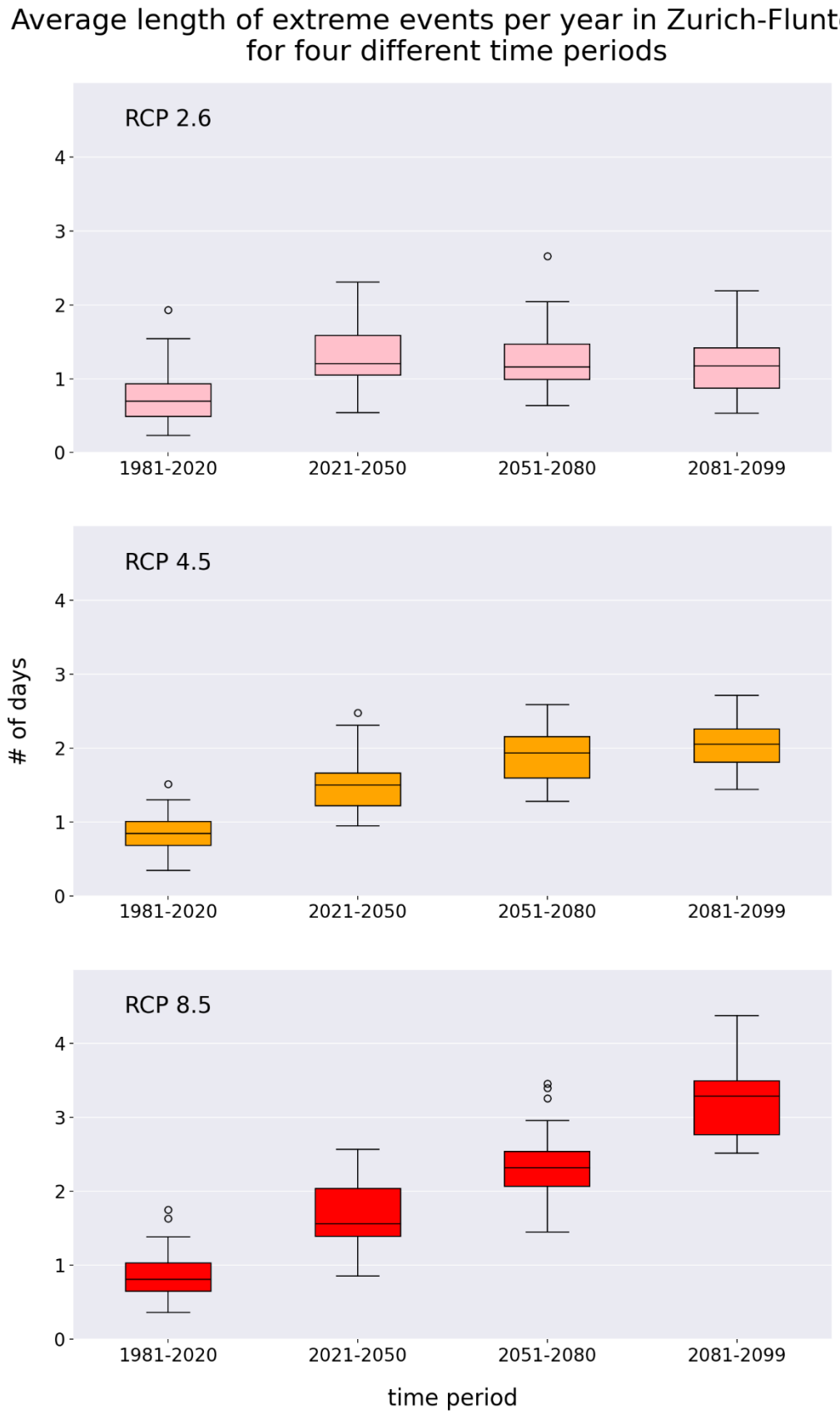

Figure 62: *LEE for four time periods for the future simulations in Zurich-Fluntern. The threshold range for an extreme day is between 26° C and 30° C. The first graph shows the RCP2.6 scenario (pink), the second graph shows the RCP4.5 scenario (orange), and the third graph shows the RCP8.5 scenario (red) (own figure).*

Sensitivity analysis of policy leavers and external factors – Basel

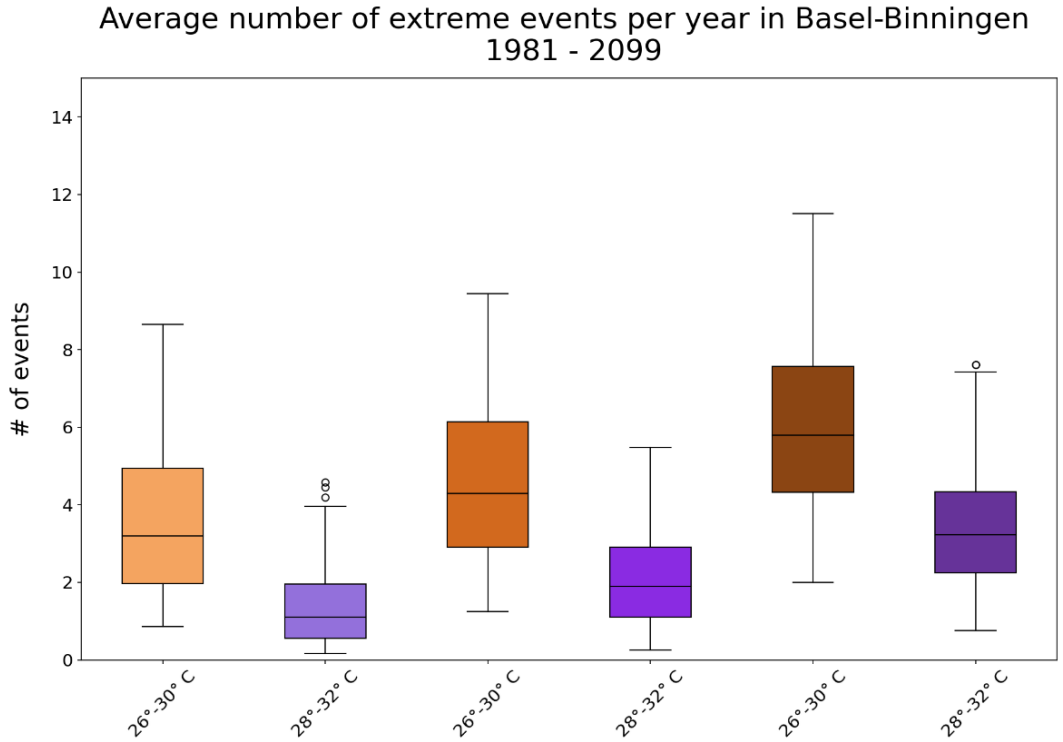

Figure 63: *Average NEE per year of the future simulations in Basel-Binningen. Threshold range 26°-30° C in brown and 28°-32° C in violet (own figure).*

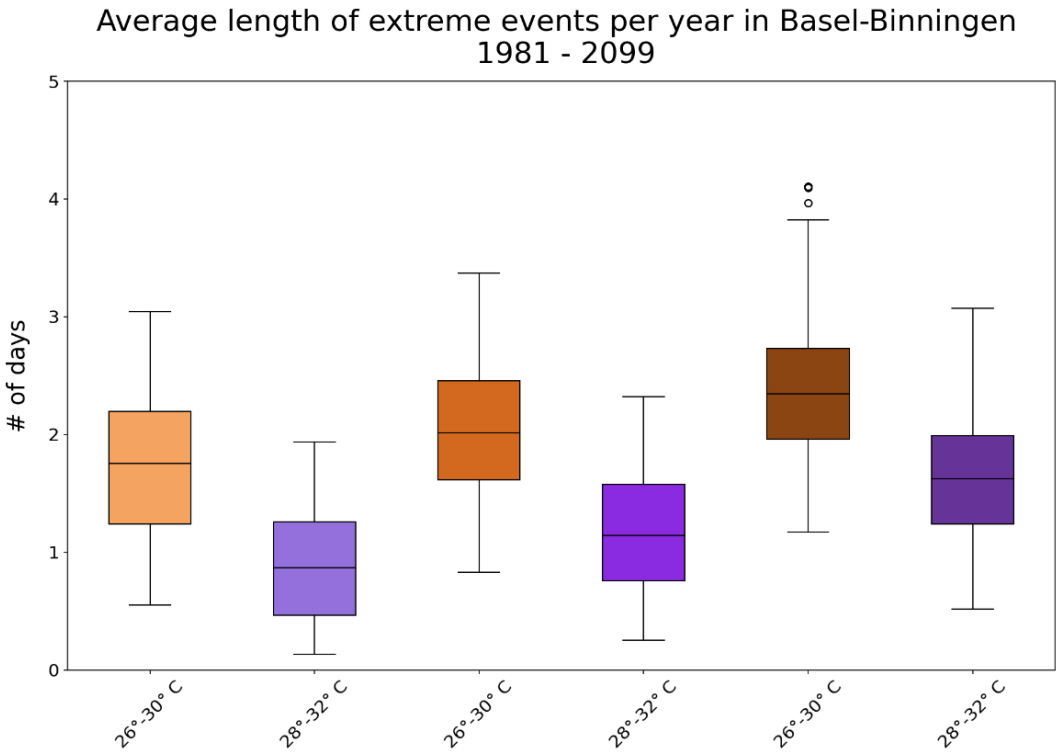

Figure 64: *LEE per year of the future simulations in Basel-Binningen. Threshold range 26°-30° C in brown and 28°-32° C in violet (own figure).*

Difference from the measuring station to the hottest places in the city – Basel

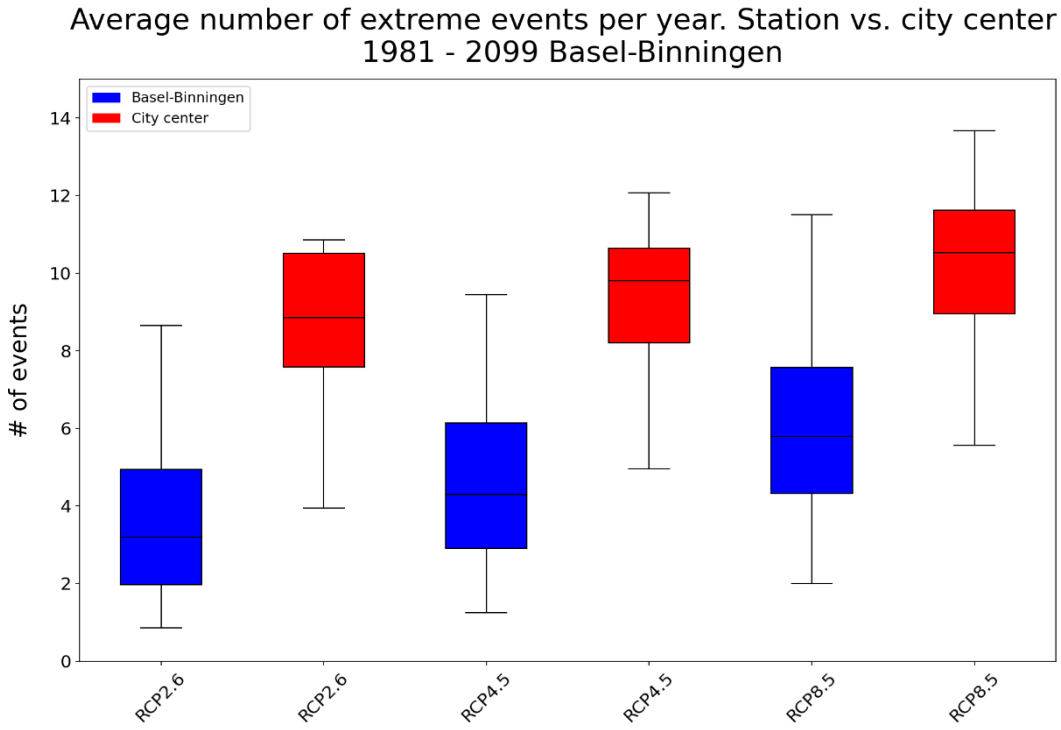

Figure 65: *Simulated NEE per year at the measuring station in Basel-Binningen in blue and simulated NEE per year for potential heat conditions in the city center in red (adapted WBGT values according to chapter 4.6) for the simulated period (1981-2099). Comparison between RCP2.6, RCP4.5, and RCP8.5 (own figure).*

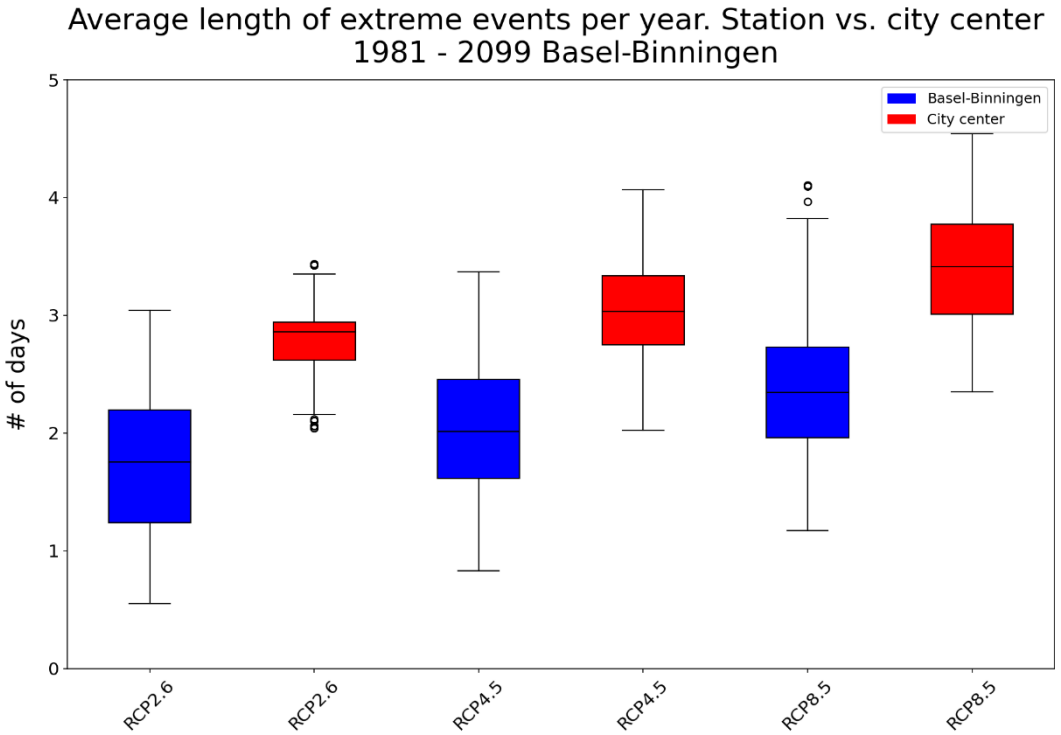

Figure 66: *Simulated LEE per year at the measuring station in Basel-Binningen in blue and simulated LEE per year for potential heat conditions in the city center in red (adapted WBGT values according to chapter 4.6) for the simulated period (1981-2099). Comparison between RCP2.6, RCP4.5, and RCP8.5 (own figure).*

Sensitivity analysis of policy leavers and external factors – Zurich

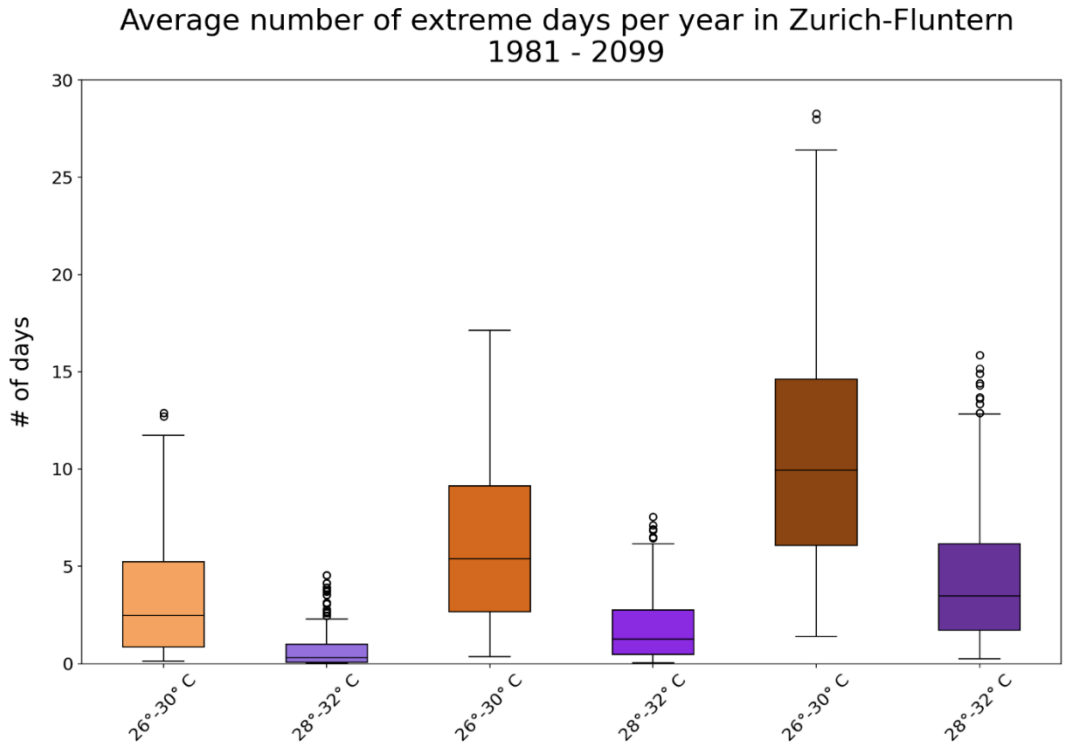

Figure 67: *Average NED per year of the future simulations in Zurich-Fluntern. Threshold range 26°-30° C in brown and 28°-32° C in violet (own figure).*

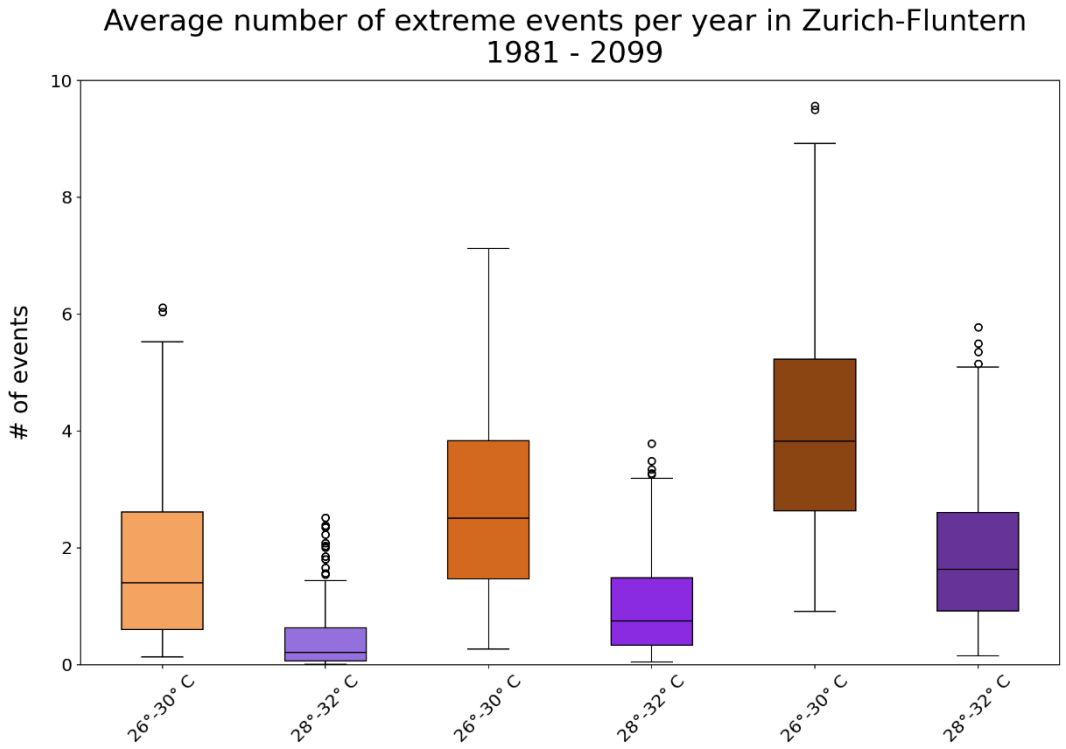

Figure 68: *Average NEE per year of the future simulations in Zurich-Fluntern. Threshold range 26°-30° C in brown and 28°-32° C in violet (own figure).*

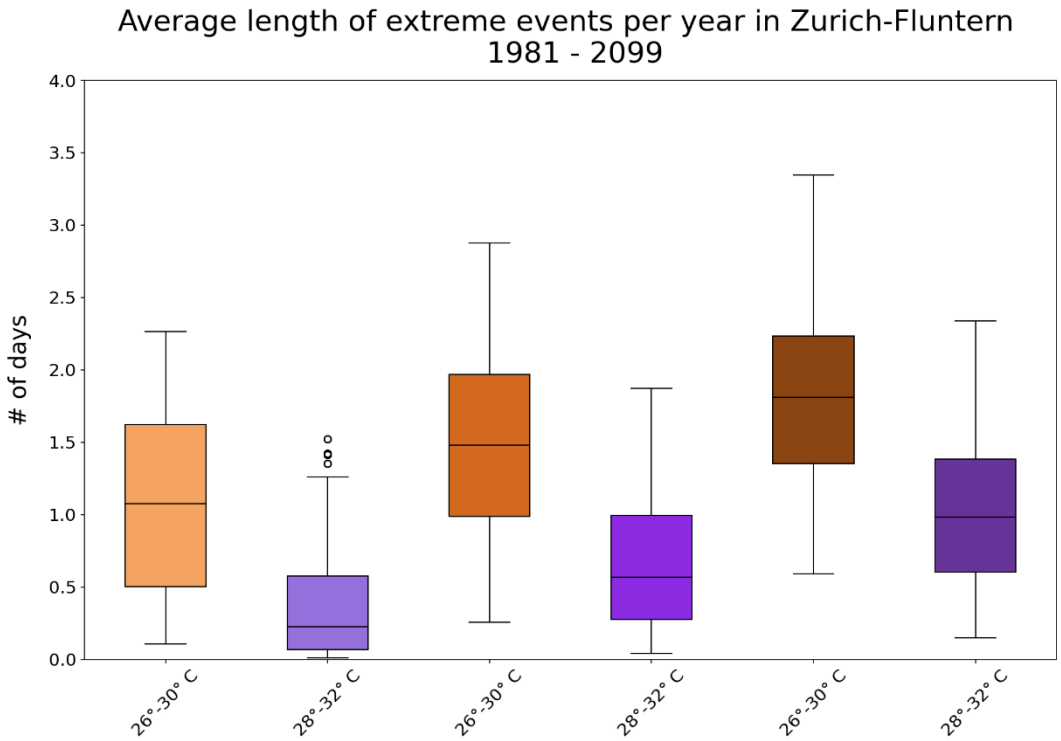

Figure 69: *LEE per year of the future simulations in Zurich-Fluntern. Threshold range 26°-30° C in brown and 28°-32° C in violet (own figure).*

Effects of adaptation options on heat indicators – Zurich

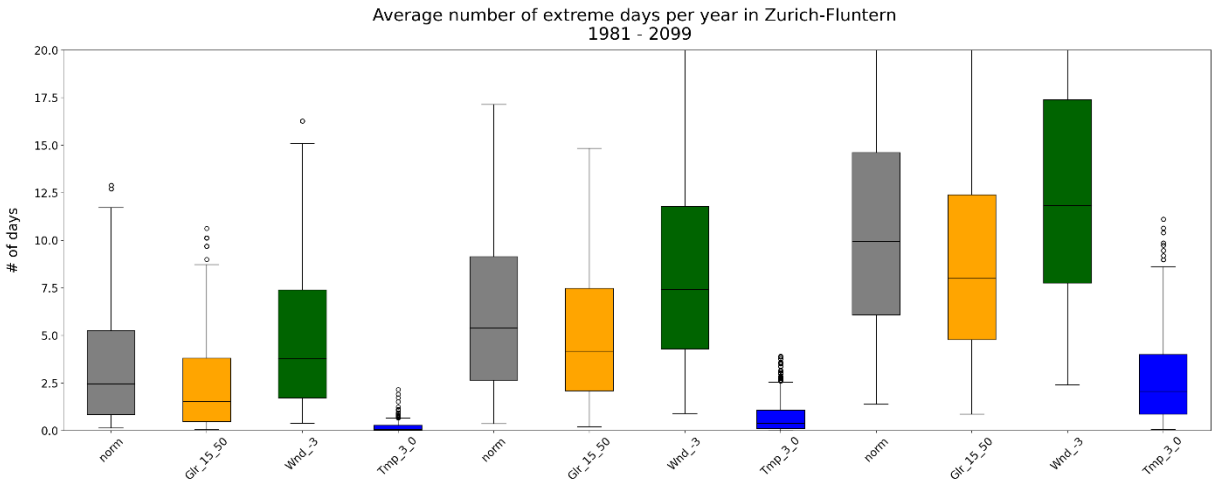

Figure 70: *Average NED per year of the future simulations in Zurich-Fluntern. No simulated adaptation effects in grey. Reduced global radiation in orange (transmissivity under trees during summer months of 15%, during winter months of 50%), decreased wind speed in dark green (by 3 m/s when initial value is greater than 3 m/s, otherwise 0 m/s), and decreased air temperature in blue (by 3° C during summer months, otherwise by 0° C). Results for three different climate scenarios (RCP2.6, RCP4.5, RCP8.5) (own figure).*

Difference from the measuring station to the hottest places in the city – Zurich

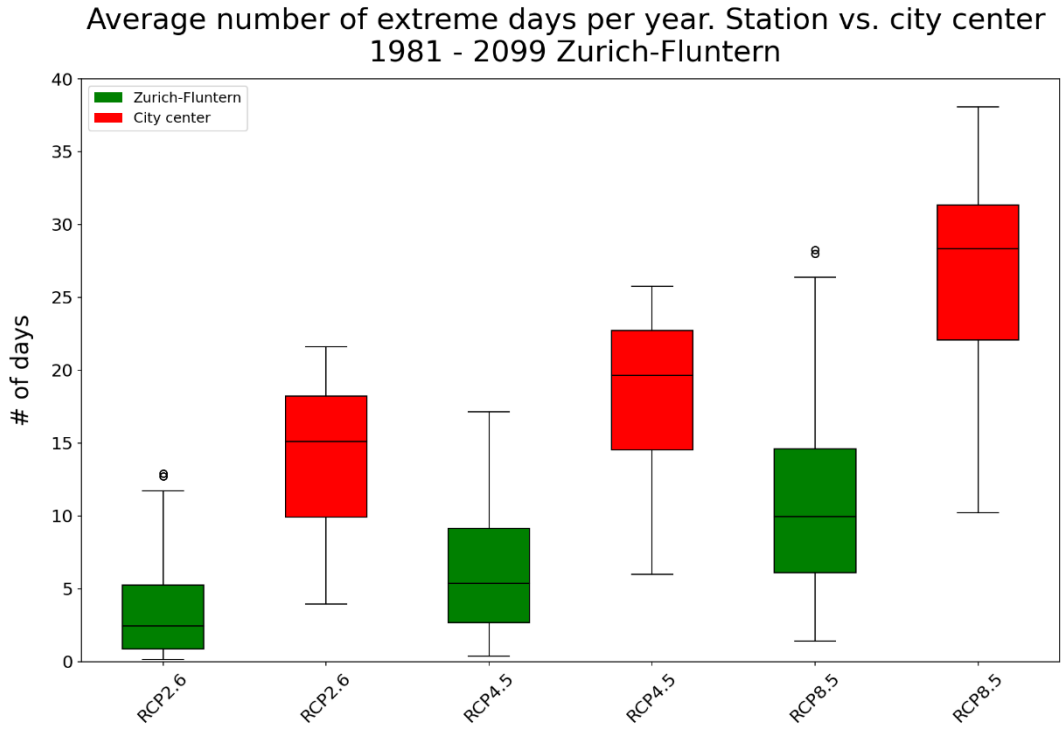

Figure 71: *Simulated NED per year at the measuring station in Zurich-Fluntern in green and simulated NED per year for potential heat conditions in the city center in red (adapted WBGT values according to chapter 4.6) for the simulated period (1981-2099). Comparison between RCP2.6, RCP4.5, and RCP8.5 (own figure).*

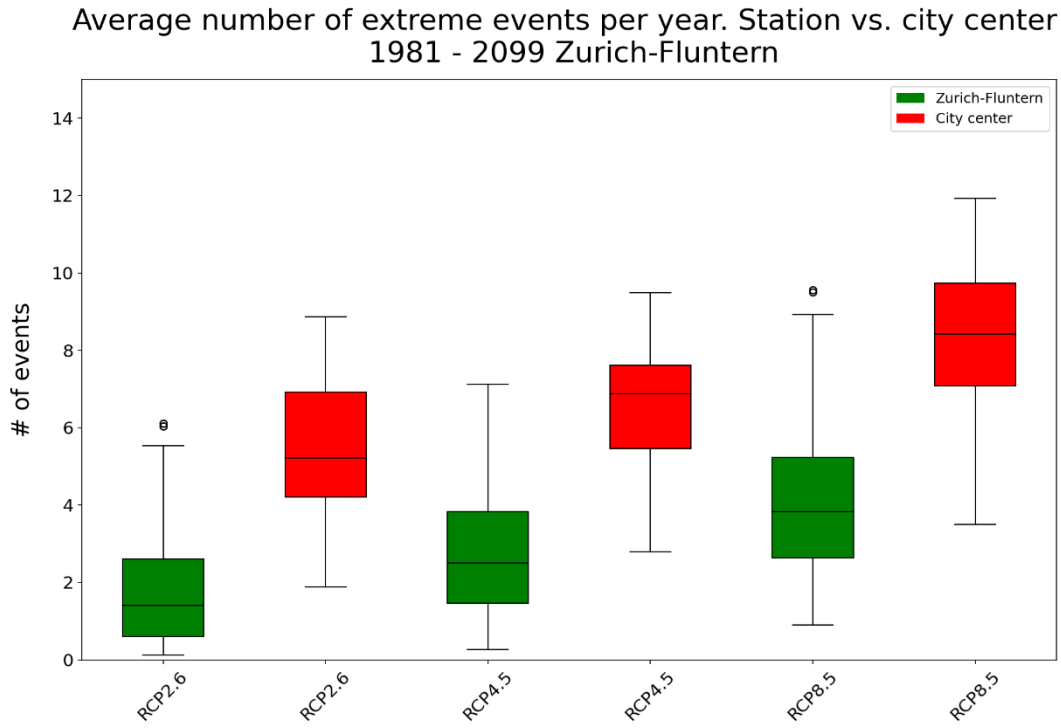

Figure 72: *Simulated NEE per year at the measuring station in Zurich-Fluntern in green and simulated NEE per year for potential heat conditions in the city center in red (adapted WBGT values according to chapter 4.6) for the simulated period (1981-2099). Comparison between RCP2.6, RCP4.5, and RCP8.5 (own figure).*

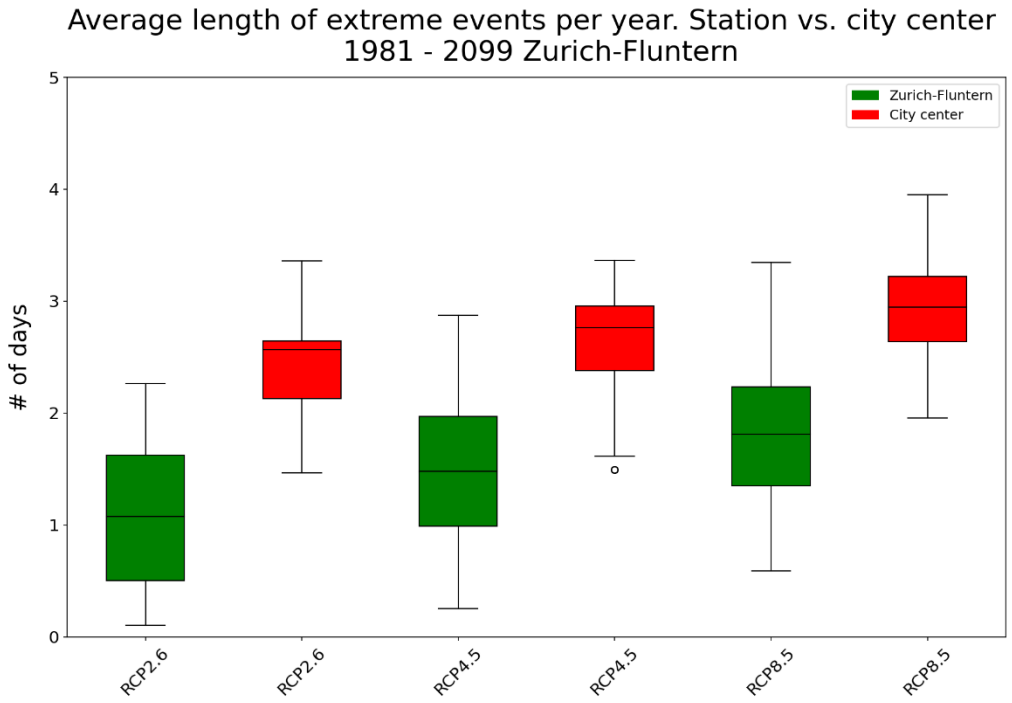

Figure 73: *Simulated LEE per year at the measuring station in Zurich-Fluntern in green and simulated LEE per year for potential heat conditions in the city center in red (adapted WBGT values according to chapter 4.6) for the simulated period (1981-2099). Comparison between RCP2.6, RCP4.5, and RCP8.5 (own figure).*

Basel vs. Zurich

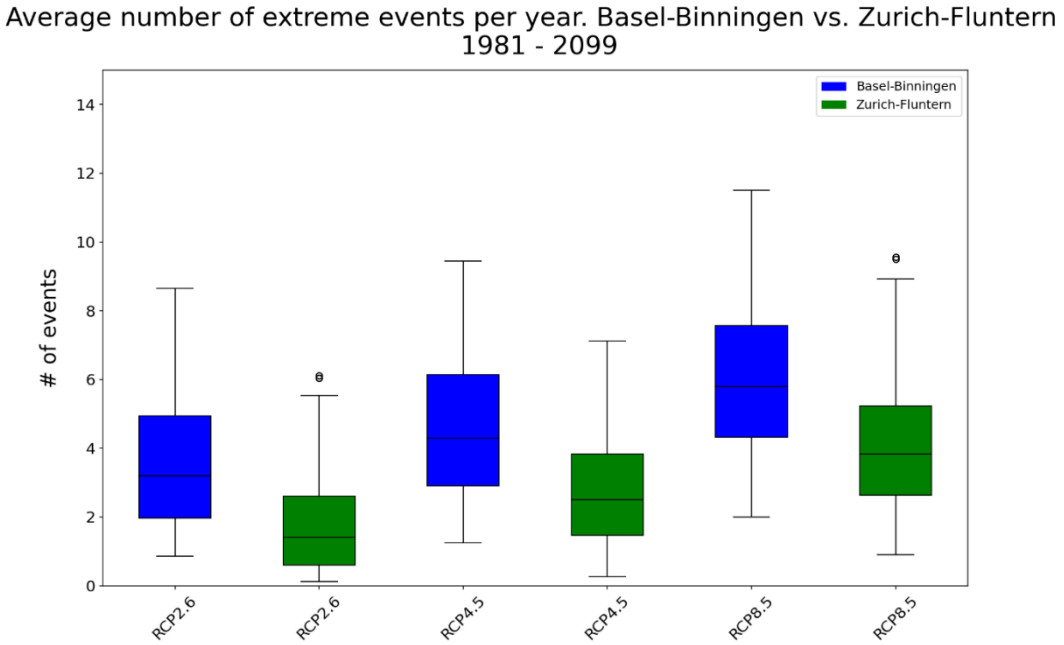

Figure 74: *Comparison of the average NEE per year between Basel-Binningen and Zurich-Fluntern for three different climate scenarios (RCP2.6, RCP4.5, RCP8.5) (own figure).*

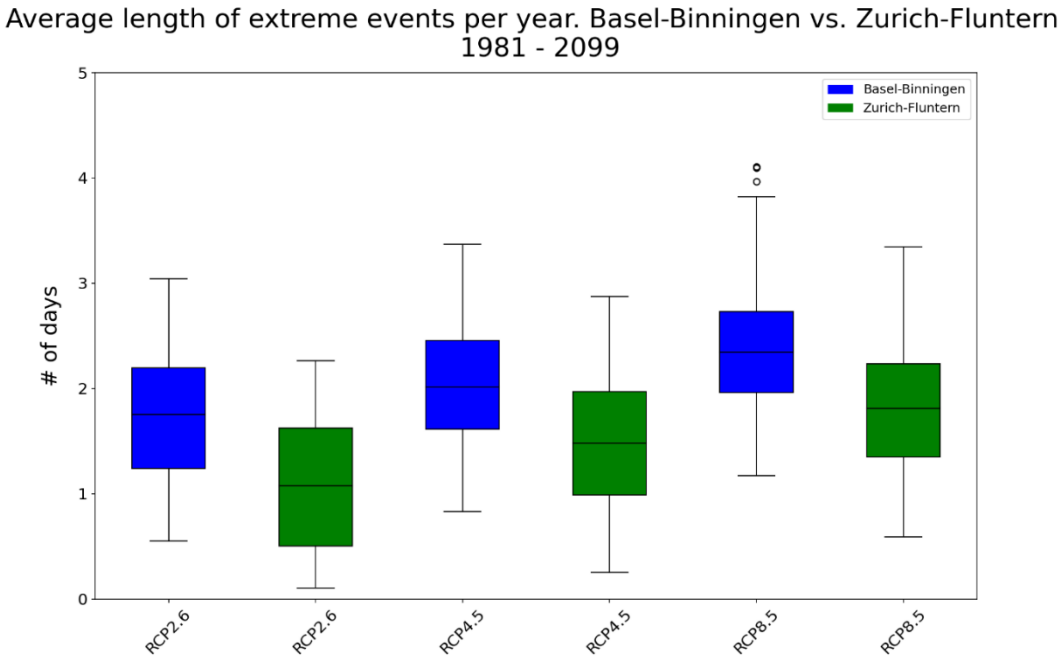

Figure 75: *Comparison of LEE per year between Basel-Binningen and Zurich-Fluntern for three different climate scenarios (RCP2.6, RCP4.5, RCP8.5) (own figure).*

Personal declaration

I hereby declare that the submitted Thesis is the result of my own, independent work. All external sources are explicitly acknowledged in the Thesis.

F. Weibel

29.09.2022, Zurich Fabian Weibel